From individual to collective behaviors based on optical flow

Franck RUFFIER

CNRS Research Director
Institute of Movement Sciences

CNRS / Aix-Marseille University, France

franck.ruffier@univ-amu.fr www.ism.univ-amu.fr/ruffier

***WS*: Collective motions of animals and robots, Cargese, Corsica**

Thanks to :

Lucia Bergantin (PhD student)

Xavier Daïni (PhD student)

Diego Castro-Rondon (PhD student)

Charles Coquet (Postdoc)

José Castillo (Postdoc)

J.-M. Ingargiola (Staff Engineer)

Syrphid flies: hover flight

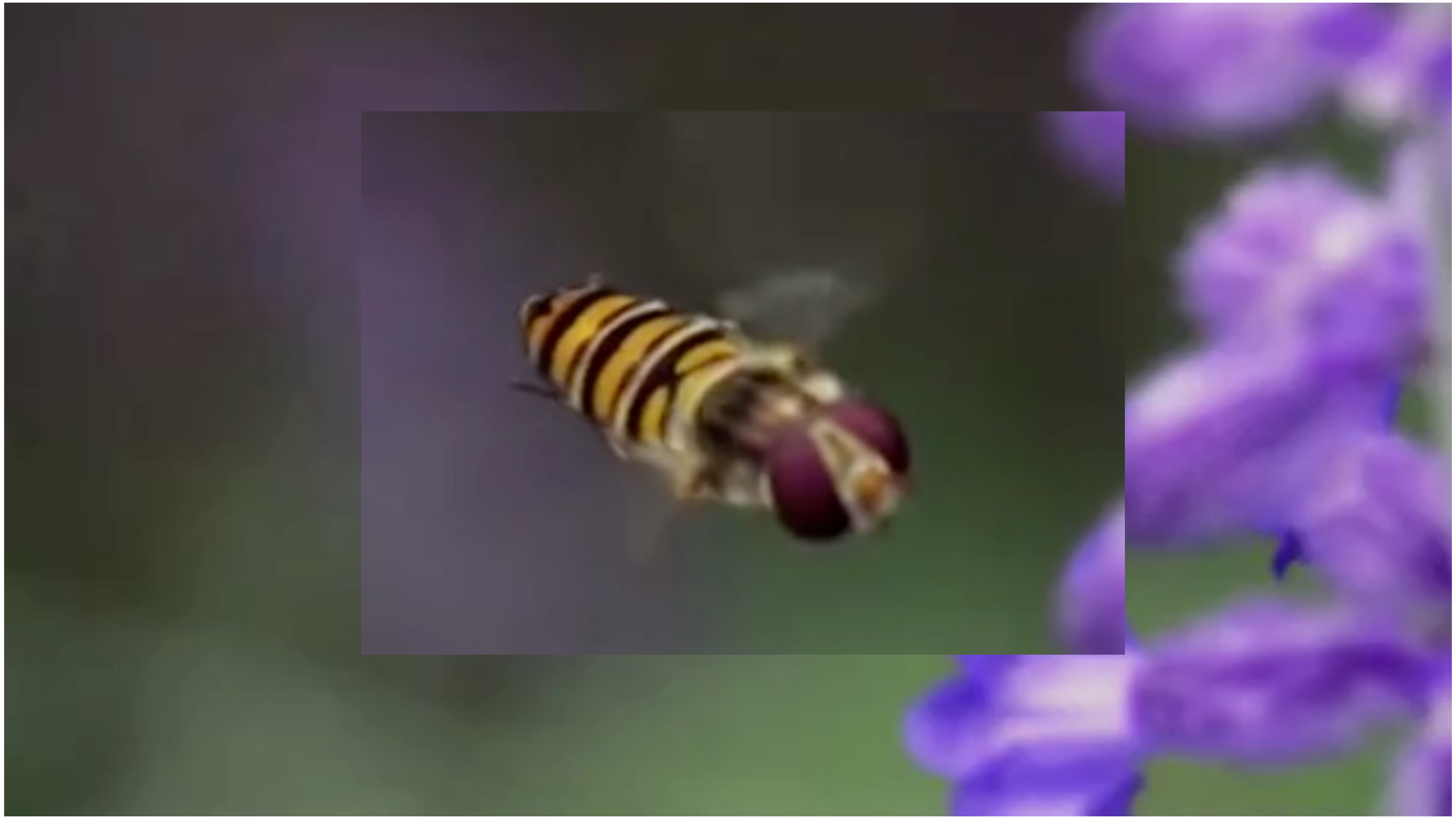

Conquest of the skies (BBC)

Visual cues of insects navigation

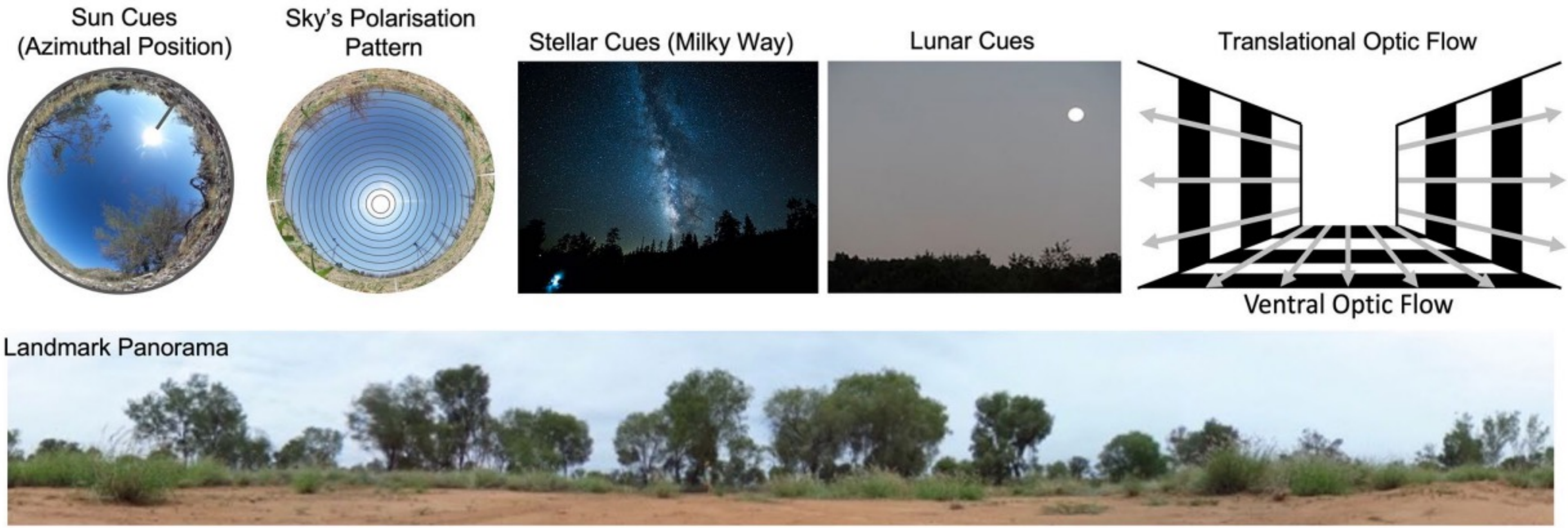

[Freas and Spetch, 2022]

Insect-scale flying robot

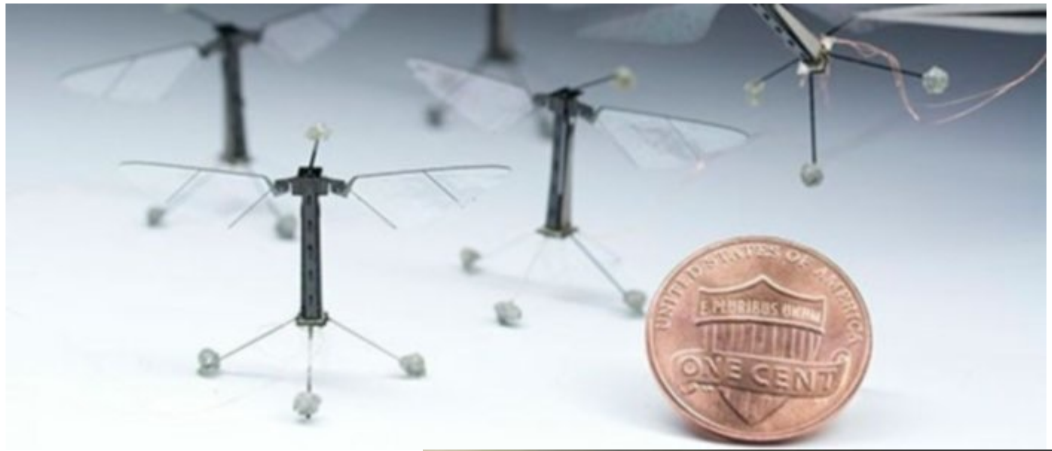

RoboBee, Harvard, USA

Biorobotics : a scientific method

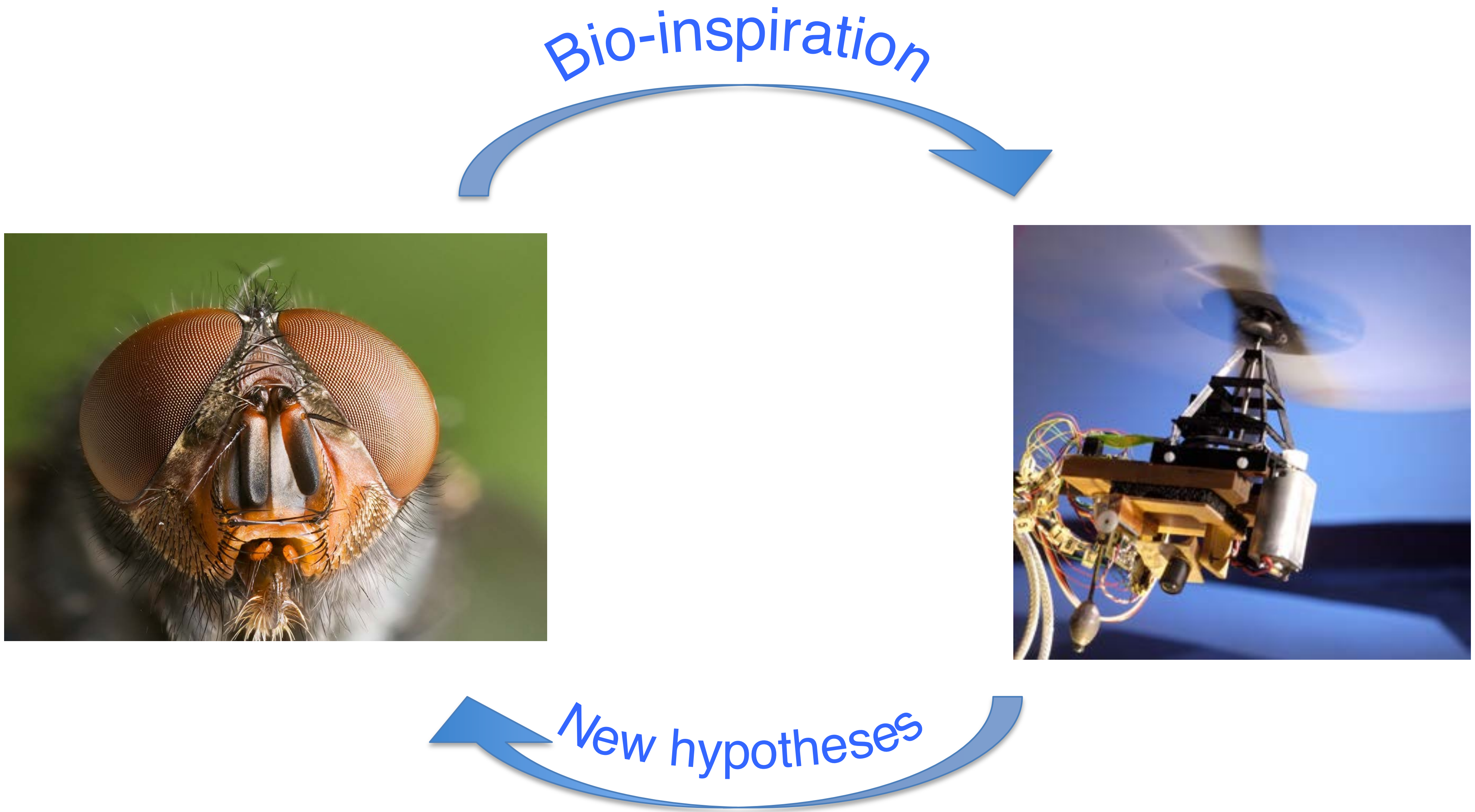


Wikimedia Common, J J Harrison

The compound eye

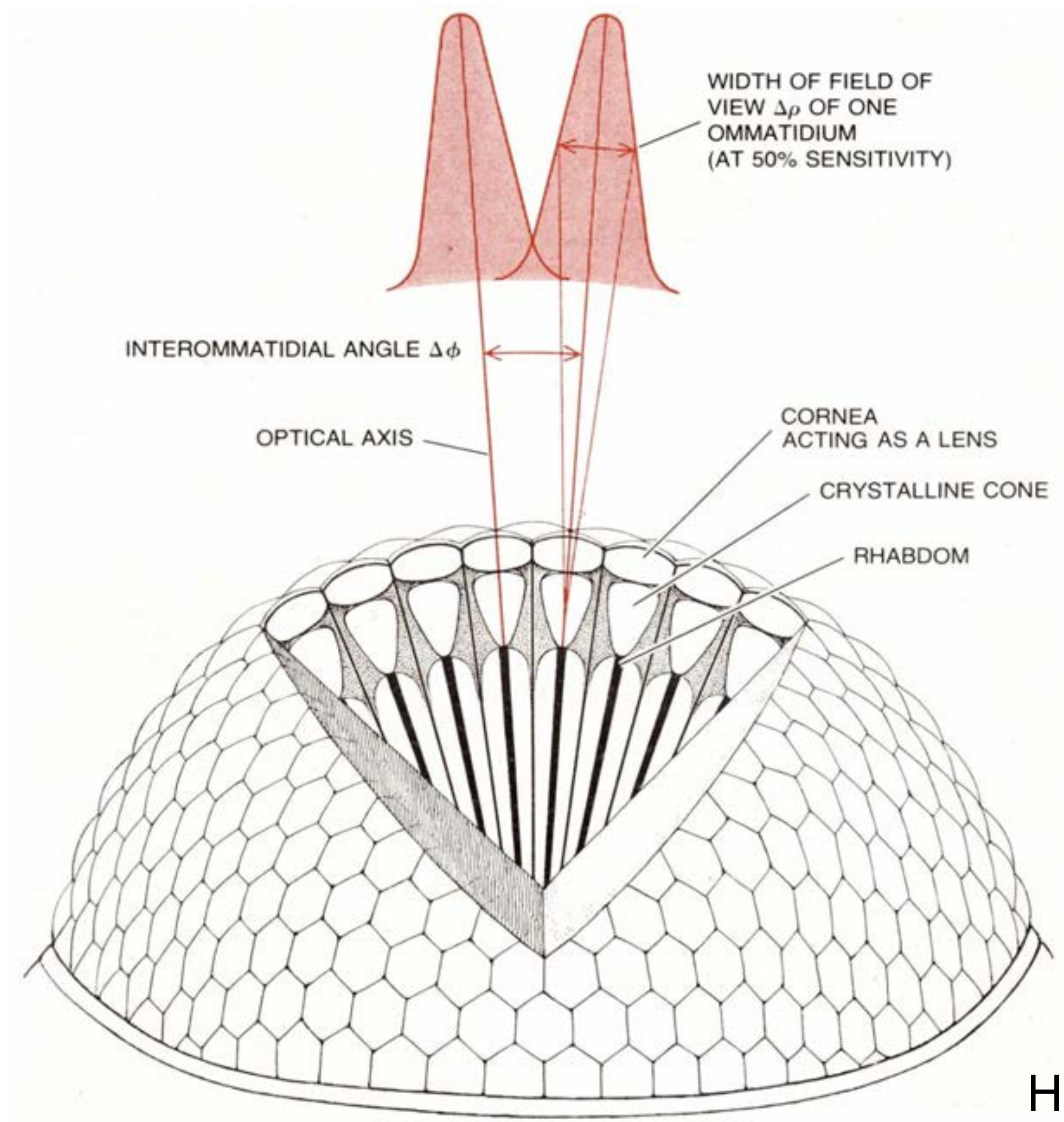

Horridge 1977

Optic flow as seen by a wingsuiter

Winged insects used the optic flow to navigate : $\omega \sim \dfrac{V}{D} \sin \Phi$

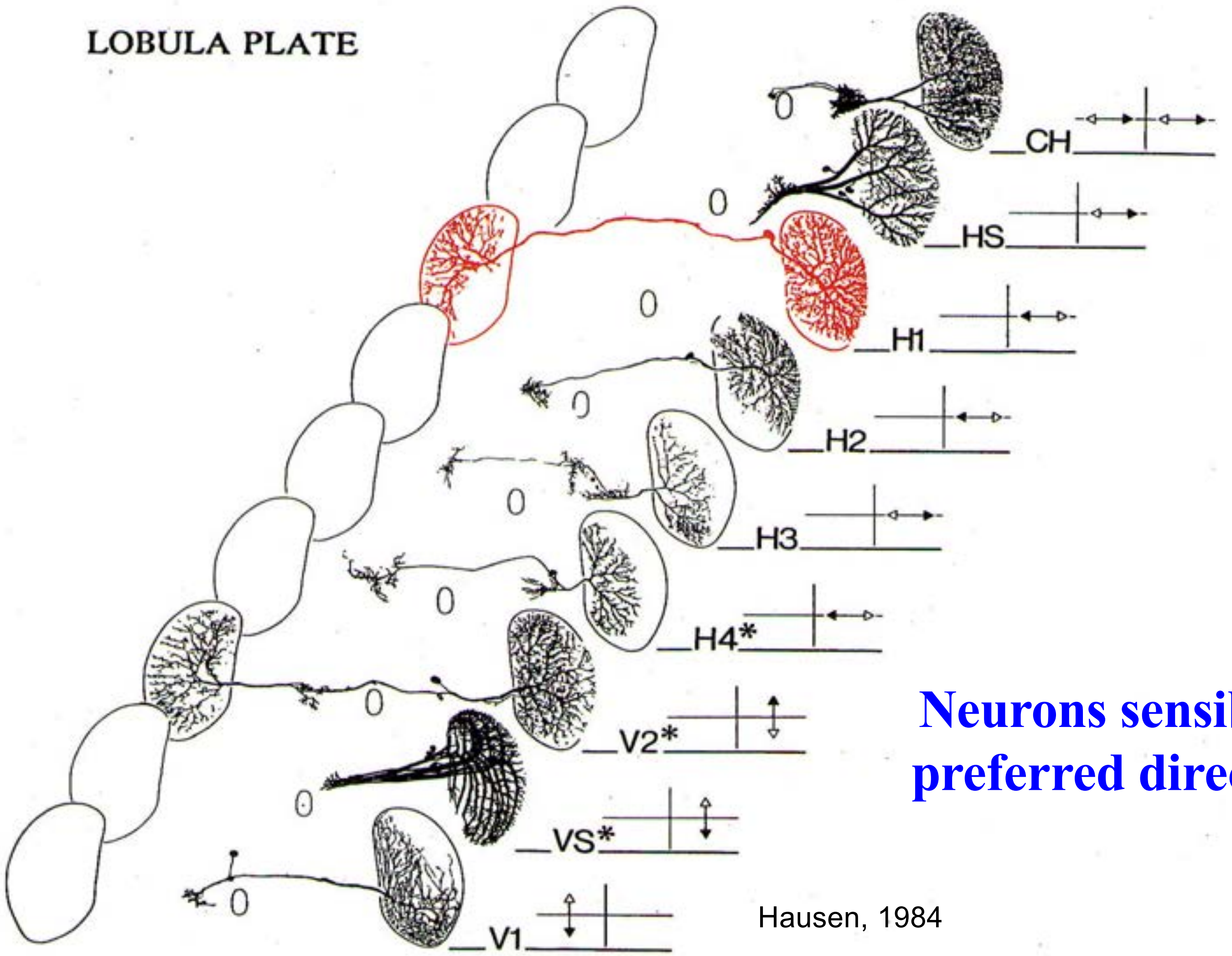

Neurons sensible to preferred directions

Hausen, 1984

I. The optic flow regulation principle for visual guidance

3 robots: Octave, Lora, Beerotor

Ventral optic flow in the vertical plane

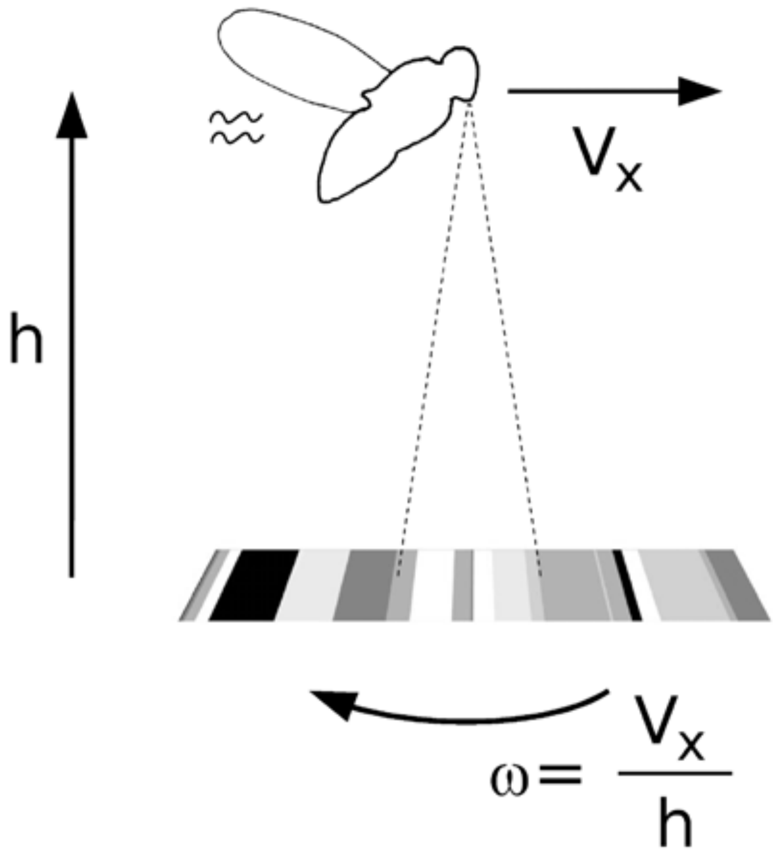

Franceschini, Ruffier, Serres, Current Biology 2007

Ventral Optic flow is kept constant by insects

1/ Kennedy's *"preferred retinal velocity" theory* (1951): qualitative data on locusts

2/ Srinivasan et al. (1996): quantitative data on landing Bees

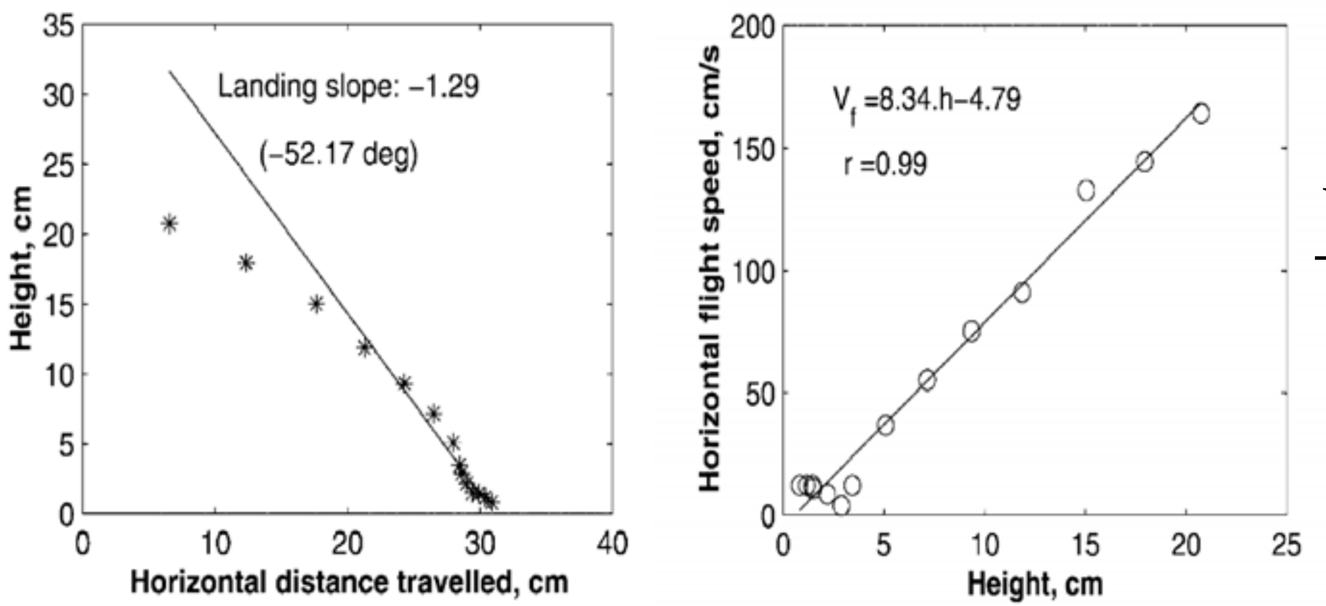

Srinivasan et al. (1996)

$$\frac{\mathrm{V_x}(t)}{h(t)} \approx \text{Constant}$$

but how?

=> Disturbing the ventral optic flow

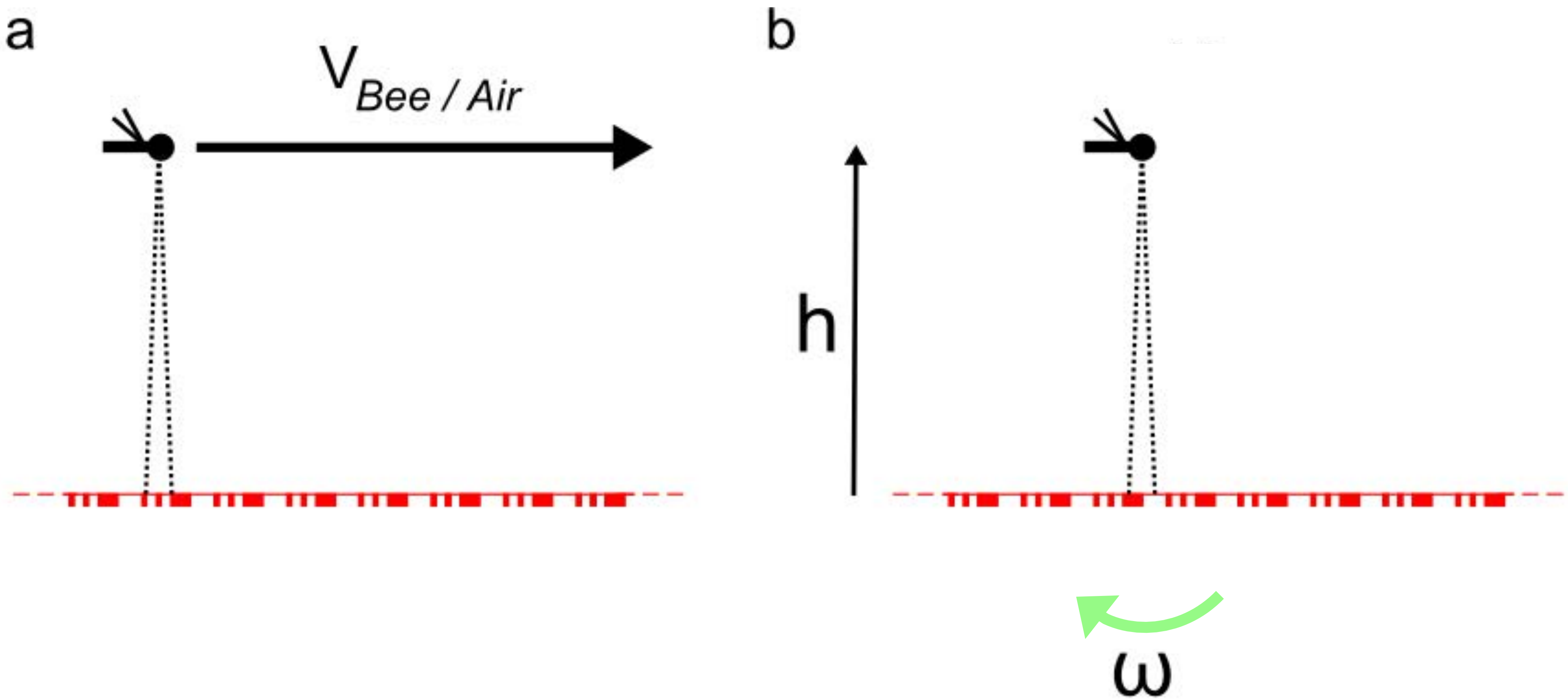

Portelli, G., Ruffier, F., & Franceschini, N. (2010) J. Comp. Physiol. A, 196:307-313

While the floor moves, honeybees decreased their height

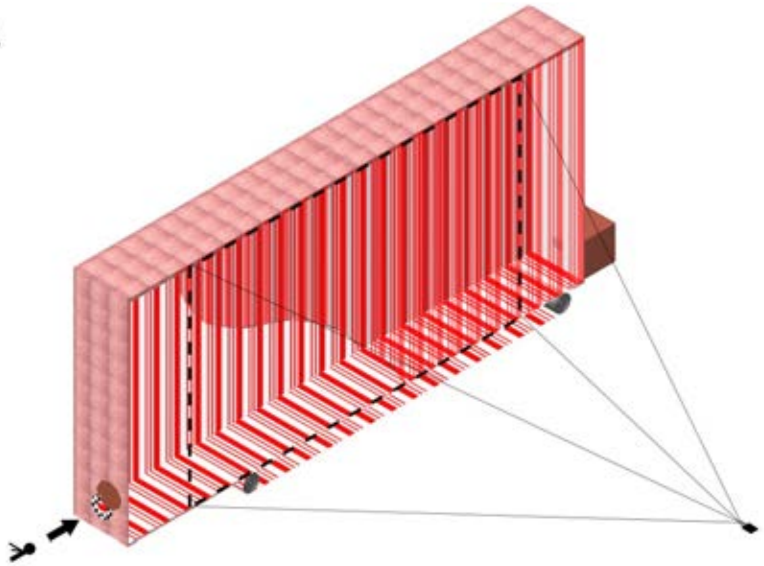

High-roof tunnel
equipped with rollers

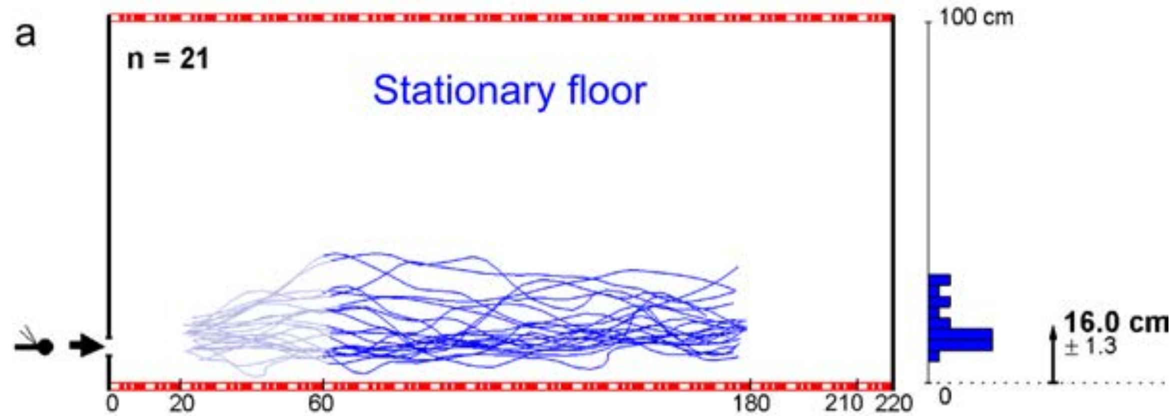

Portelli, G., Ruffier, F., & Franceschini, N. (2010) J. Comp. Physiol. A, 196:307-313

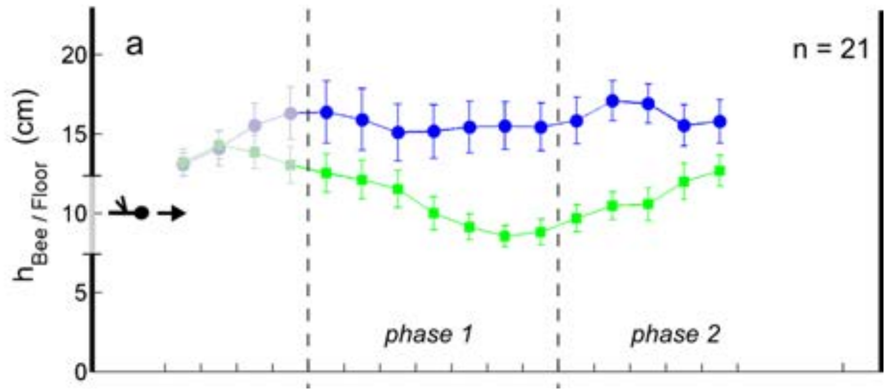

⇒ Honeybees decreased their height, thus restoring their Optic Flow

⇒ Ventral Optic flow may be regulated by adjusting altitude

Portelli, G., Ruffier, F., & Franceschini, N. (2010) J. Comp. Physiol. A, 196:307-313

OCTAVE robot: ventral Optic flow regulator that adjusts the altitude

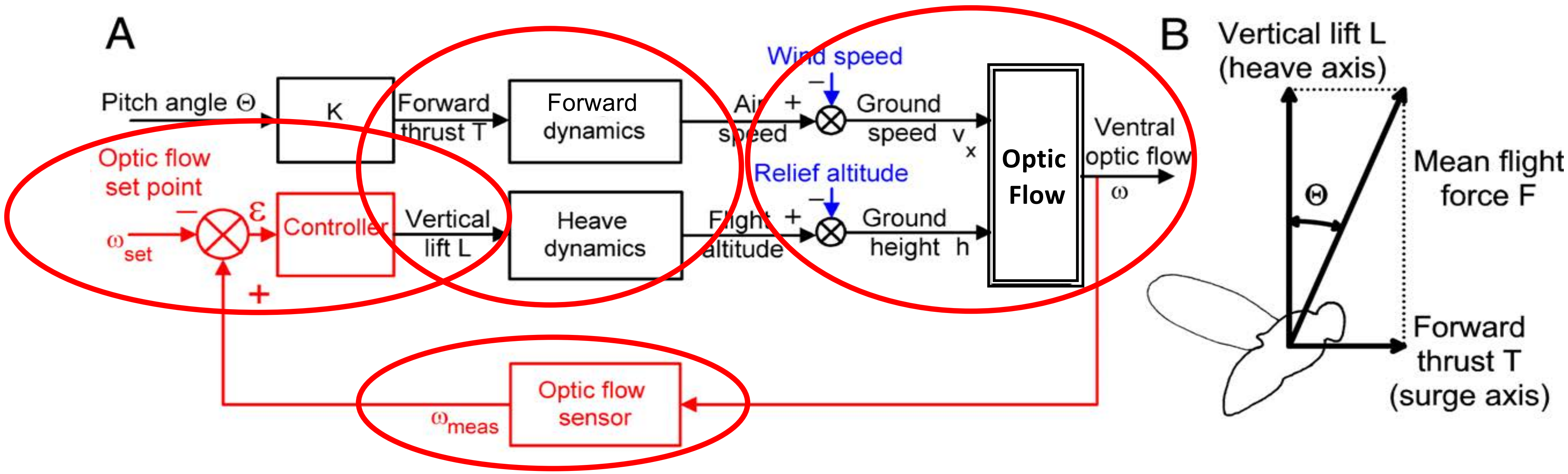

Franceschini, Ruffier, Serres (2007) *Current Biology 17, 329-335*
Ruffier, Franceschini (2003, 2004, 2005)

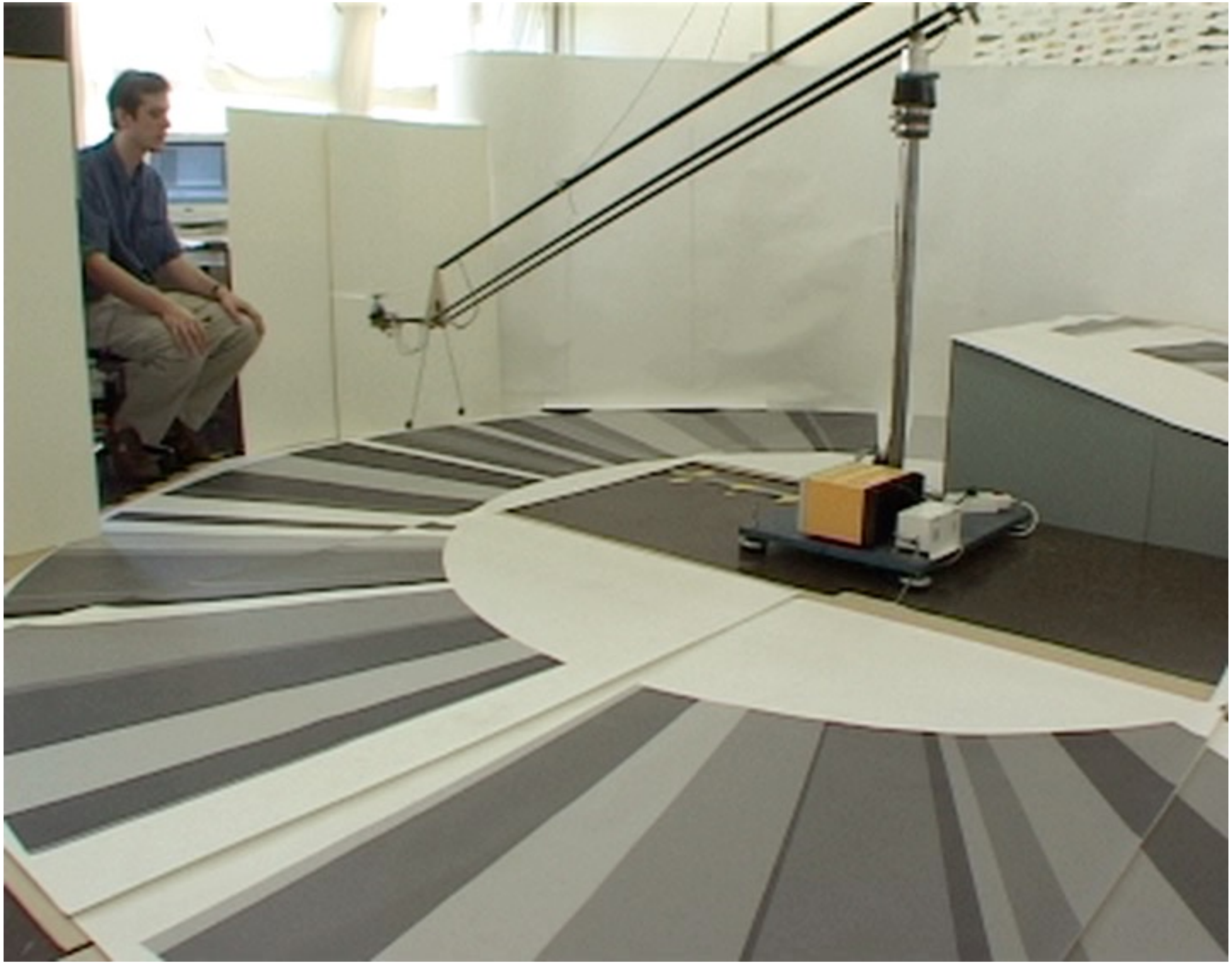

Landing by backward pitching

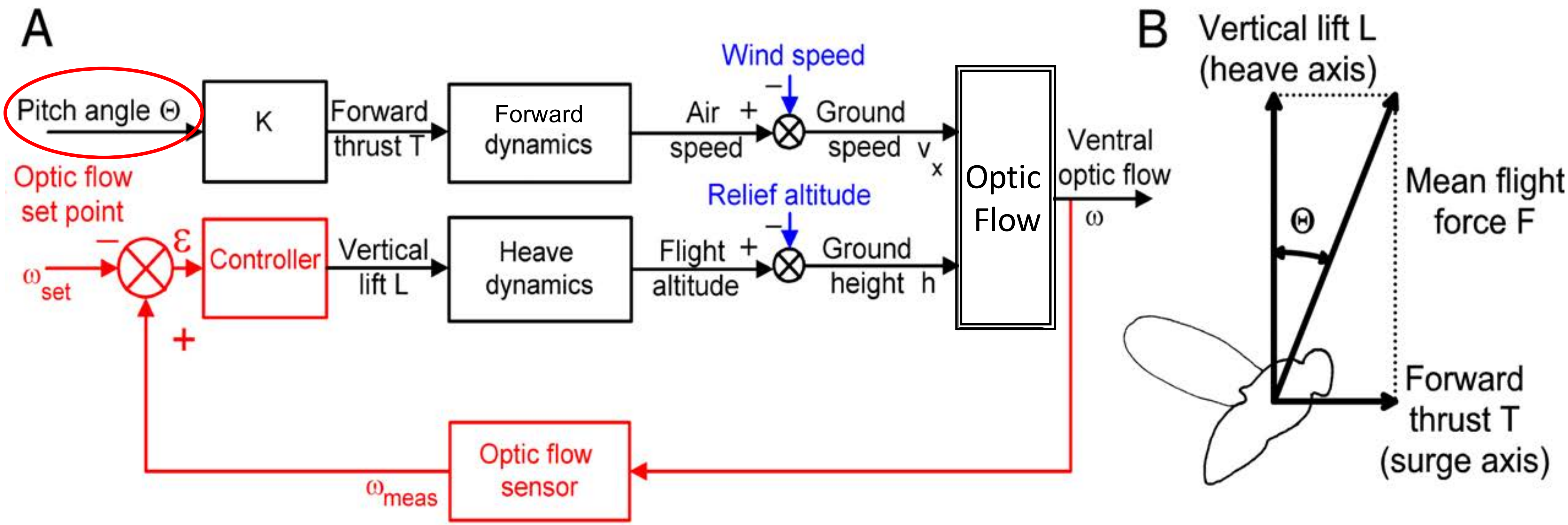

Franceschini, Ruffier, Serres (2007) *Current Biology 17, 329-335*
Ruffier, Franceschini (2003, 2004, 2005)

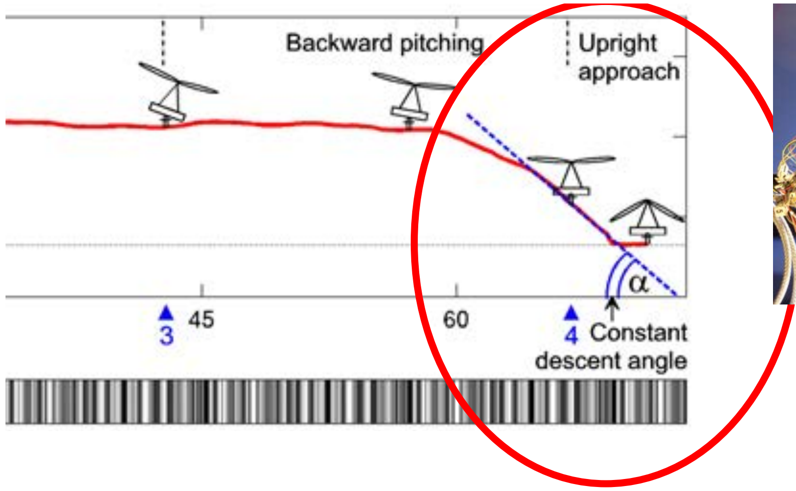

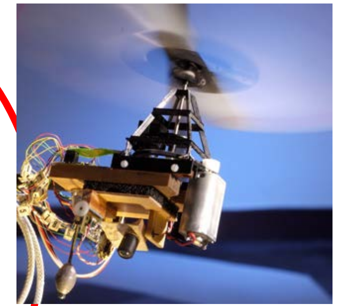

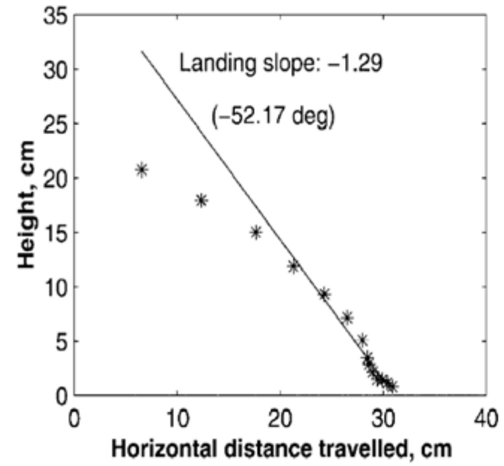

Srinivasan et al. (1996, 2000)

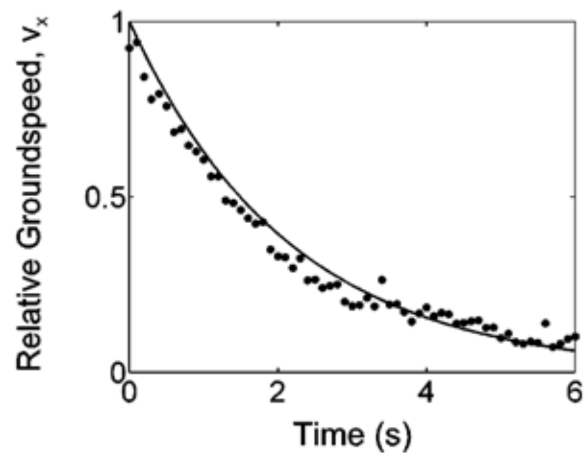

Vx is an exponential function of time

⇒ h is an exponential

⇒ Vz is an exponential

⇒ Vz/Vx is therefore constant

In addition, we show that ***landing with a constant slope*** is not a *requirement* but a *consequence* of the optical flow regulator.

Franceschini, Ruffier, Serres (2007) *Current Biology 17: 329-335*

Landing on a moving target

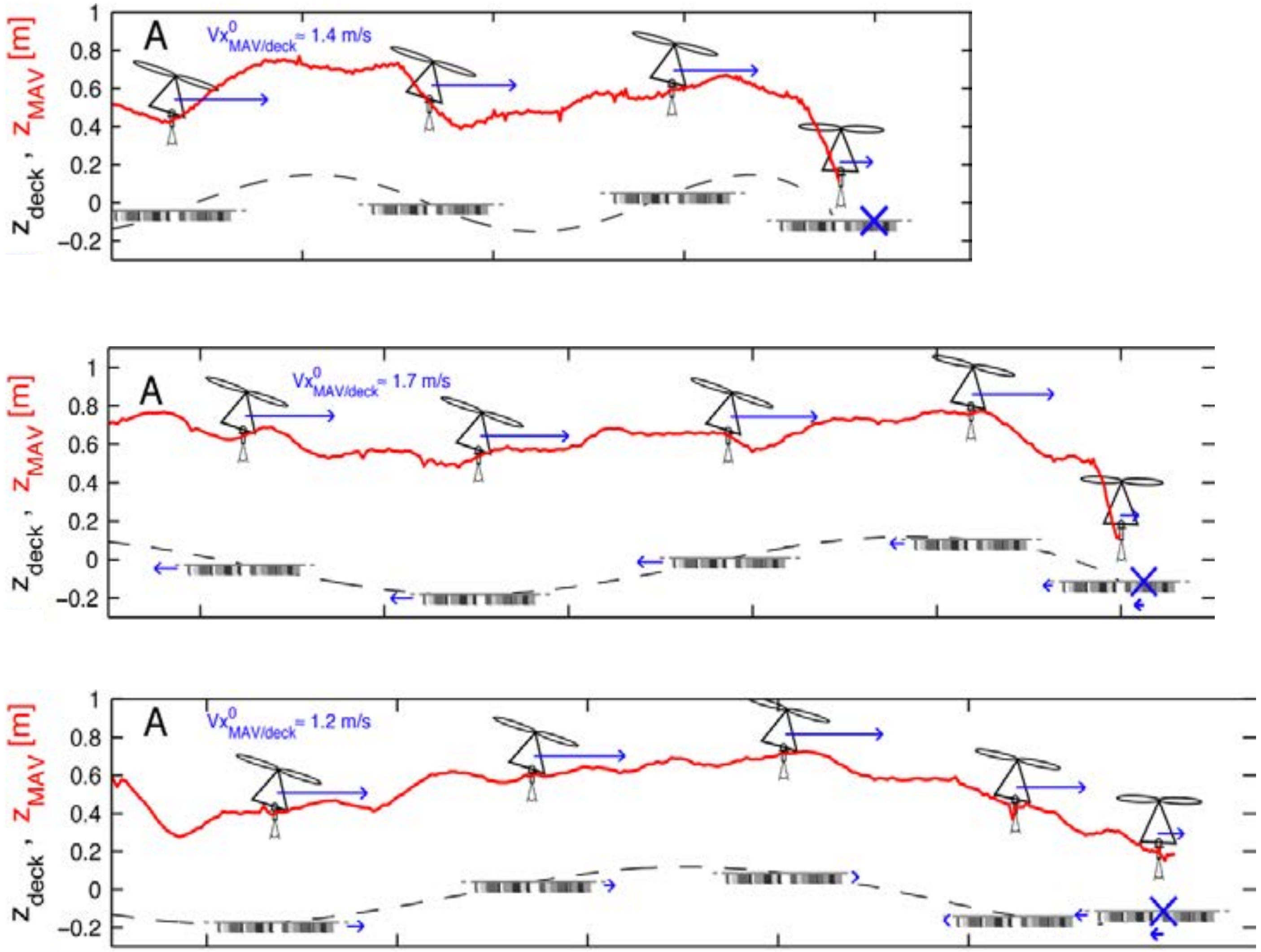

Ruffier Franceschini (2015)
J Intell Robot Syst

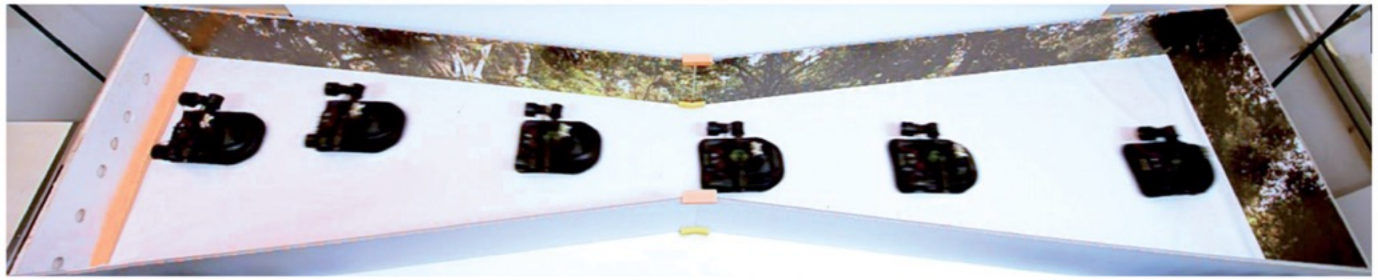

LORA robot

Roubieu et al. (2014)
Bioinspir. Biomim.

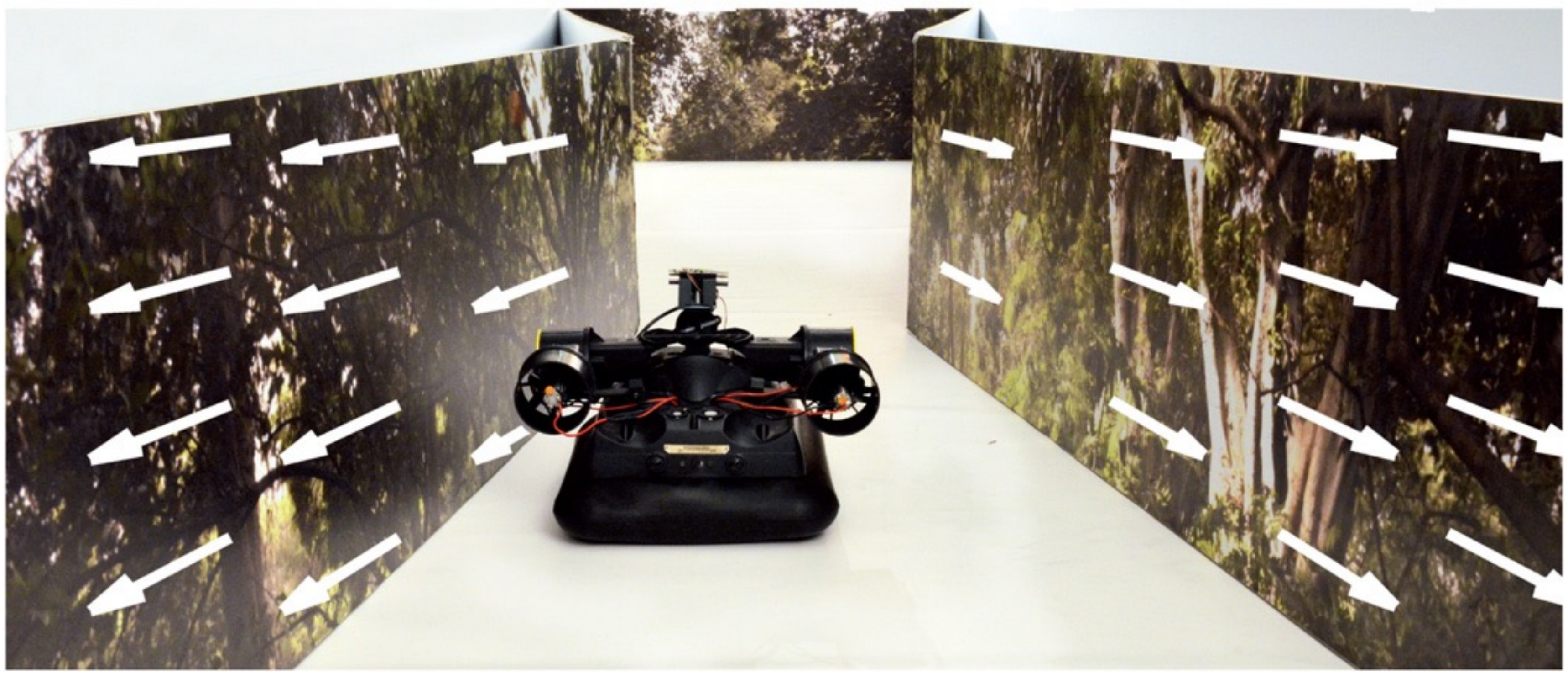

Optic flow (OF) measurement

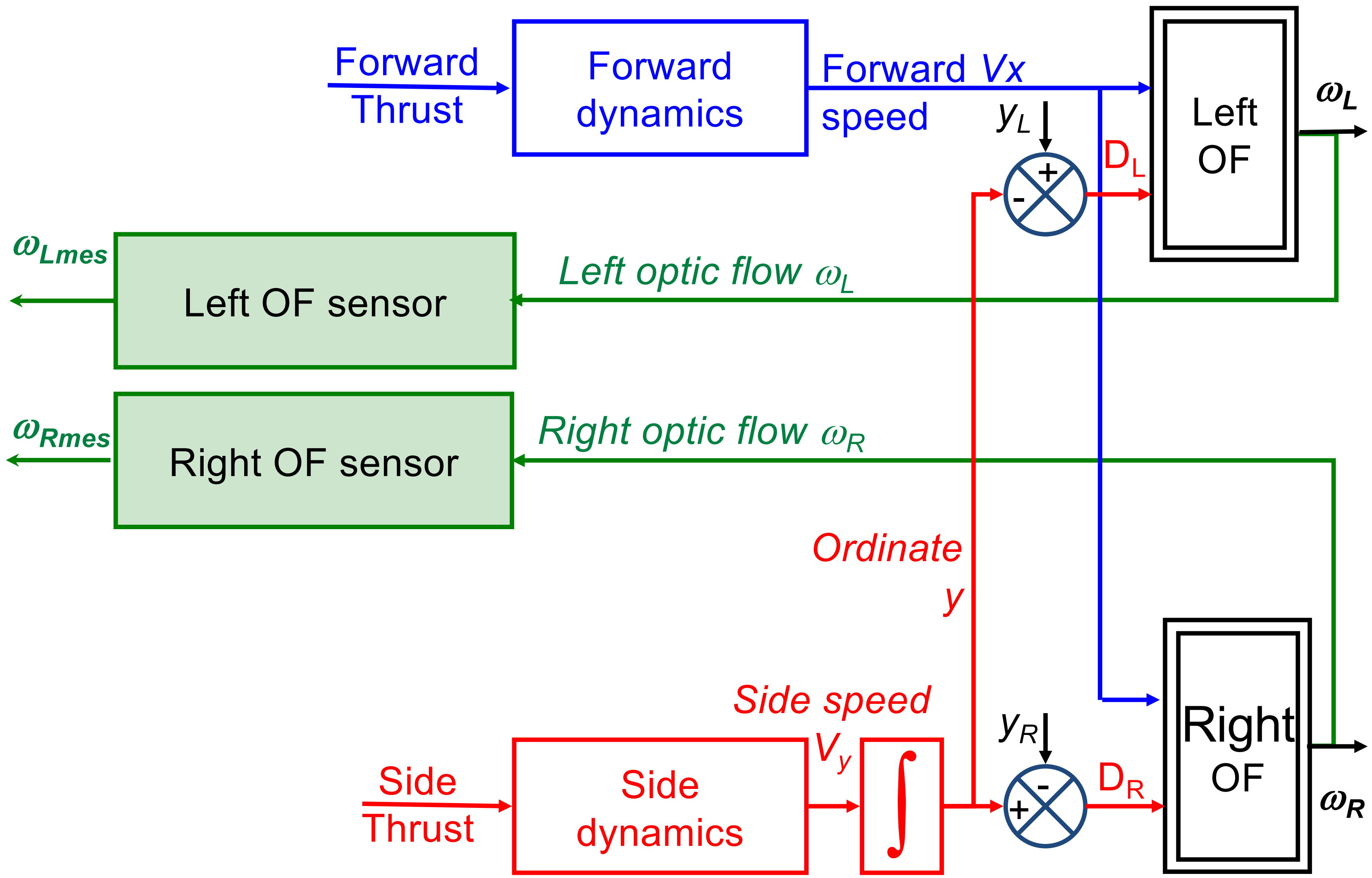

Selection of the wall to follow

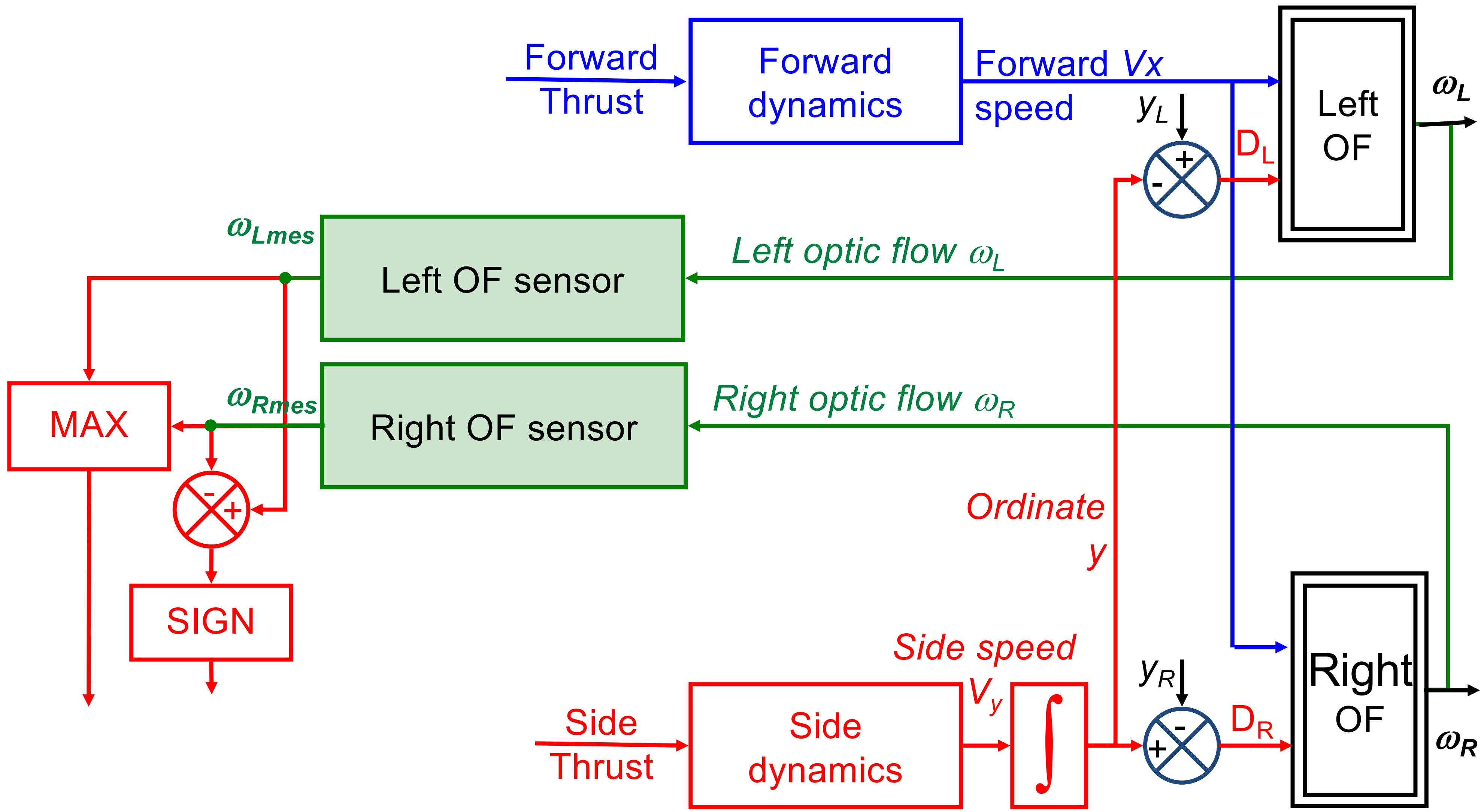

The side control loop

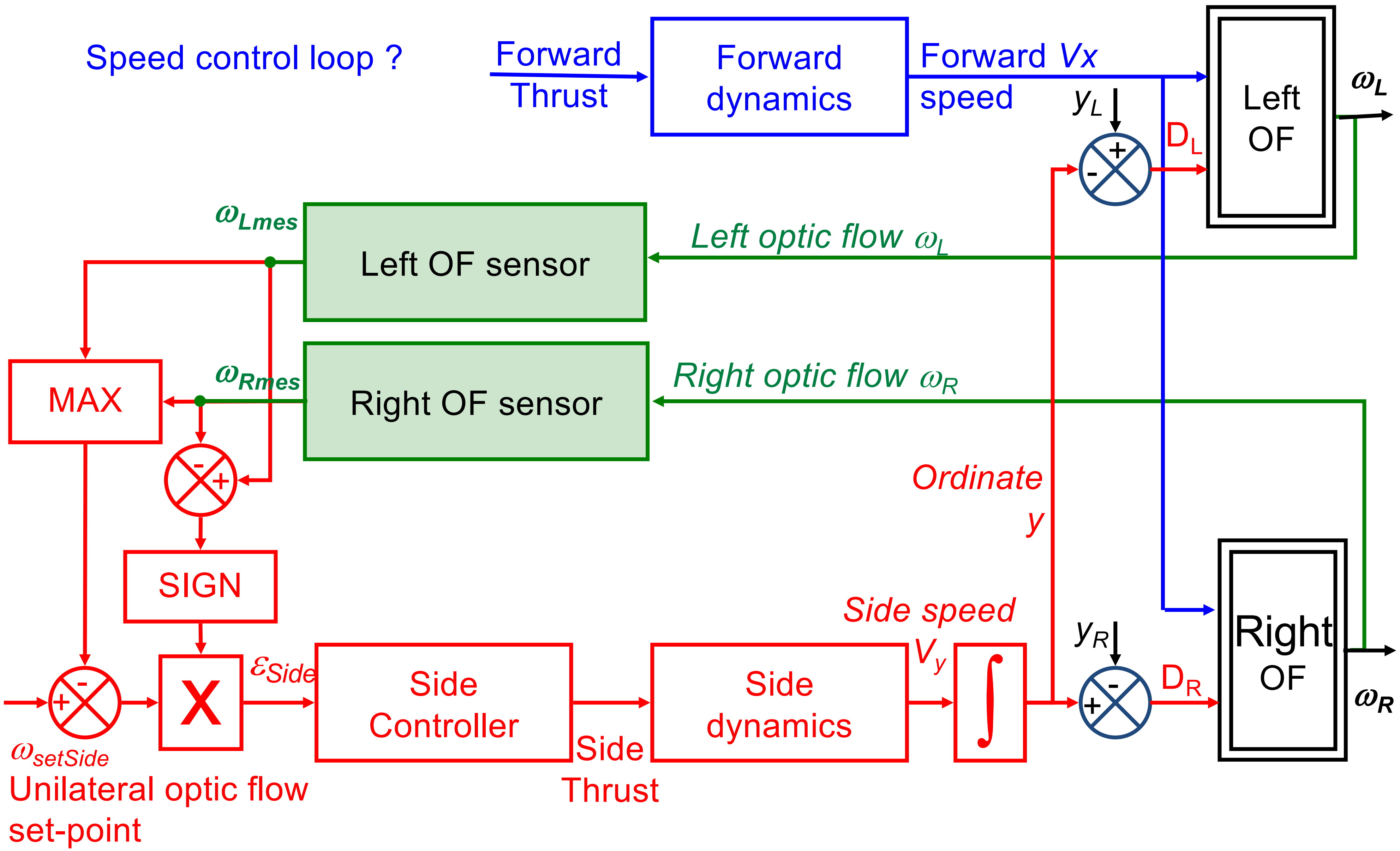

Speed control loop: Source of inspiration

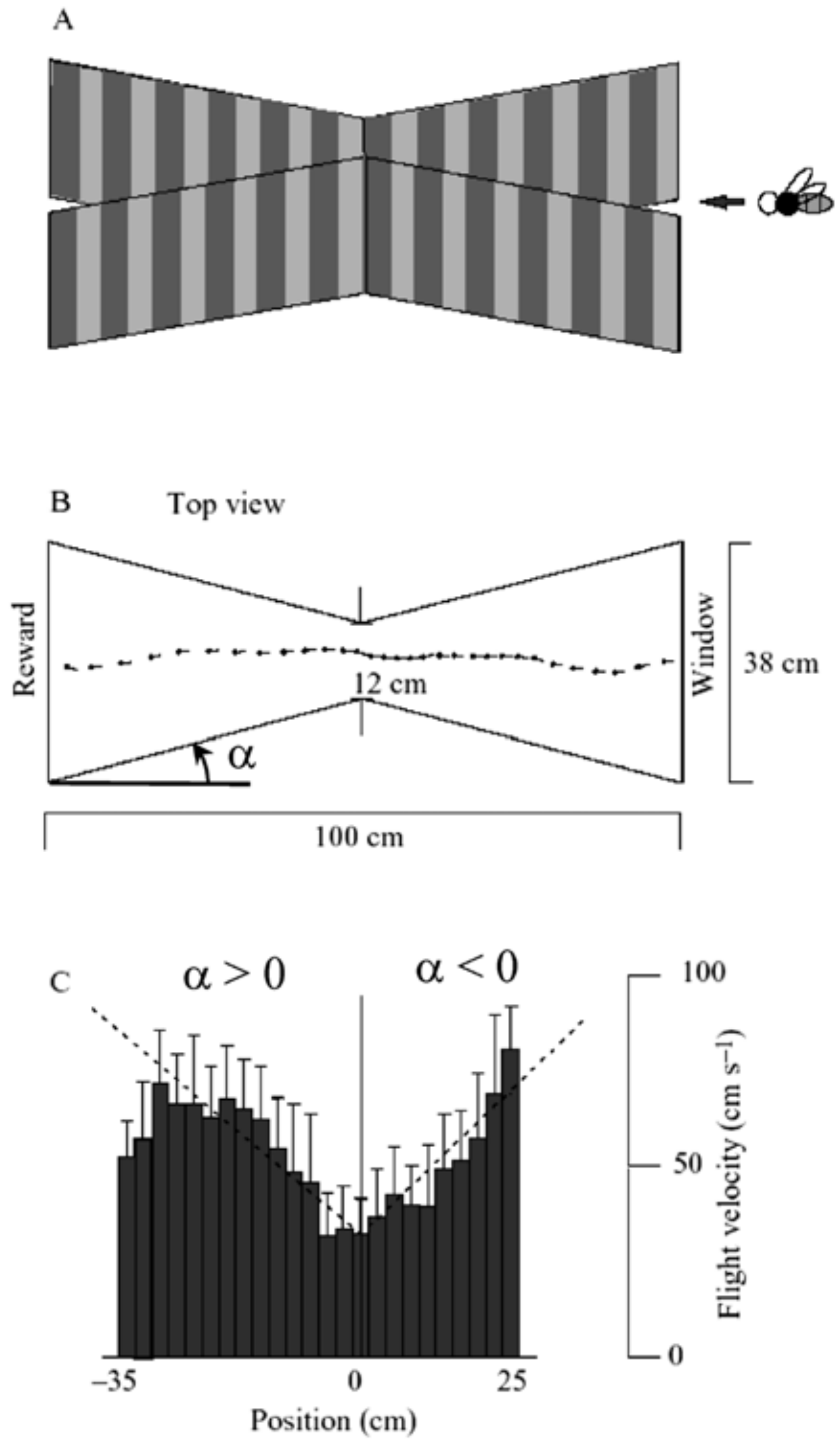

Observation:

« Bees tend to keep their flight speed proportional to the corridor width »

Conclusion:

« The speed of flight is controlled by regulating the image velocity »

Srinivasan et al. (1996)

LORA III: Forward control loop+Side control loop

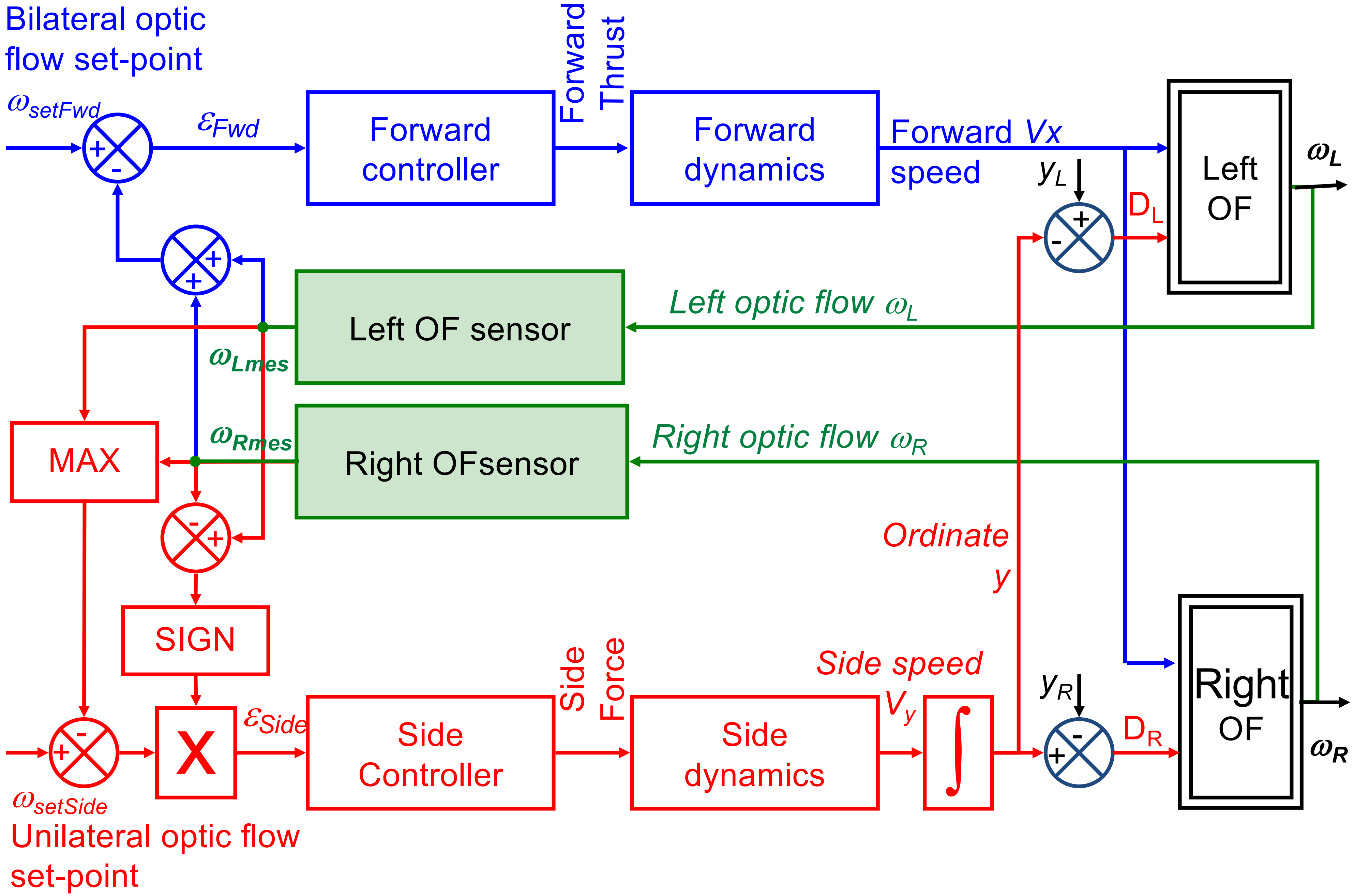

Roubieu et al. (2014) *Bioinspir. Biomim.*

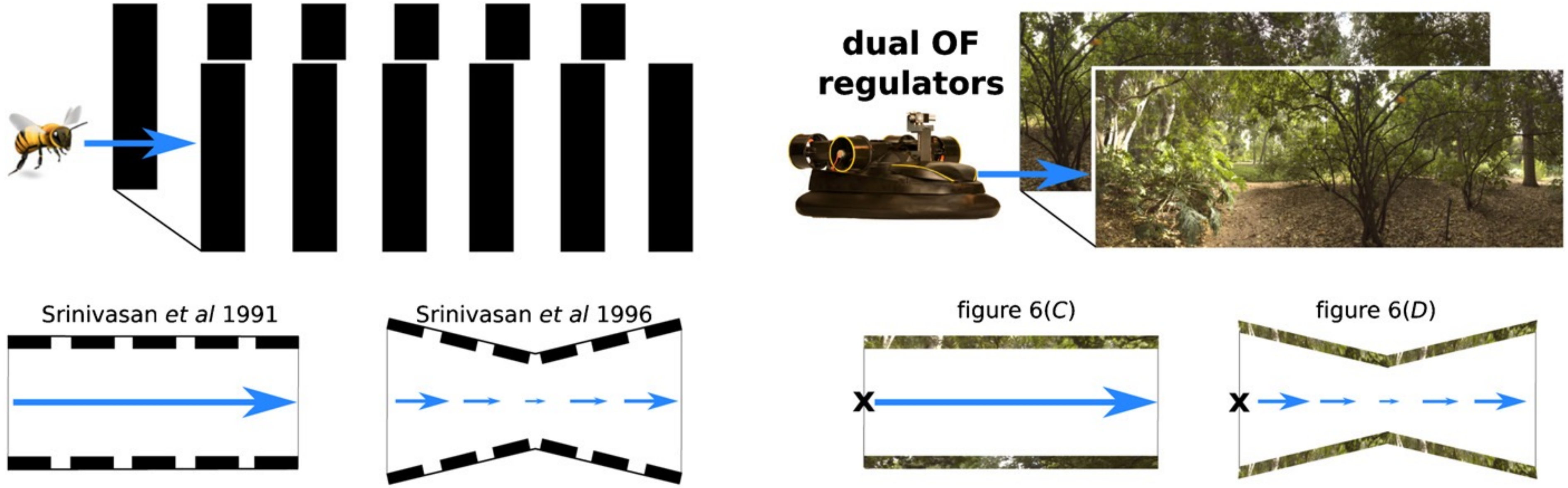

Roubieu et al. (2014) *Bioinspir. Biomim.*

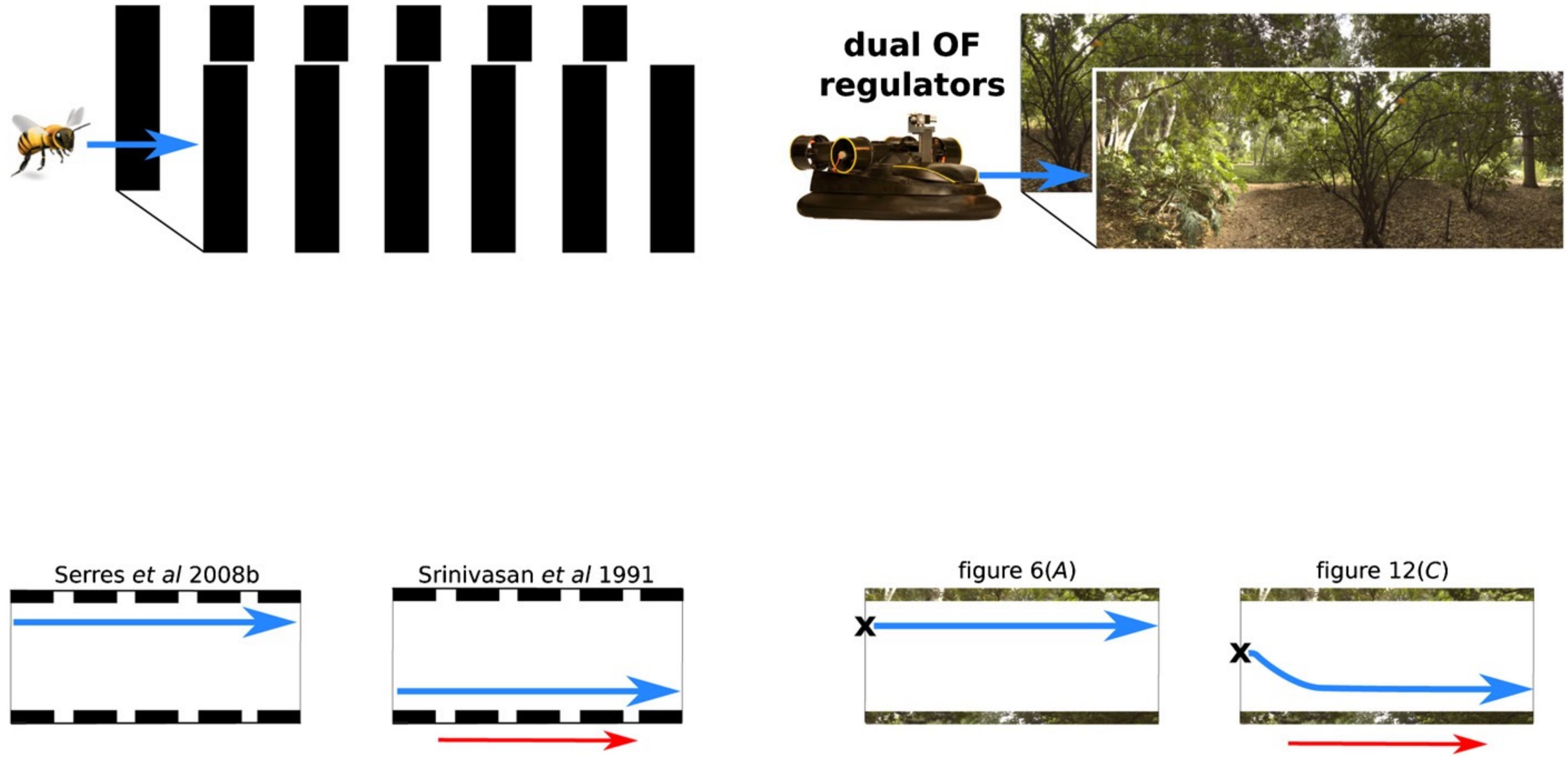

Roubieu et al. (2014) *Bioinspir. Biomim.*

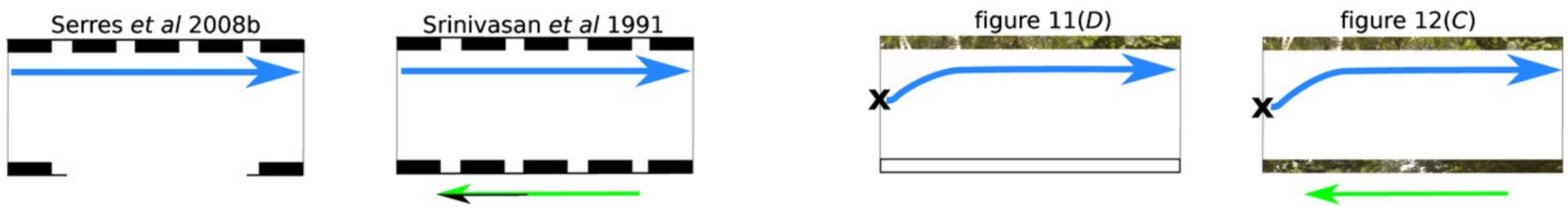

Roubieu et al. (2014) *Bioinspir. Biomim.*

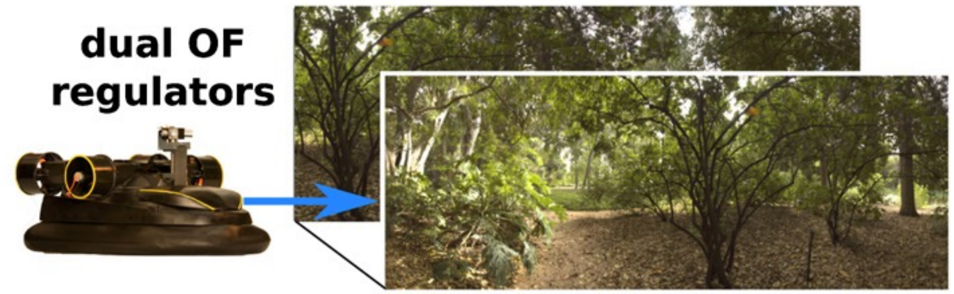
dual OF
regulators

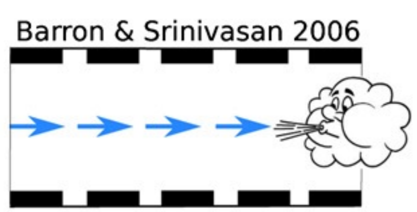
Barron & Srinivasan 2006

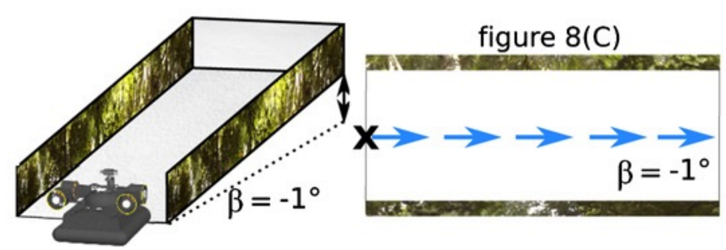
β = -1°
figure 8(C)
X
β = -1°

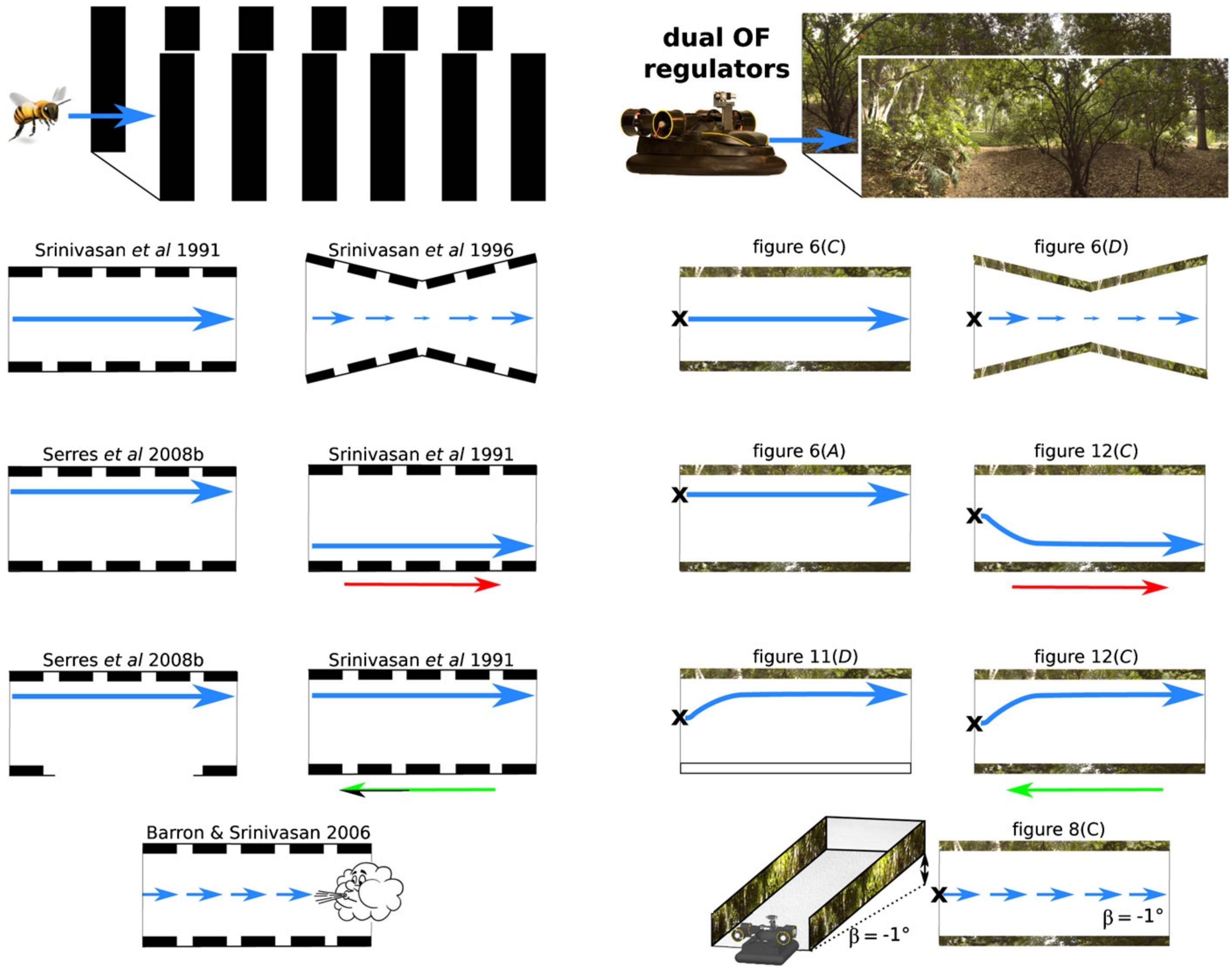
dual OF
regulators
Srinivasan et al 1991
Srinivasan et al 1996
figure 6(C)
figure 6(D)
Serres et al 2008b
Srinivasan et al 1991
figure 6(A)
figure 12(C)
Serres et al 2008b
Srinivasan et al 1991
figure 11(D)
figure 12(C)
Barron & Srinivasan 2006
figure 8(C)
β = -1°
β = -1°

Beerotor robot

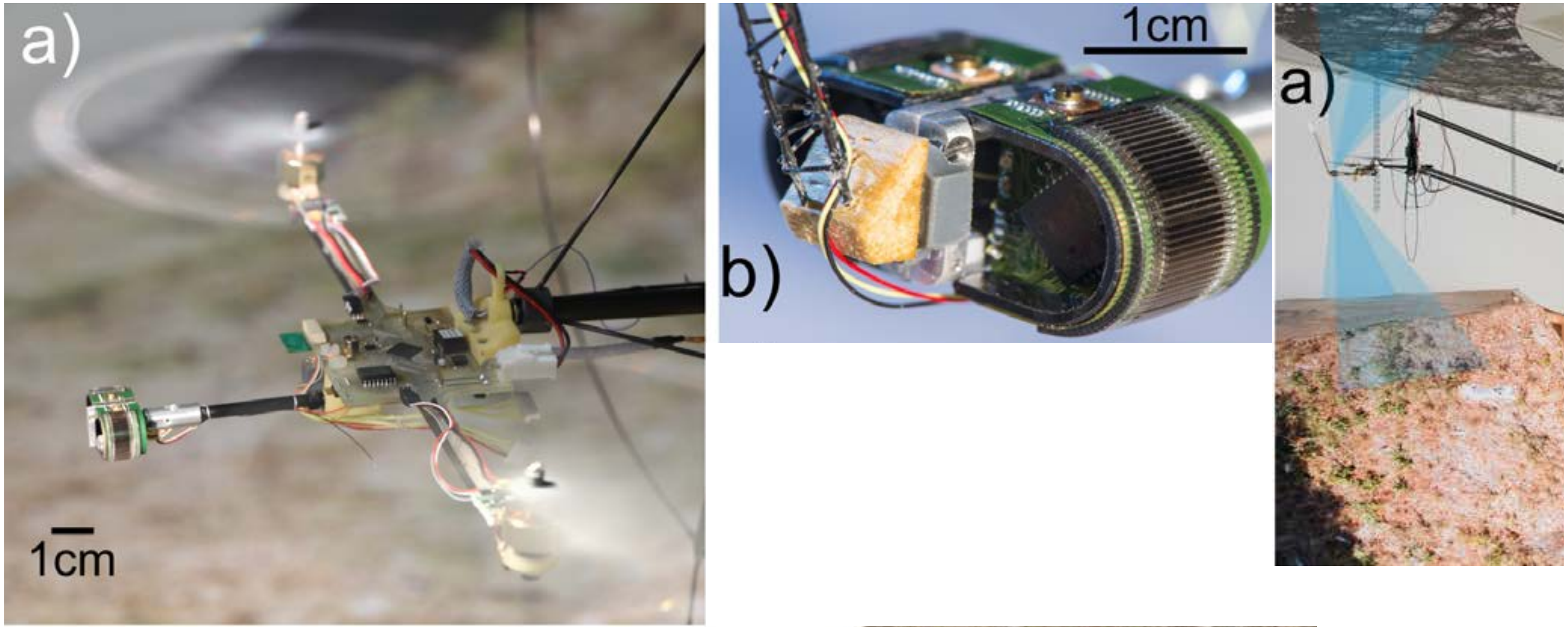

Expert, Ruffier (2015) *Bioinsp & Biomim*

Beerotor: Flying over uneven moving terrain based on optic-flow cues

3 degrees-of-freedom aerial robot

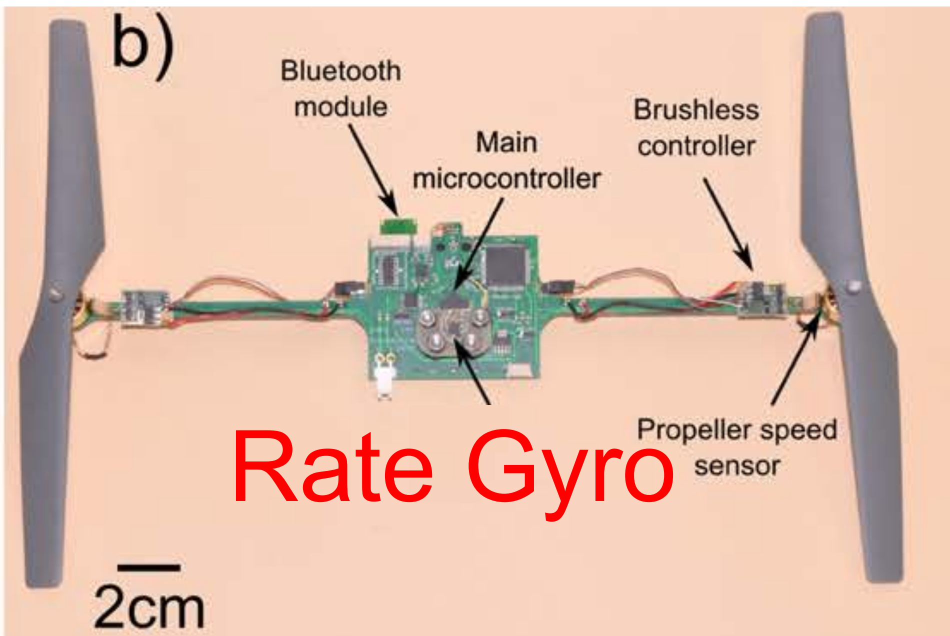

without using the inertial reference frame or accelerometer

Expert, Ruffier (2015) *Bioinsp & Biomim*

1st control law:

To regulate the maximum optic flow (ventral or dorsal)

=> by acting upon the rotors' speed

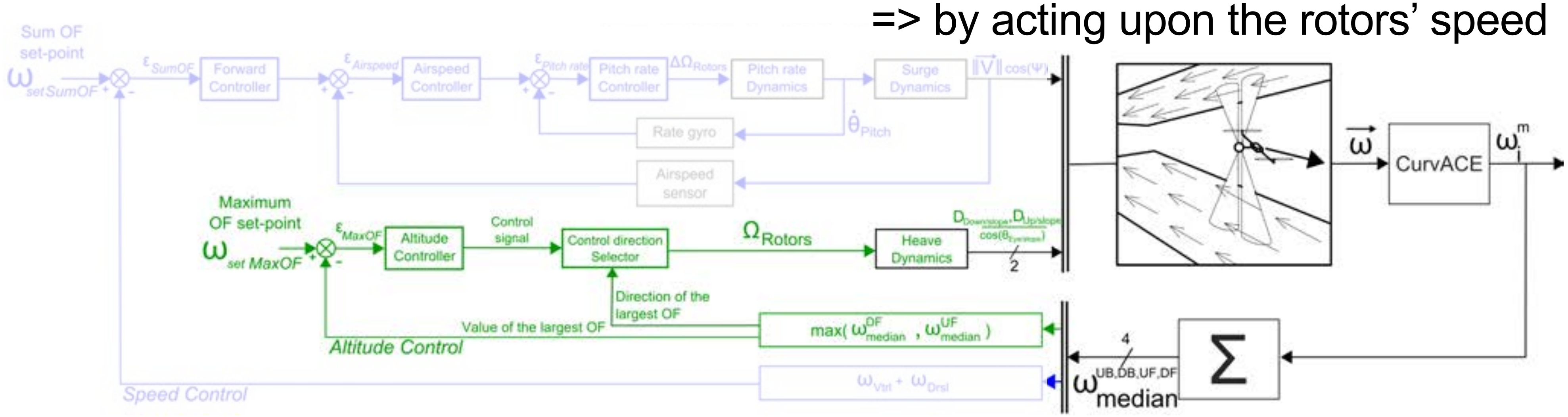

Expert, Ruffier (2015) *Bioinsp & Biomim*

2nd control law:

To regulate the sum of ventral + dorsal optic flow

=> by acting upon the rotors differentially

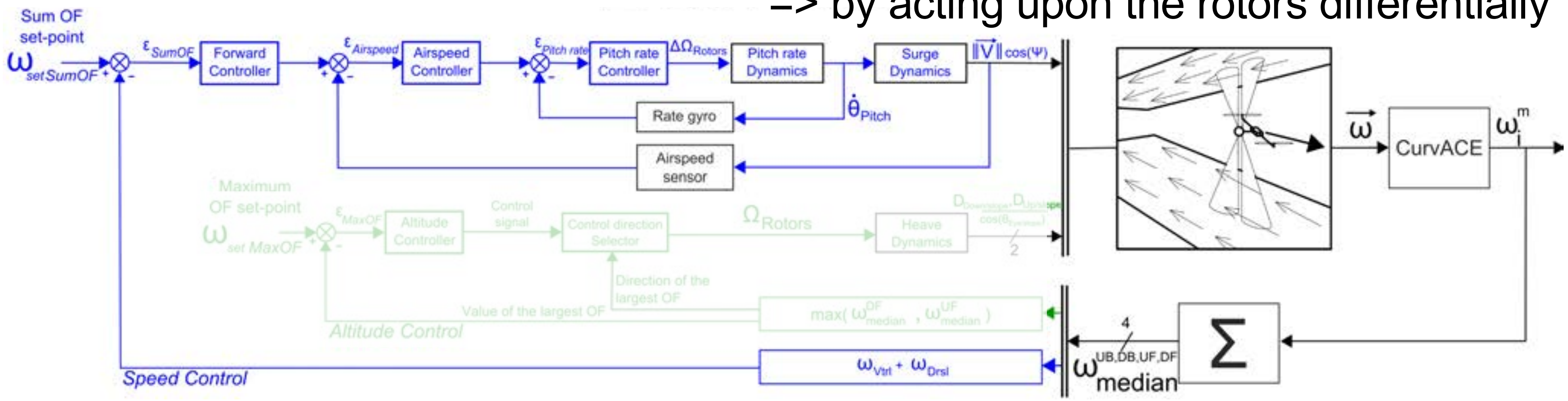

Expert, Ruffier (2015) *Bioinsp & Biomim*

3^{rd} *Beerotor* control law

- Do not orient the drone's body in relation to the earth's reference frame

- But orient its decoupled eye parallel to the slope of the ground overflown

A motor decoupling eye rotation from body rotation

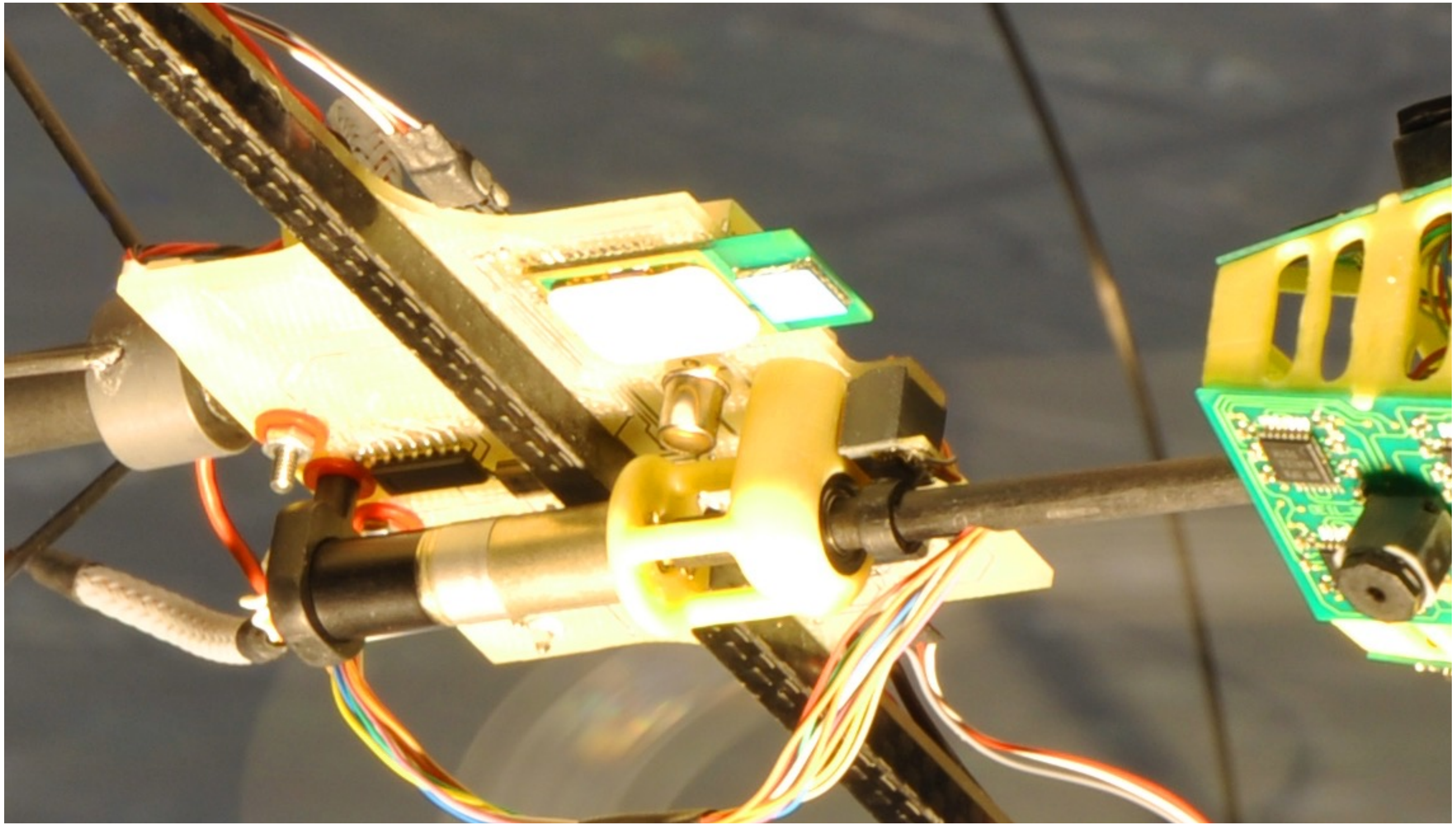

=> The idea is to reorient the eye during the flight

Without eye reorientation, the OF depends on the angle between the eye and the slope which causes the crash

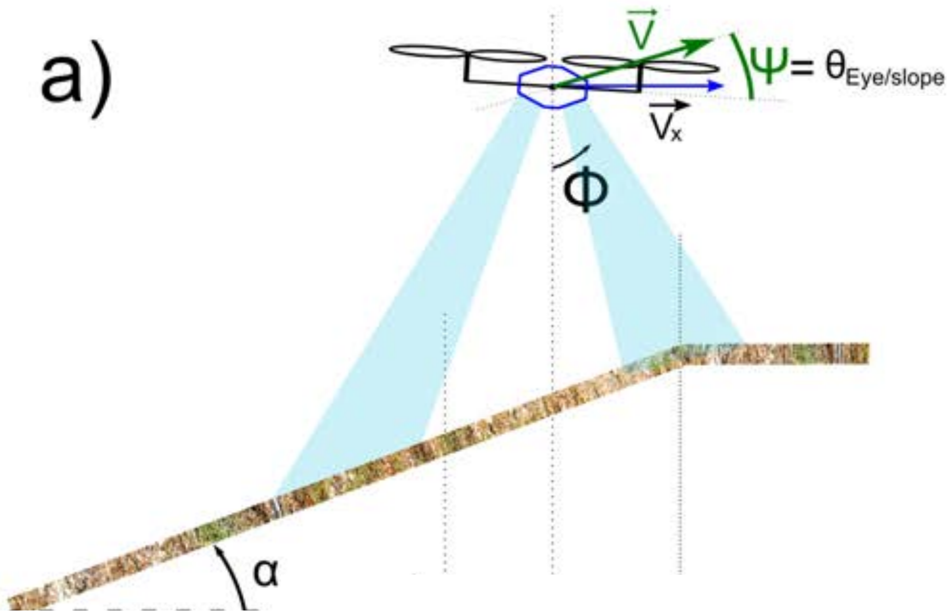

Without eye reorientation, the OF depends on the angle between the eye and the slope which causes the crash

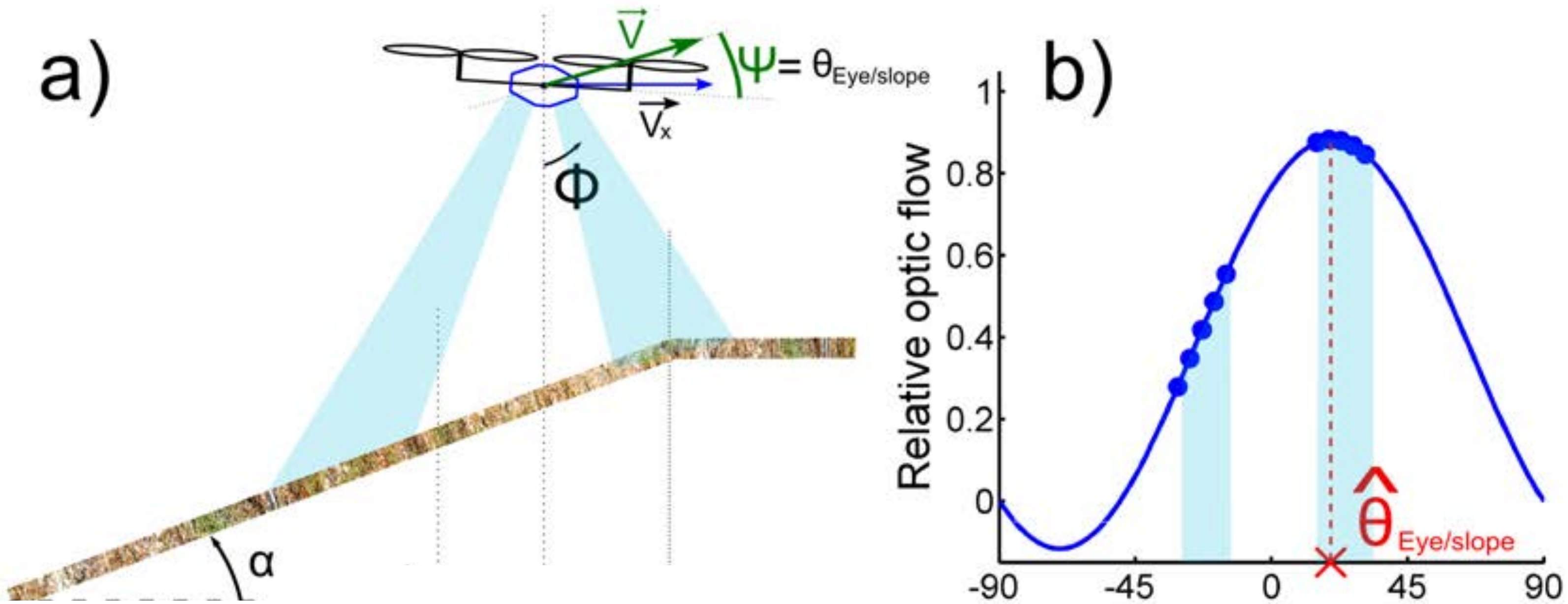

3rd control law:

To orient the OF sinus profile toward surface below

=> by acting upon the eye's pitch

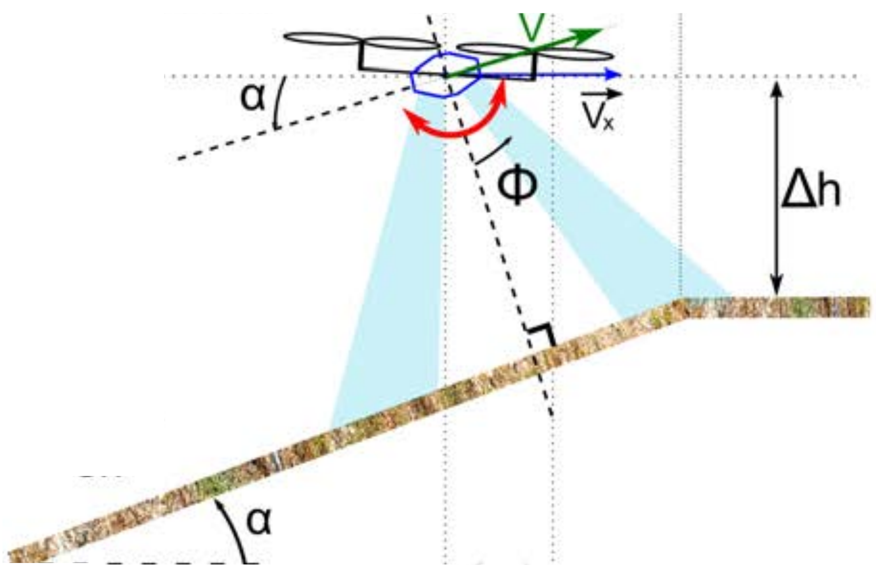

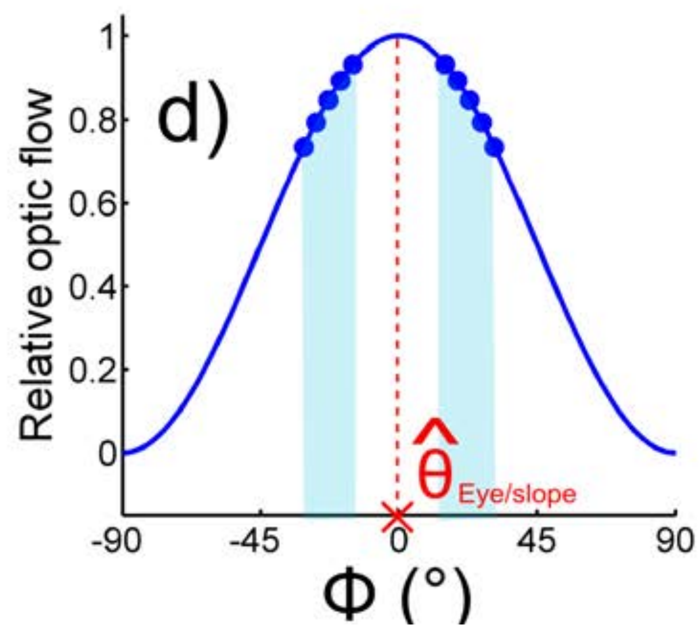

3rd control law:

To orient the OF sinus profile toward surface below

=> by acting upon the eye's pitch

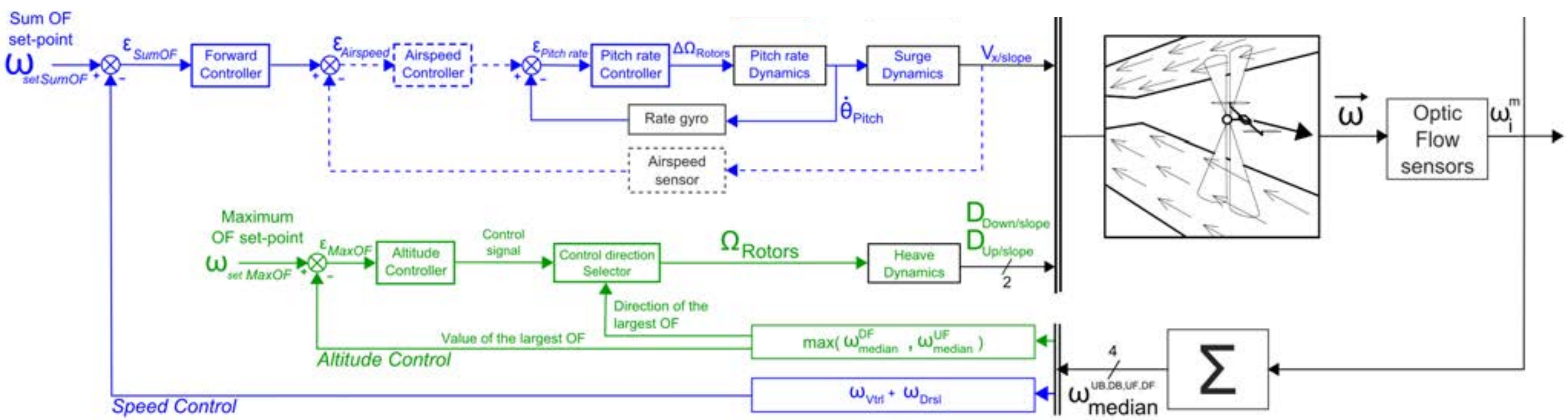

Expert, Ruffier (2015) *Bioinsp & Biomim*

3rd control law:

To orient the OF sinus profile toward surface below

=> by acting upon the eye's pitch

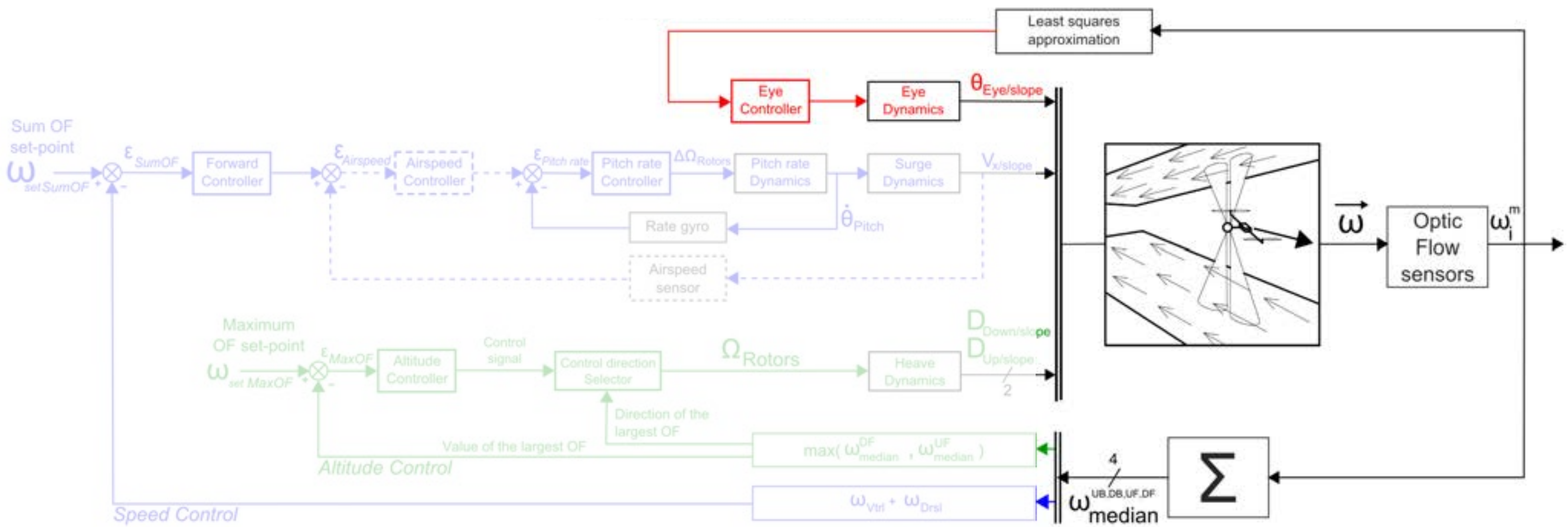

Expert, Ruffier (2015) *Bioinsp & Biomim*

Automatic landing without airspeed sensor

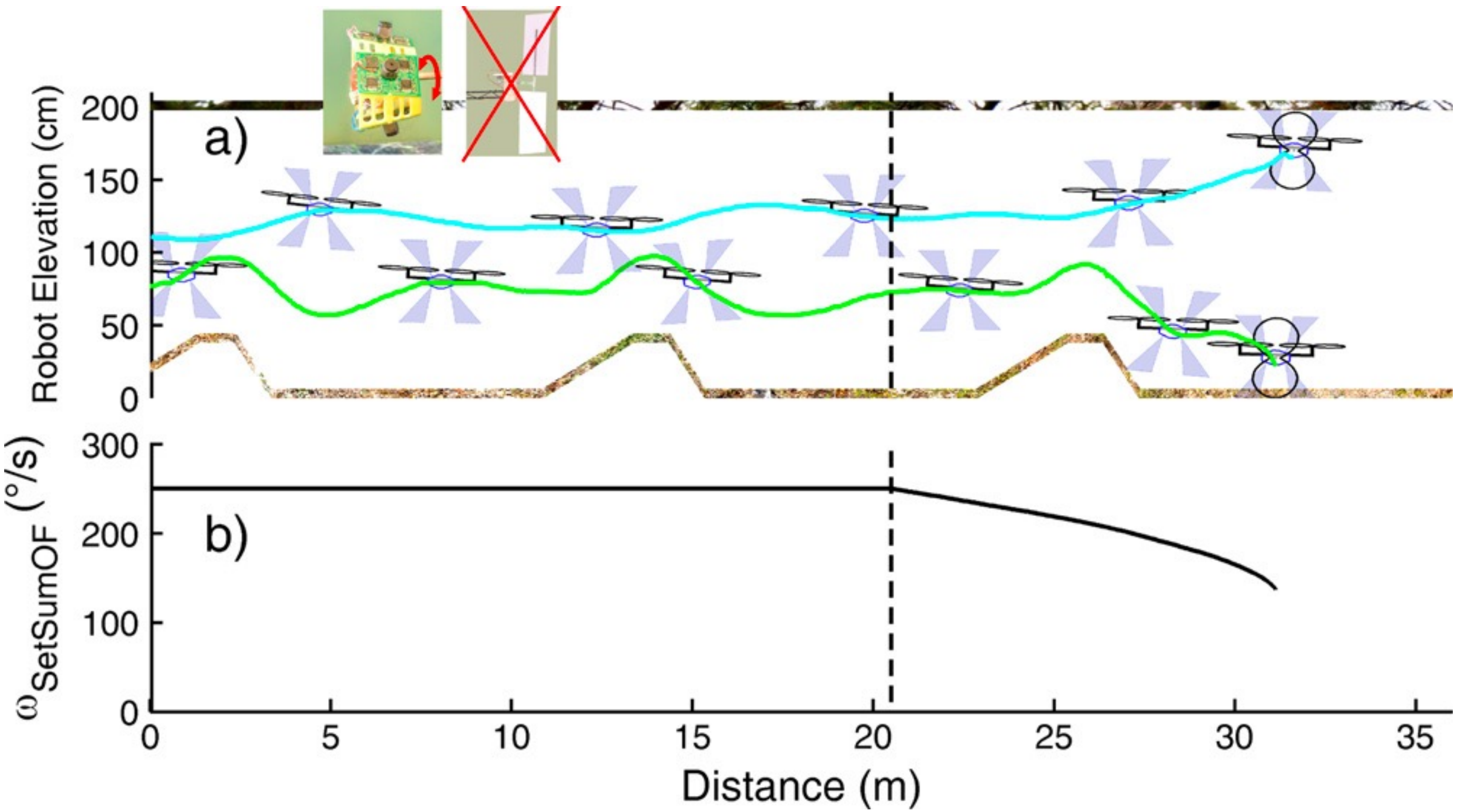

II. Enriching the optic flow with oscillations for state estimation

2 principles : SoFIa, *Embracing wobbles*

Insects oscillations

- Flying insects’ attitude wobbles
- Flying insects’ ups & downs

The up and down oscillations are enriching the optical flow vector field

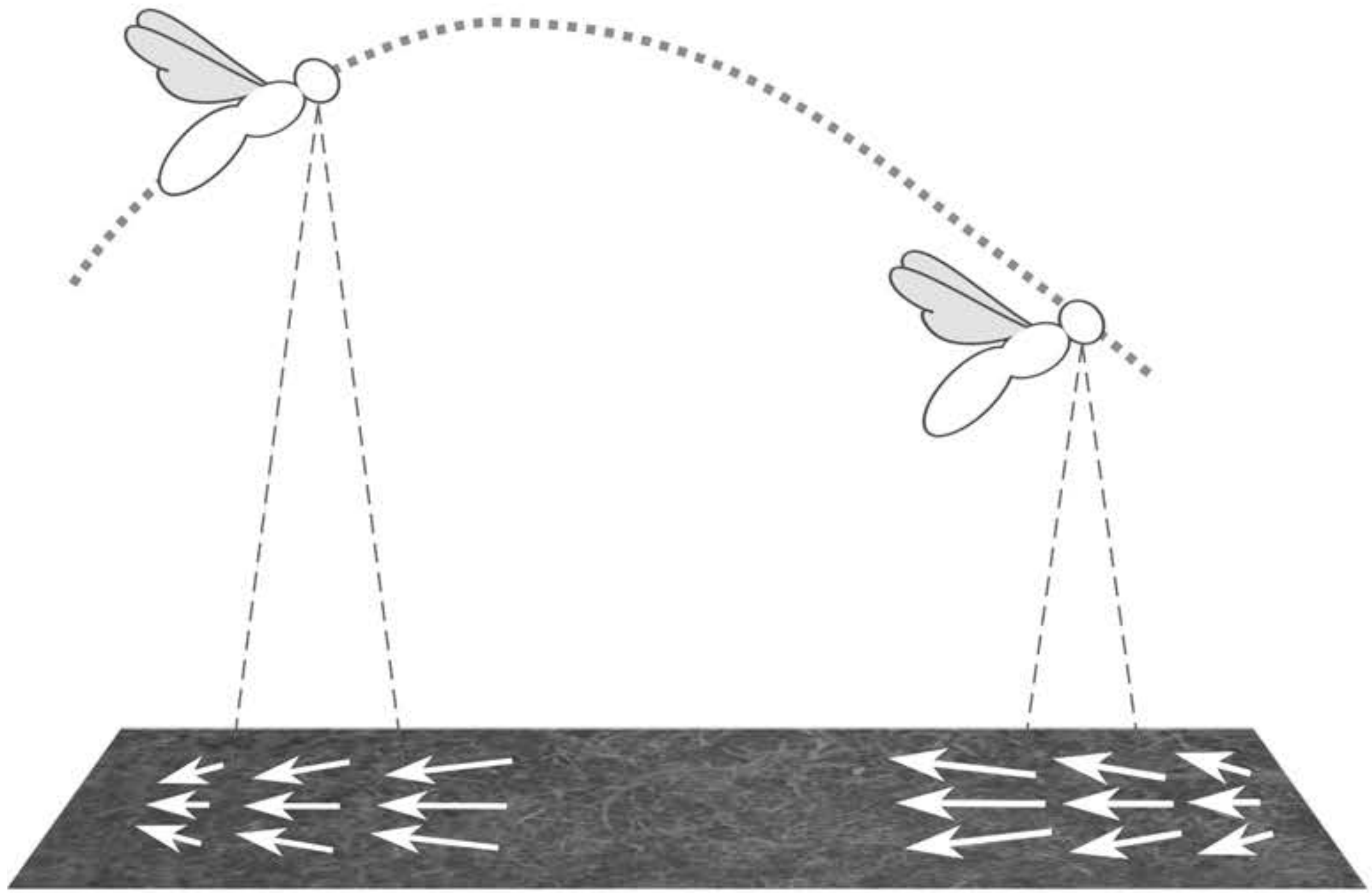

Modifed from Bergantin et al. (2021) *Interface*

Honeybees perceive their distance travelled using OF

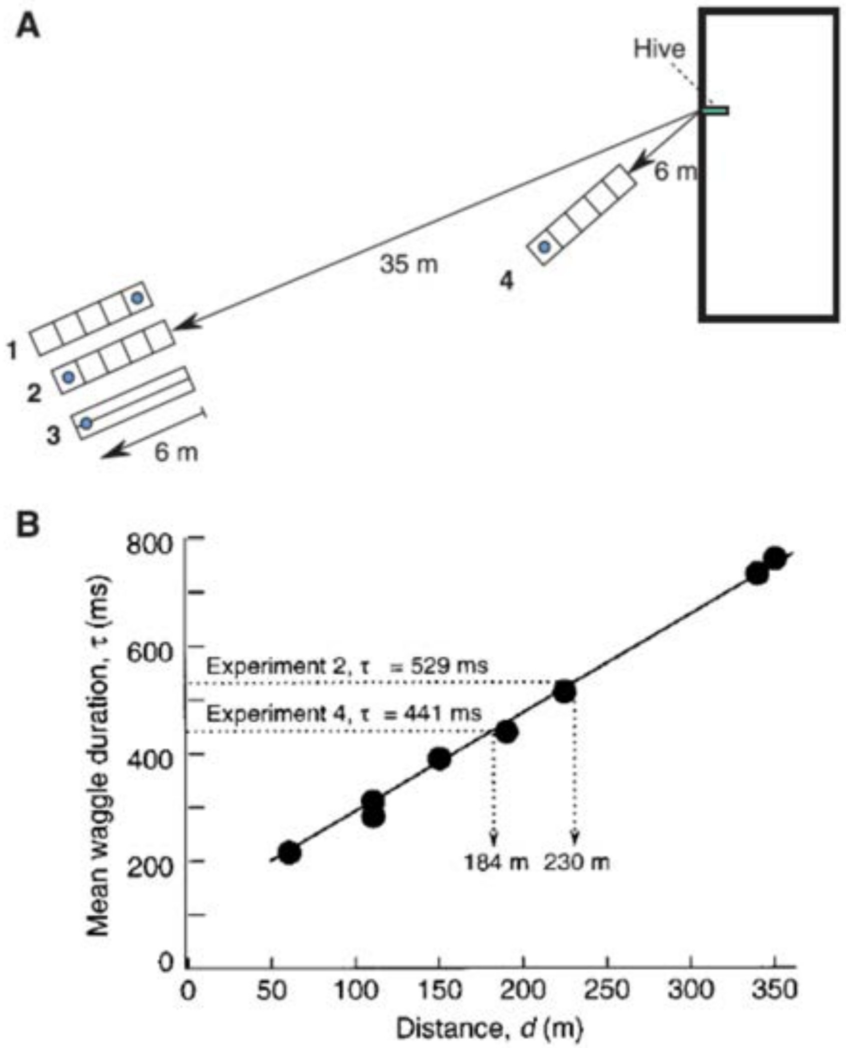

[Srinivasan et al., 2000]

Measuring the distance travelled

In the literature: accumulation of raw translational optic flow ω_T (*OFacc* model)

$$OFacc = \int \omega_T \, \mathrm{d}t \quad (1)$$

n = 630 traj.

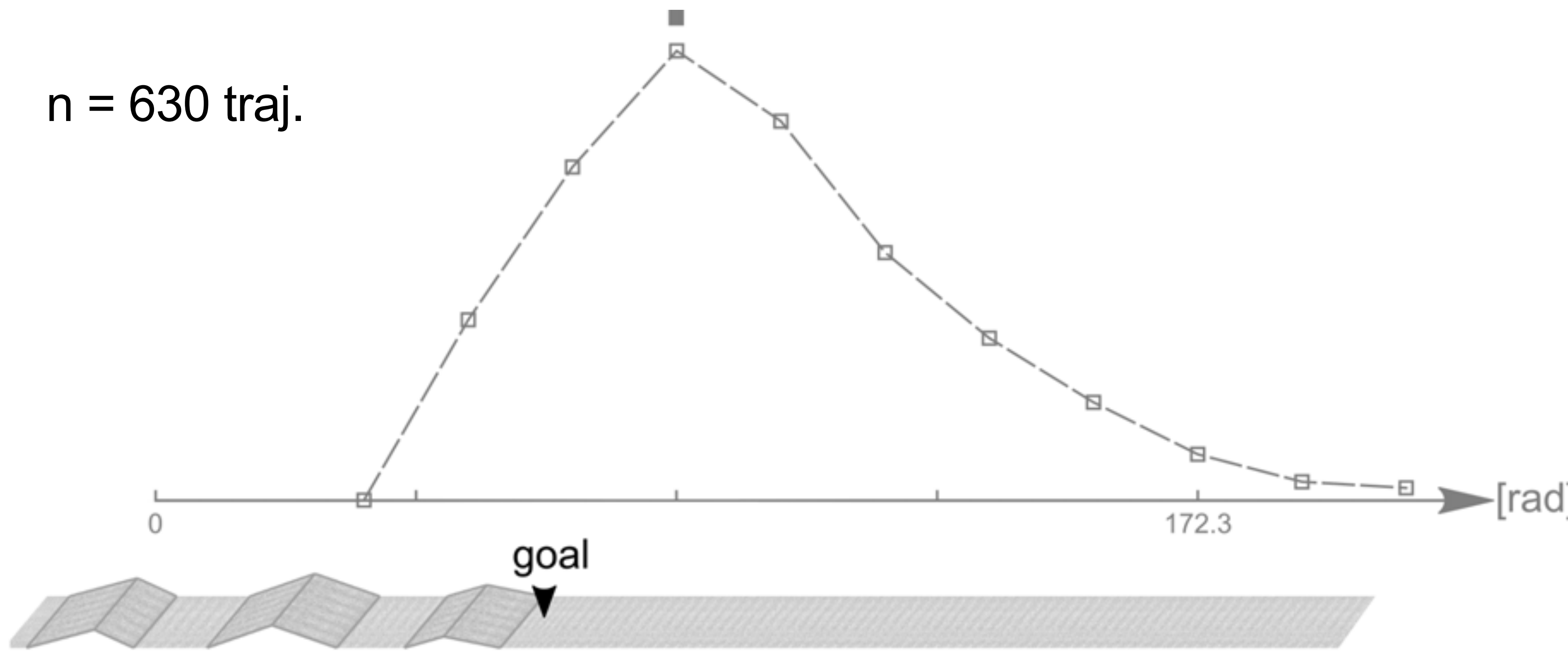

[Bergantin et al., 2021]

Oscillations in flying insects

A

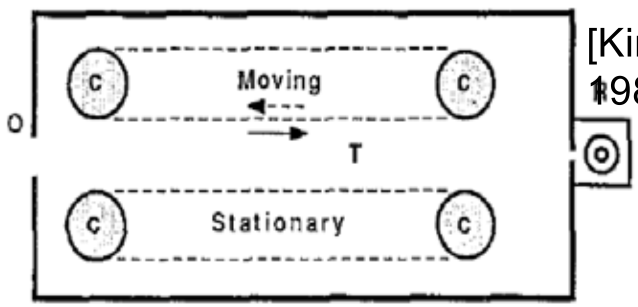

[Kirchner and Srinivasan, 1989]

B

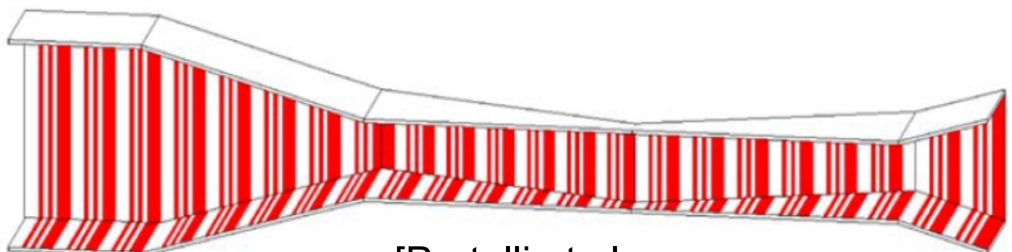

[Portelli et al., 2011]

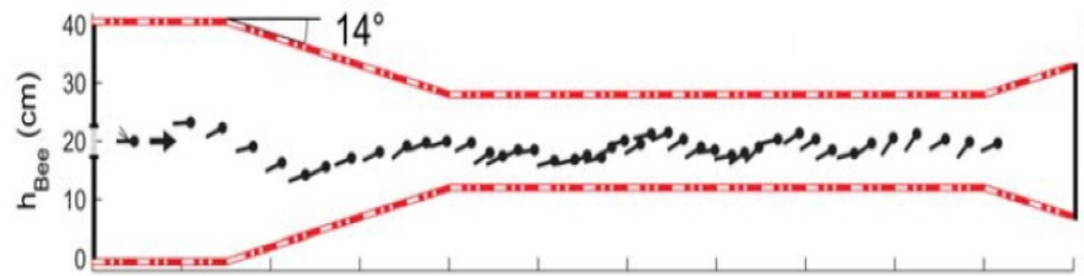

C

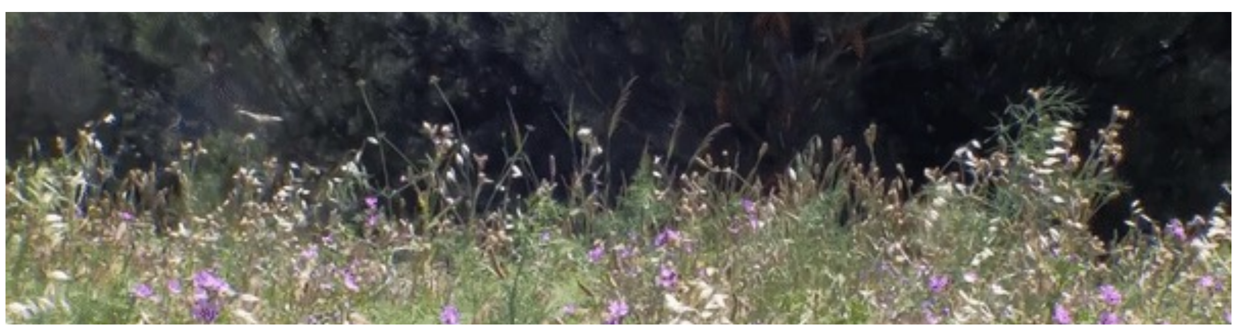

Optic flow cues

Translational optic flow:

$$\omega_T^{th} = \frac{v_x}{h} \qquad (2)$$

Optic flow divergence:

$$\omega_{div}^{th} = \frac{v_h}{h} \qquad (3)$$

used to observe the state Vector [Ho et al., 2017]

$$X = [h; v_h] \qquad (4)$$

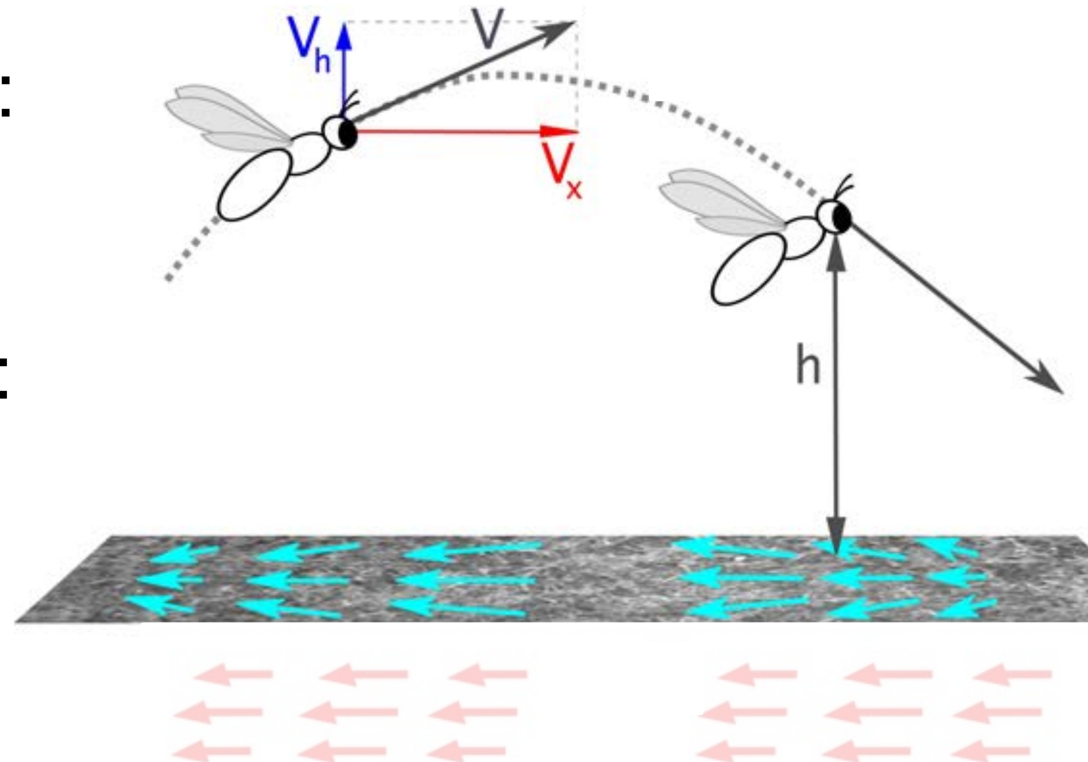

[Bergantin et al., 2021]

Optic flow cues

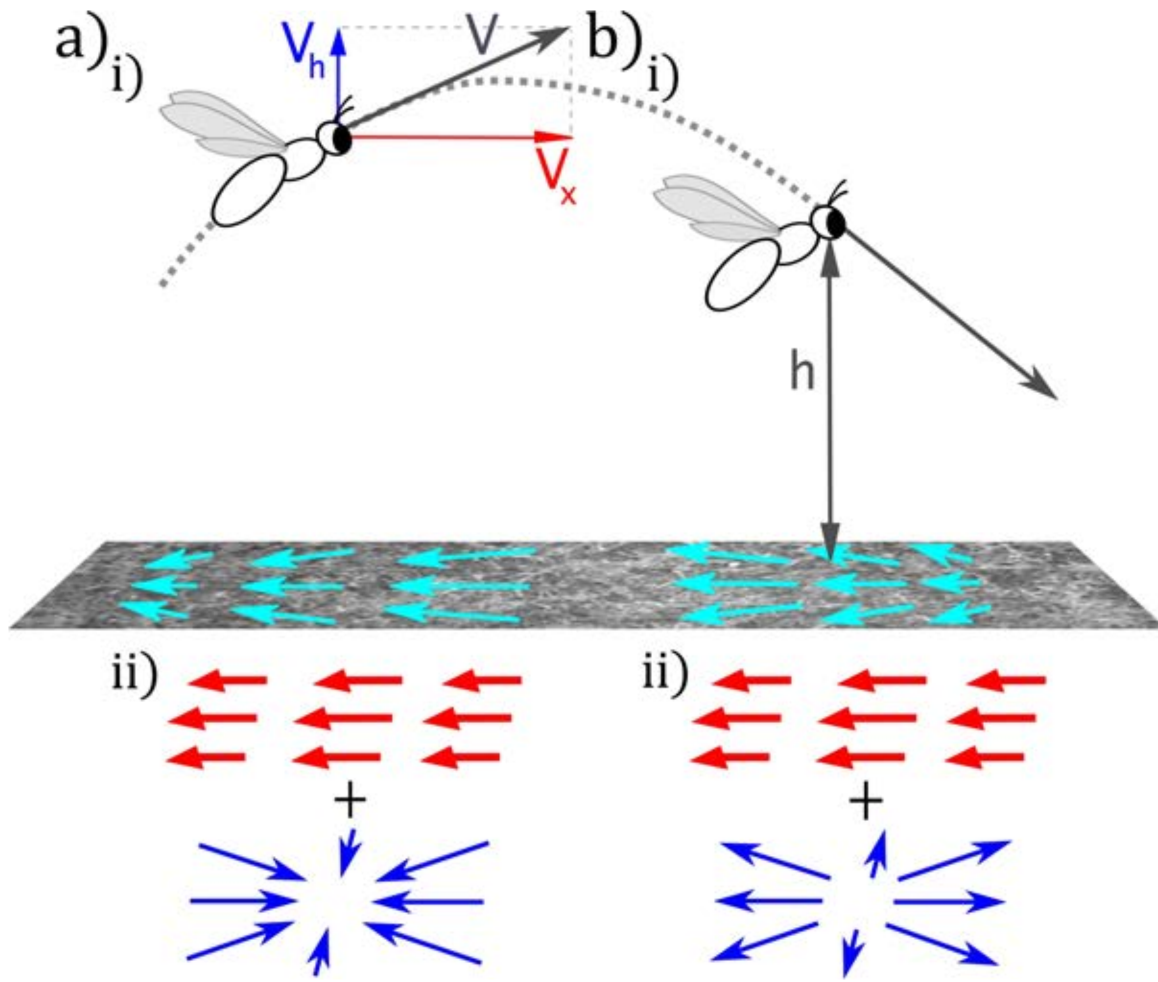

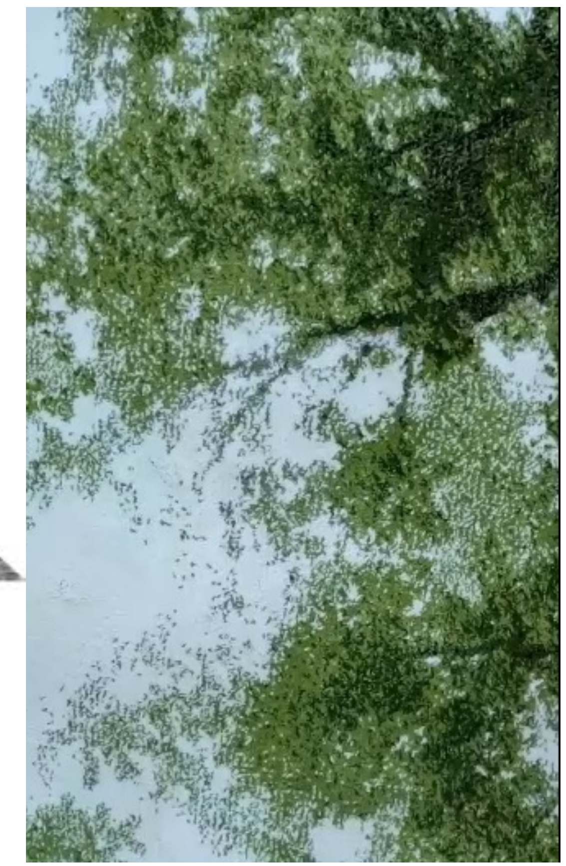

[Bergantin et al., 2021]

Observability analysis

Simplified honeybee vertical dynamics [Portelli et al., 2010]:

$$\begin{cases} \dot{h} = v_h \\ \dot{v}_h = -\dfrac{v_h}{\tau_z} + \dfrac{K_z}{\tau_z}\Delta\Phi \\ \omega_{div} = \dfrac{v_h}{h} \end{cases} \quad (5) \longrightarrow \begin{cases} \dot{x}(t) = f\big(x(t), \Delta\Phi(t)\big) = \begin{bmatrix} \dot{h}(t) \\ \dot{v}_h(t) \end{bmatrix} = \begin{bmatrix} 0 & 1 \\ 0 & -\dfrac{1}{\tau_z} \end{bmatrix} \begin{bmatrix} h \\ v_h \end{bmatrix} + \begin{bmatrix} 0 \\ \dfrac{K_z}{\tau_z} \end{bmatrix} \Delta\Phi \\ y(t) = g\big(x(t)\big) = \dfrac{v_h}{h} = \dfrac{\dot{h}}{h} = \omega_{div} \end{cases} \quad (6)$$

Observability matrix:

$$O = \begin{bmatrix} L_f^0\big(g(x(t))\big) \\ L_f^1\big(g(x(t))\big) \end{bmatrix} \longrightarrow$$

Locally observable if
$u \neq 0, h \neq 0, v_h \neq 0$
as in [Ho et al., 2017]

[Bergantin et al., 2021]

SOFIa Simulations

- Self-oscillations [Kirchner and Srinivasan, 1989; Portelli et al., 2011]
- Honeybee dynamics [Portelli et al., 2010]
- Neurons sensitive to translational optic flow [Ibbotson, 1991; Stone et al., 2017]
- Neurons sensitive to optic flow divergence [Bidwell and Goodman, 1993]
- Optic flow regulator [Franceschini et al., 2007]

$$\begin{cases}\dot{x}(t) = f\big(x(t),\Delta\Phi(t)\big) = \begin{bmatrix}\dot{h}(t)\\ \dot{v}_h(t)\end{bmatrix} = \begin{bmatrix}0 & 1\\ 0 & -\frac{1}{\tau_z}\end{bmatrix}\begin{bmatrix}h\\ v_h\end{bmatrix} + \begin{bmatrix}0\\ \frac{K_z}{\tau_z}\end{bmatrix}\Delta\Phi \\ y(t) = g\big(x(t)\big) = \frac{v_h}{h} = \frac{\dot{h}}{h} = \omega_{div}\end{cases} \qquad (6)$$

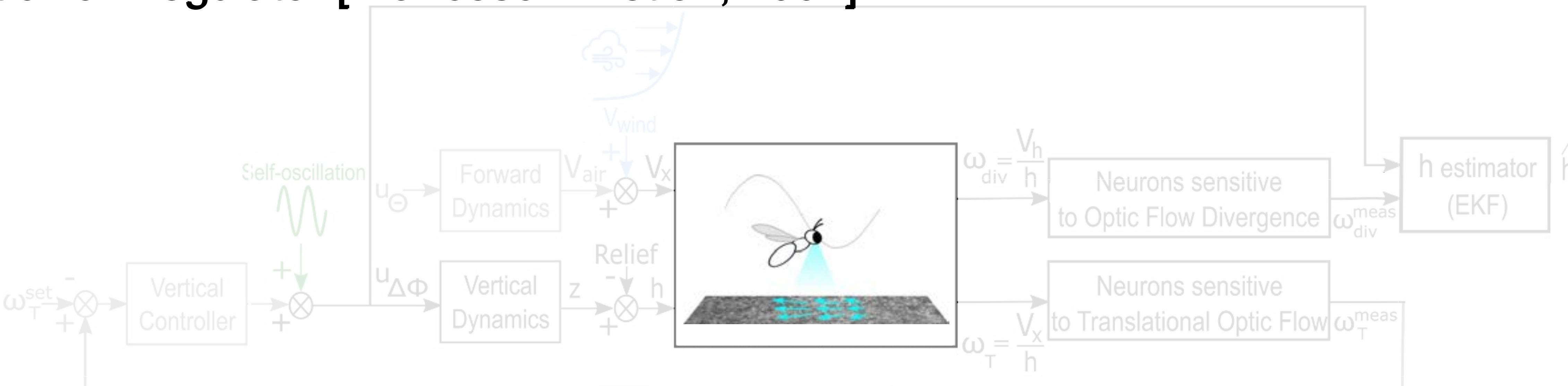

[Bergantin et al., 2021]

SOFIa Simulations

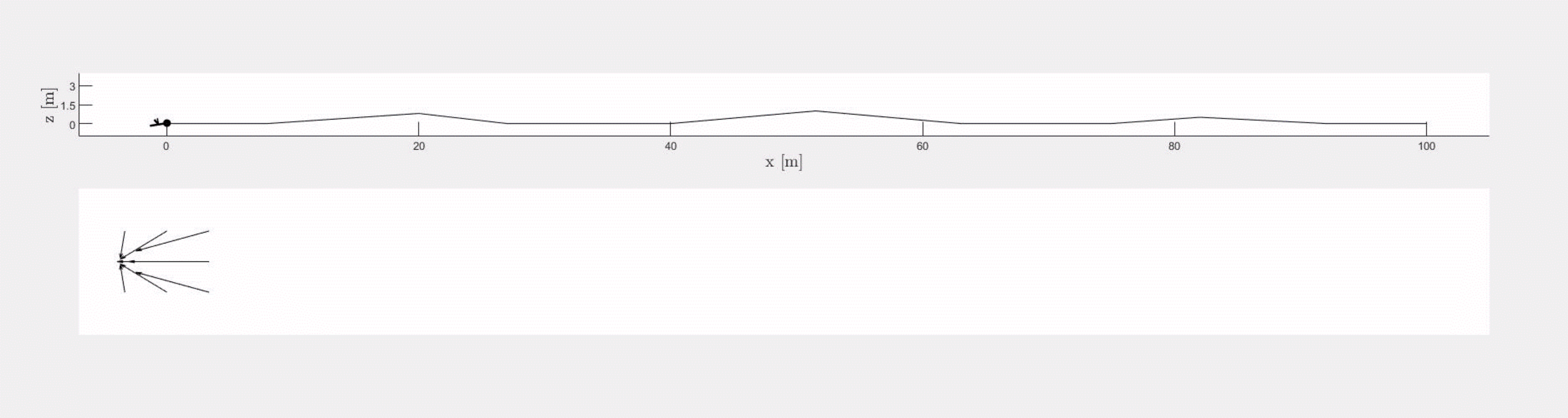

Estimation of the ground height

Estimation of the ground height with an **Extended Kalman Filter** (EKF)

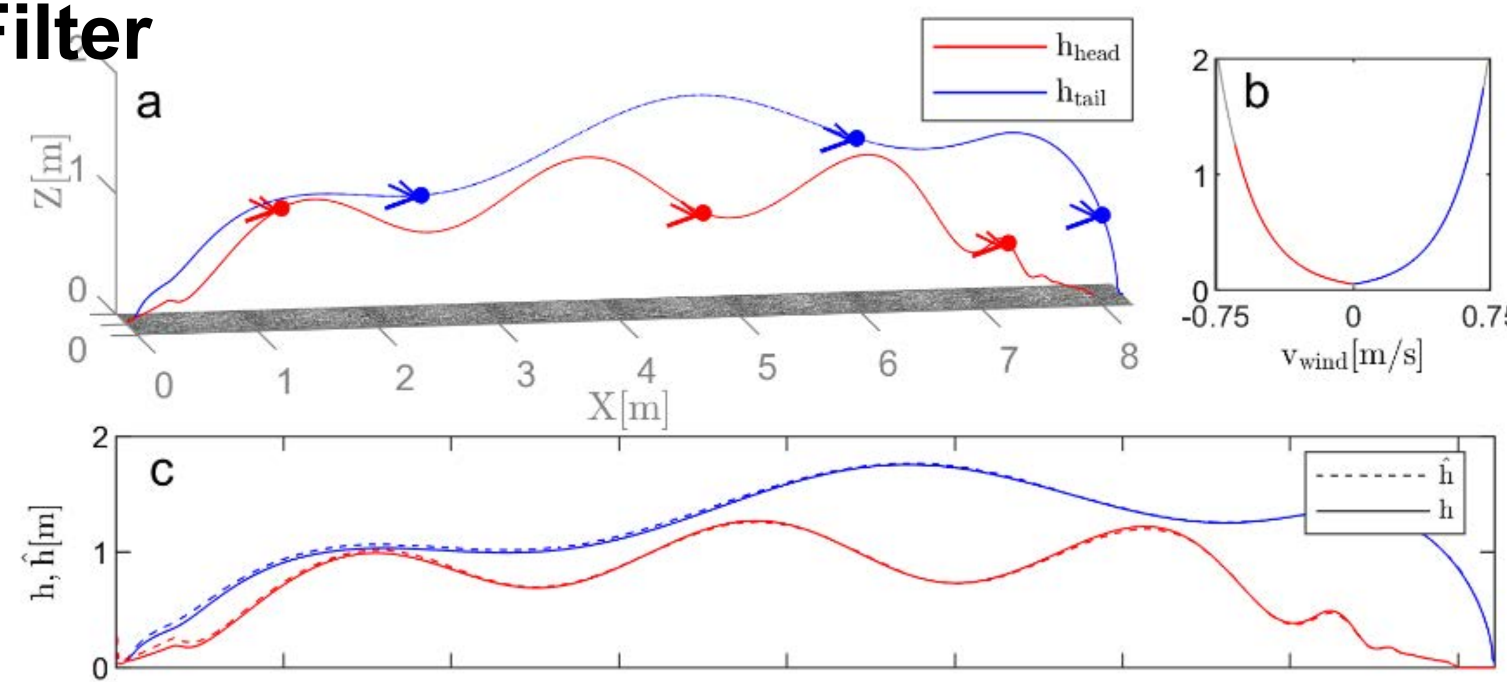

→ $\hat{h}$ can be used as a scaling factor

[Bergantin et al., 2021]

The *SOFIa* odometer model

(Self-scaled Optic Flow Integration)

$$\hat{X}_{SOFIa} = \int \omega_T^{meas} \cdot \hat{h}\, \mathrm{d}t \qquad (8)$$

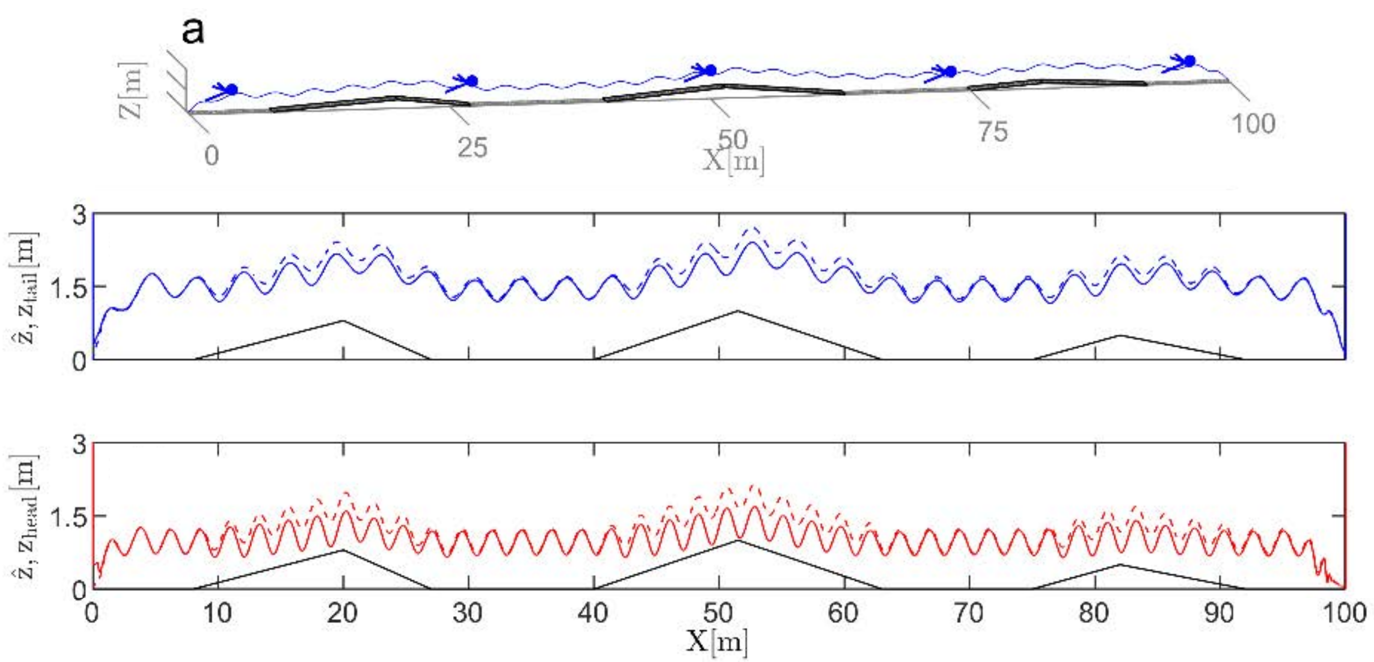

Final % error ($\widehat{\mathbf{X}}_{SOFIa} - \mathbf{X}_{\mathrm{gt}}$) odometry of example:

- 0,69% tail wind
- -1,8% head wind

[Bergantin et al., 2021]

Comparison of models

n=630

n = 630 traj.

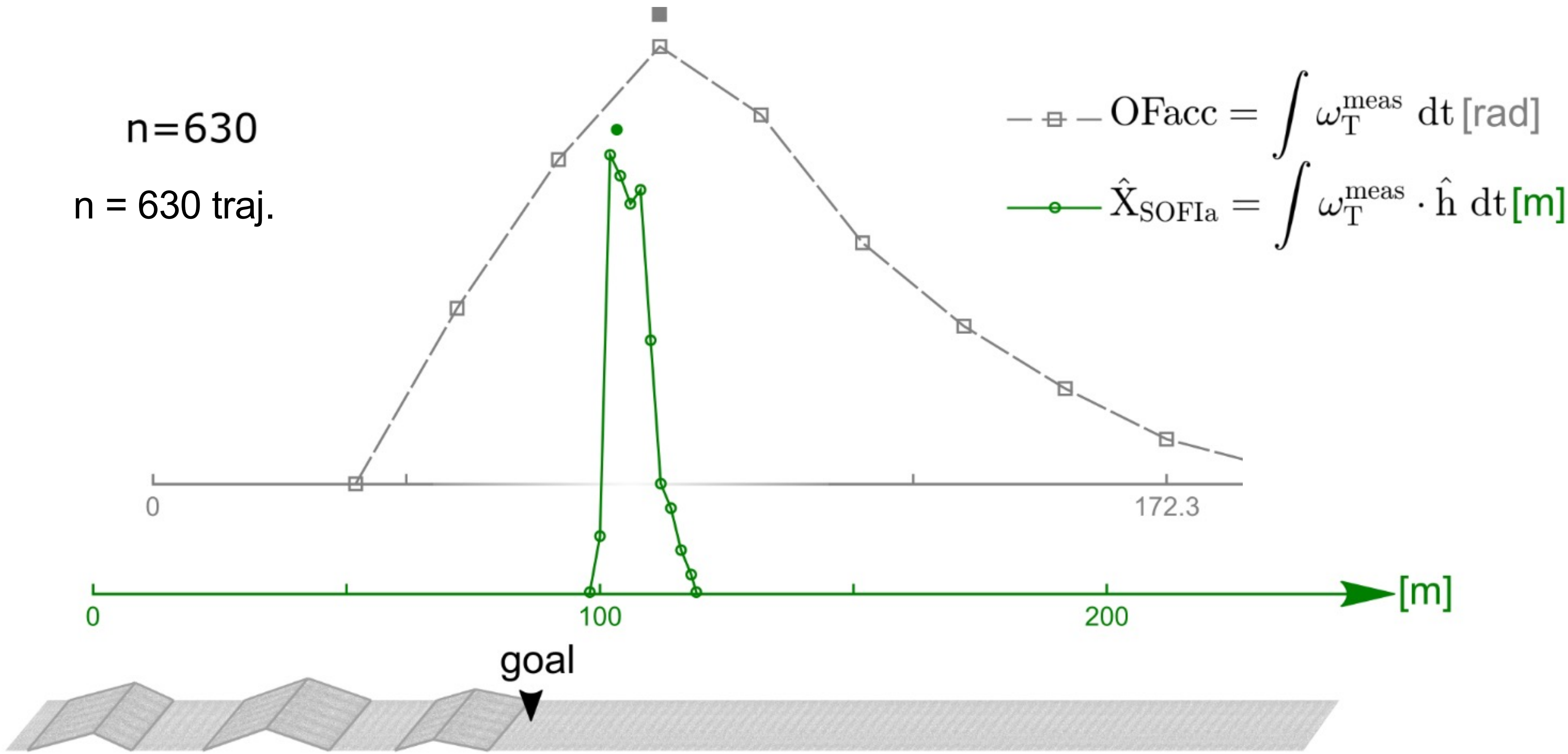

[Bergantin et al., 2021]

SOFIa results for head and tail wind

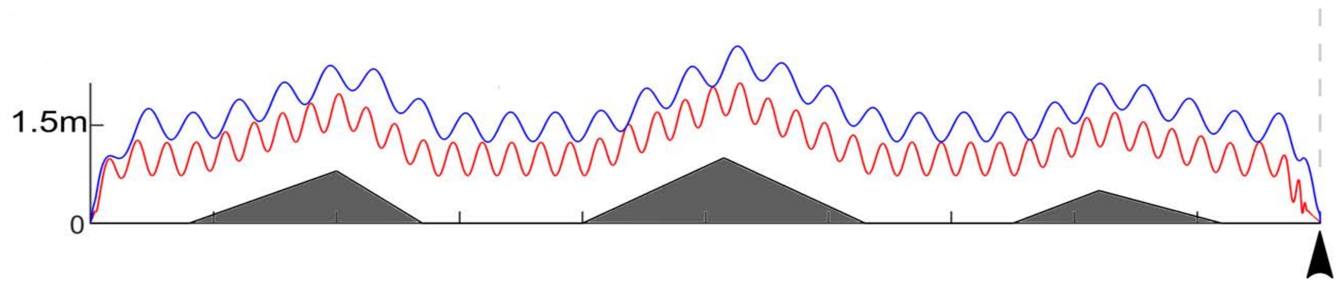

$$\hat{X}_{SOFIa} = \int \omega_T^{meas} \cdot \hat{h}\, \mathrm{d}t$$

Reliability of the odometer in different winds

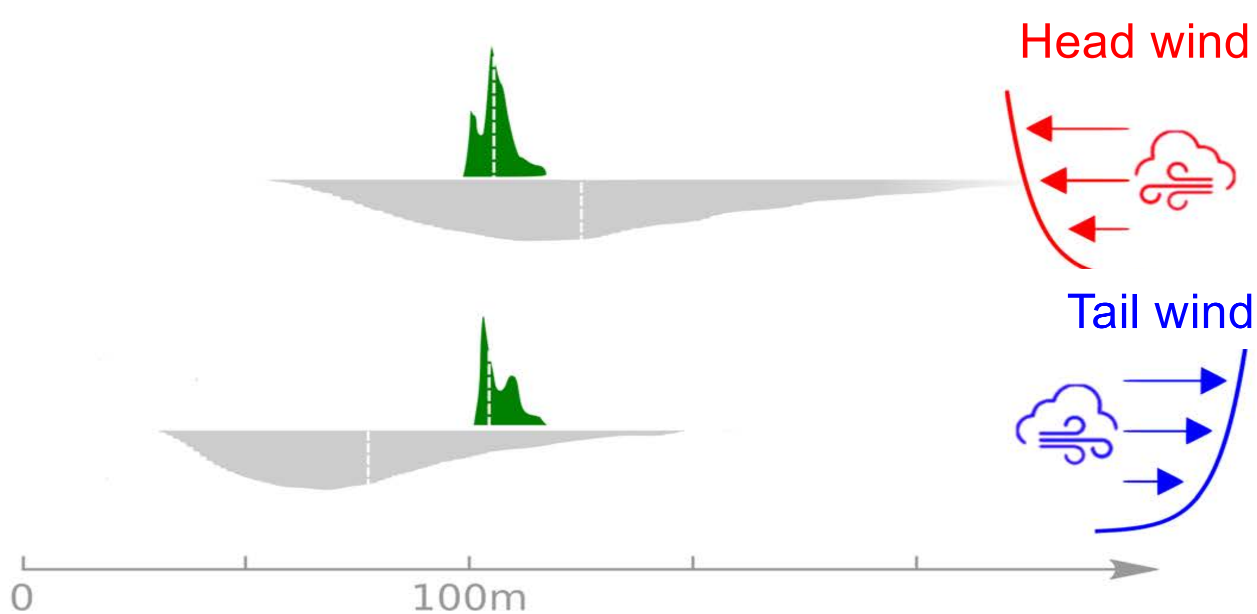

Modifed from Bergantin et al. (2021) *Interface*

Fusion strategy with 4 optic flow sensors

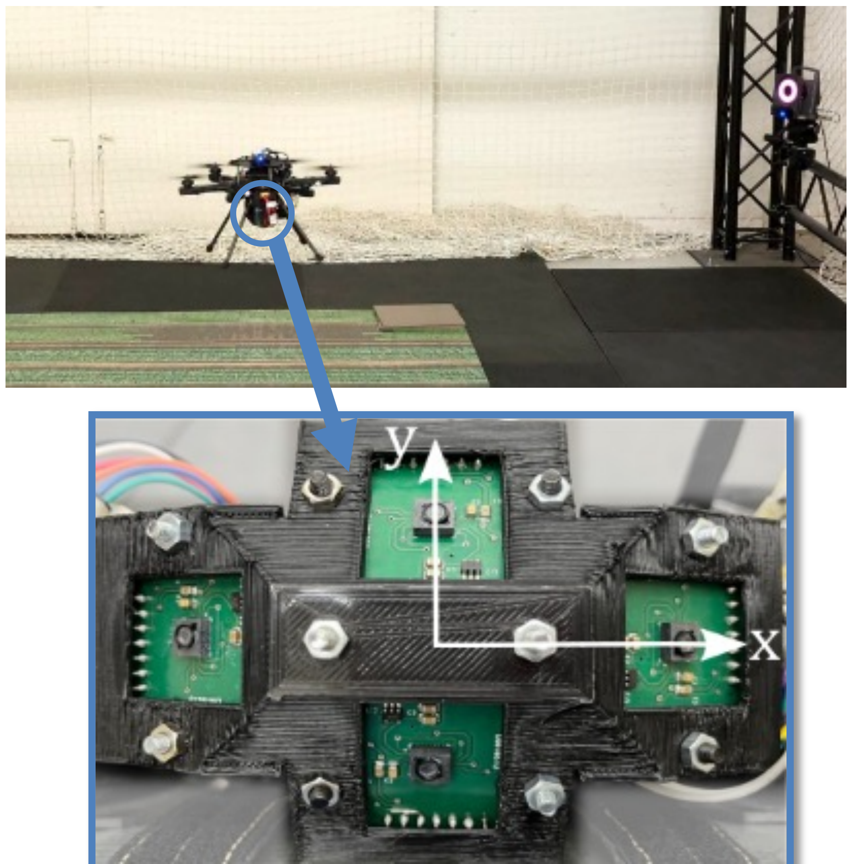

- 3 translational optic flow cues
- 2 optic flow divergence cues

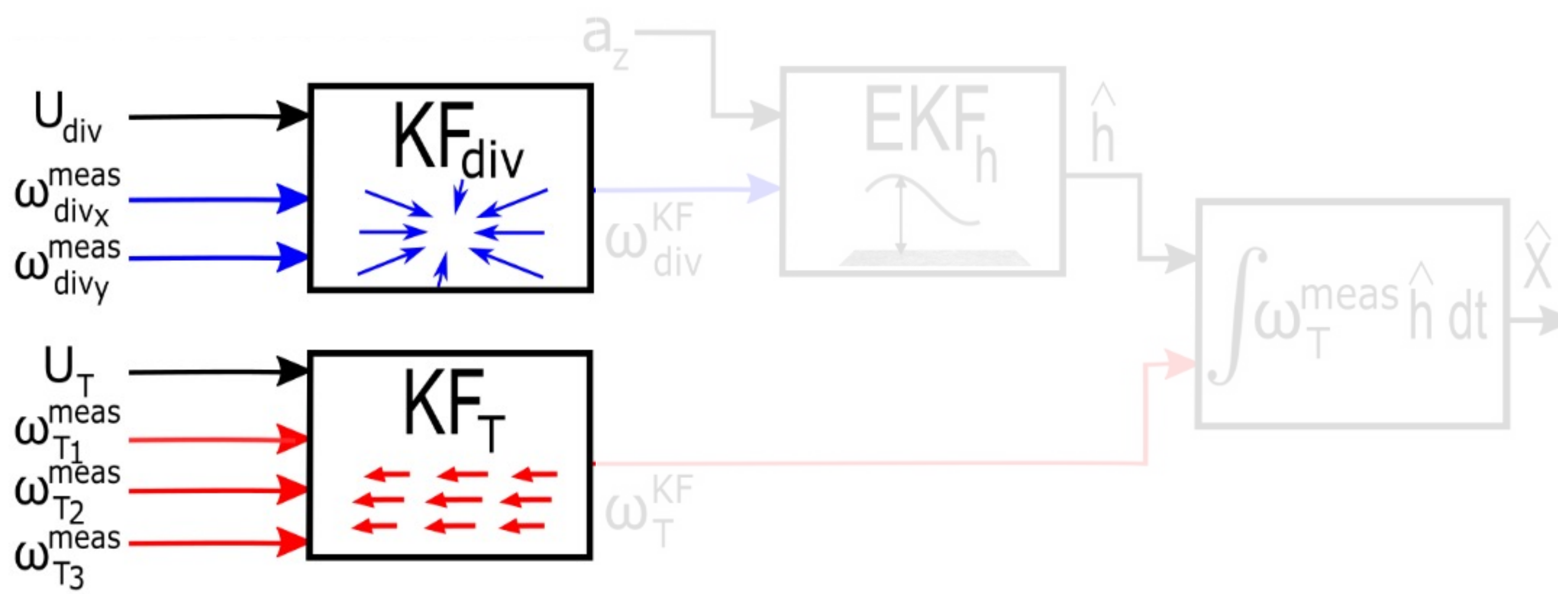

[Bergantin et al., 2023]

SOFIa onboard a flying robot

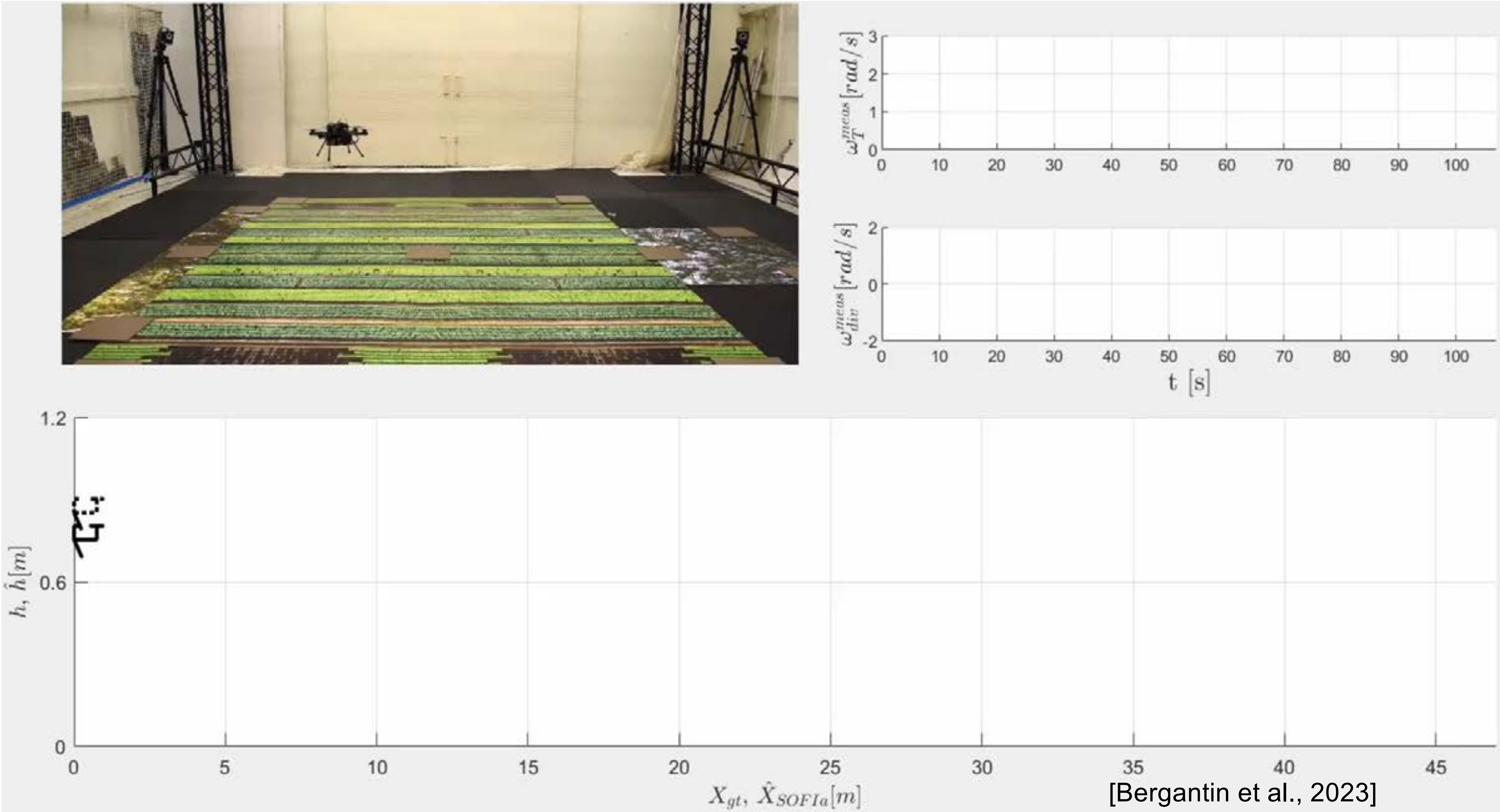

[Bergantin et al., 2023]

Outdoor test

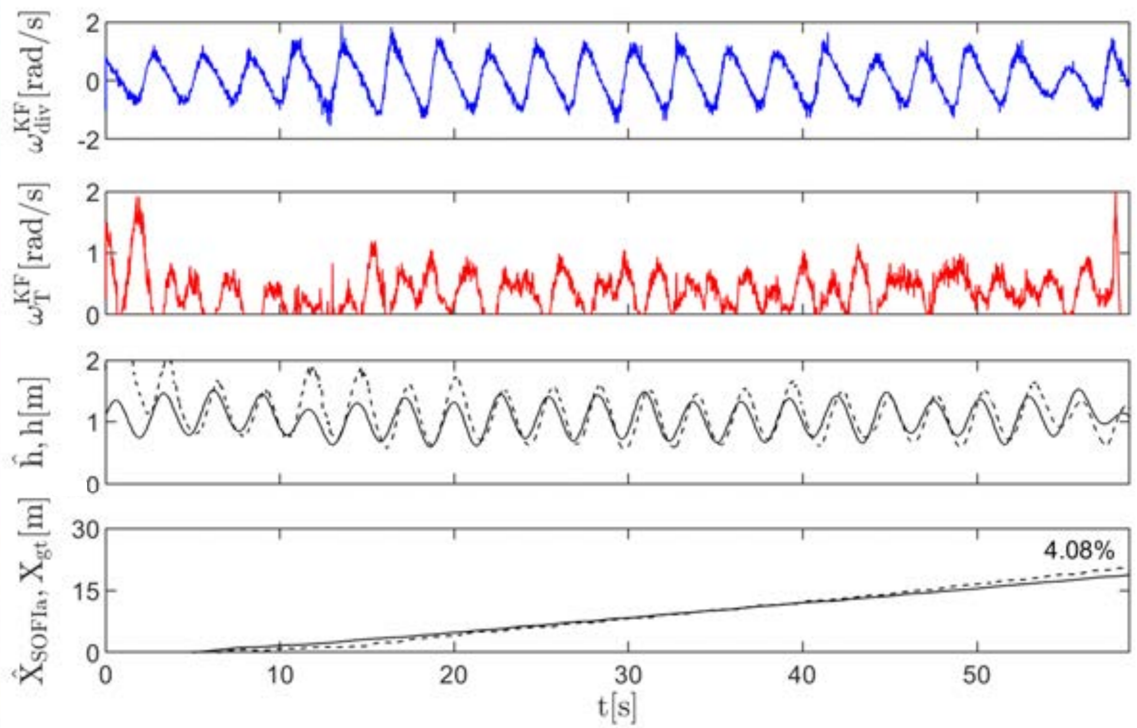

[Bergantin et al., 2023]

Embracing wobble to control attitude without accelerometer

G.C.H.E. de Croon[1], J.J.G. Dupeyroux[1], C. De Wagter[1],

A. Chatterjee[1], D.A. Olejnik[1], F. Ruffier[2]

1. Micro Air Vehicle laboratory, Control and Simulation, Faculty of Aerospace Engineering, Delft University of Technology, the Netherlands

2. Aix Marseille Univ, CNRS, ISM, Marseille, France.

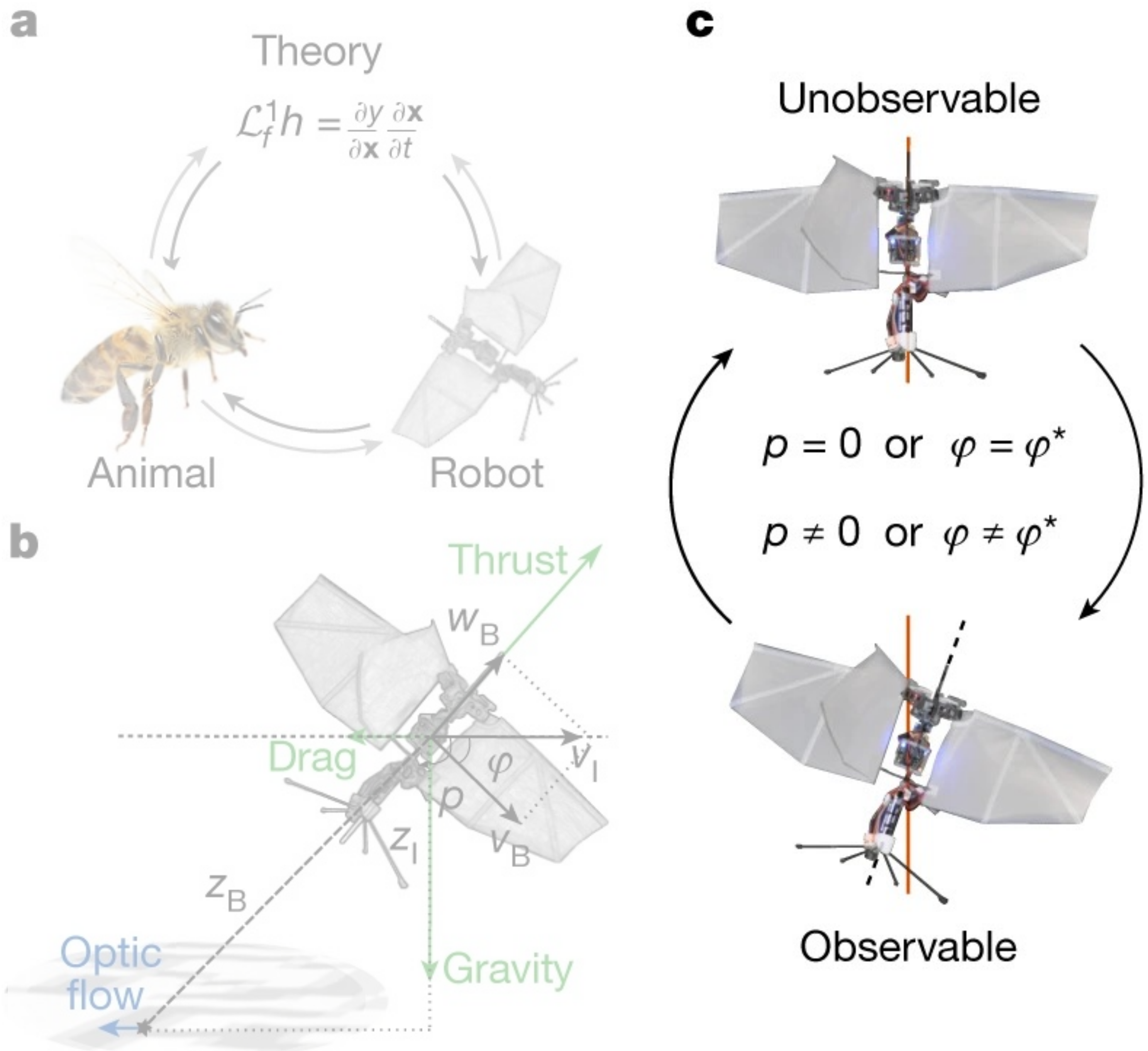

de Croon et al., *Nature*, 2022

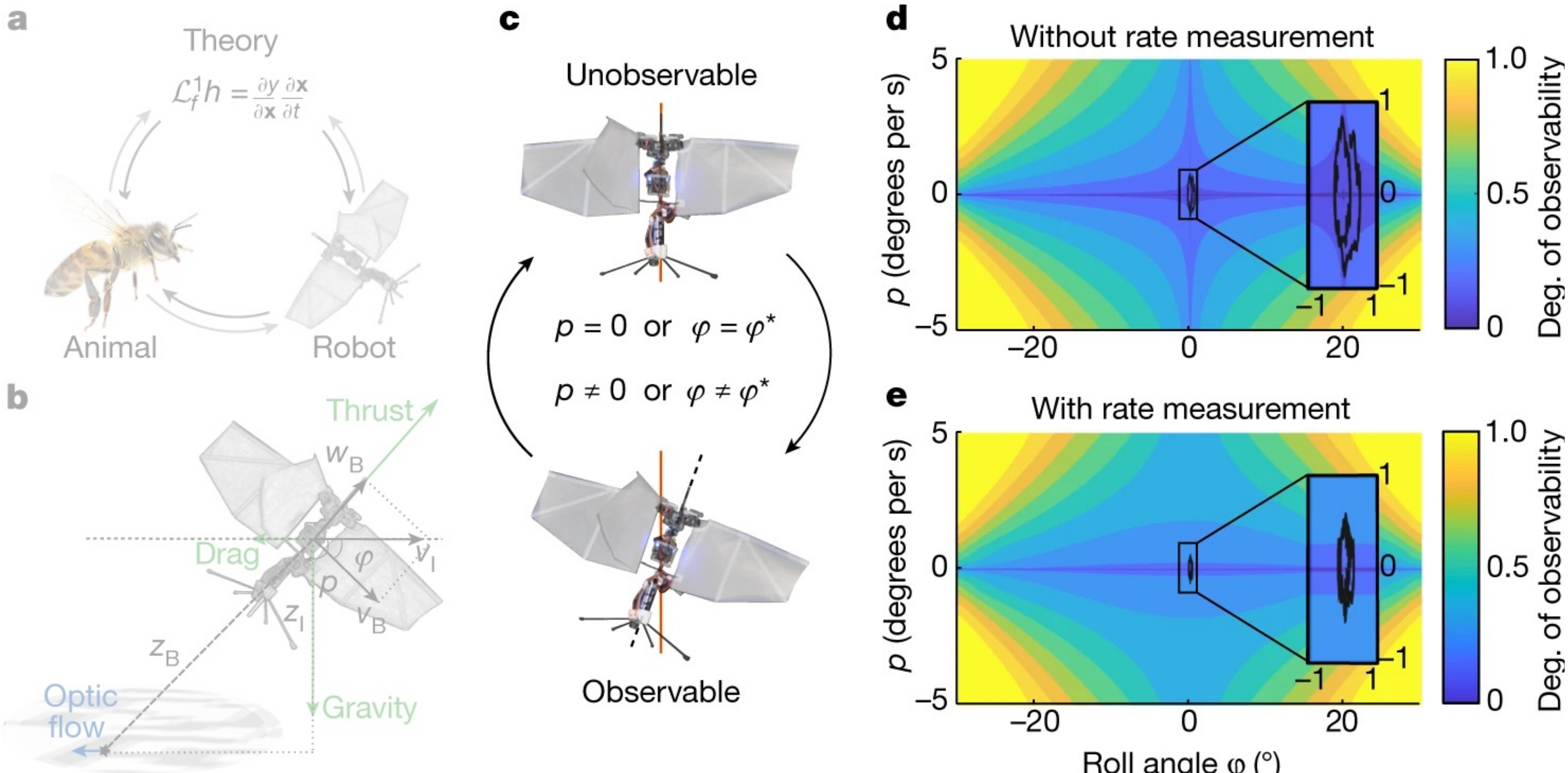

de Croon et al., *Nature*, 2022

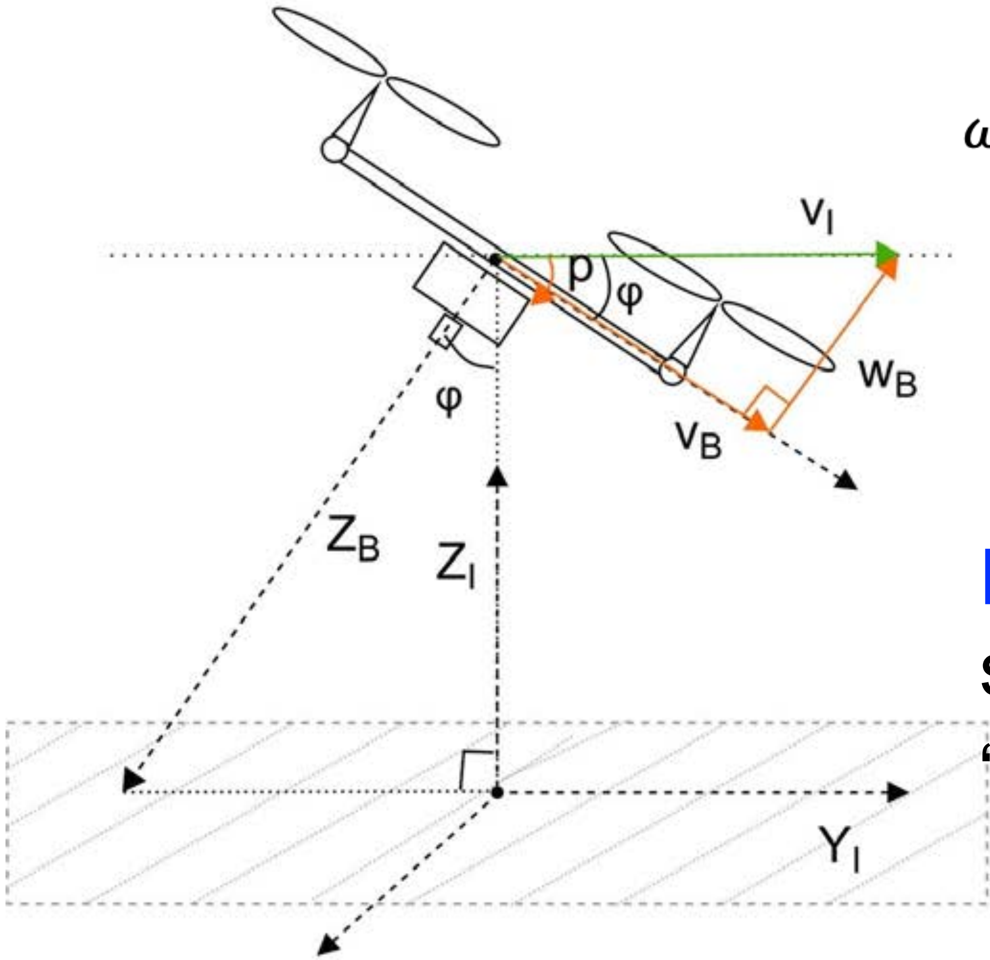

Observation model

$$\omega_y = -\frac{v_B}{Z_B} + p = -\frac{cos^2(\varphi) v_I}{Z_I} + p \qquad \text{(Eq. 1)}$$

State update equation

$$f(\vec{x}, u) = \begin{bmatrix} \dot{v}_I \\ \dot{\varphi} \\ \dot{Z}_I \end{bmatrix} = \begin{bmatrix} g\, tan(\varphi) \\ p \\ 0 \end{bmatrix} \qquad \text{(Eq. 2)}$$

Nonlinear observation analysis based on taking subsequent Lie derivatives $\mathcal{L}_f^i h$, which lead to an "observability mapping"

$$\mathrm{H}(\vec{x}) = \begin{bmatrix} h \\ \mathcal{L}_f^1 h \\ \mathcal{L}_f^2 h \end{bmatrix} = \begin{bmatrix} y \\ \dot{y} \\ \ddot{y} \end{bmatrix} = \begin{bmatrix} -\frac{cos^2(\varphi) v_I}{Z_I} + p \\ \frac{(2pv_I - g) sin(2\varphi)}{2\, Z_I} \\ p \frac{2(pv_I - g) cos(2\varphi) + g}{Z_I} \end{bmatrix} \qquad \text{(Eq. 5)}$$

$$y = \omega_y = h(\vec{x})$$

de Croon et al., *Nature*, 2022

The common way to proceed with (nonlinear) observability analysis is then to perform a local analysis by differentiating $\mathrm{H}(\vec{\boldsymbol{x}})$ with respect to the state to obtain the observability matrix $\mathcal{O}$:

$$\mathcal{O} = \frac{\partial \mathrm{H}(\vec{\boldsymbol{x}})}{\partial \vec{\boldsymbol{x}}} = \begin{bmatrix} \frac{\partial y}{\partial \vec{\boldsymbol{x}}} & \frac{\partial \dot{y}}{\partial \vec{\boldsymbol{x}}} & \frac{\partial \ddot{y}}{\partial \vec{\boldsymbol{x}}} \end{bmatrix} = \begin{bmatrix} -\frac{cos^2(\varphi)}{Z_I} & \frac{p\ sin(2\varphi)}{Z_I} & \frac{2\,p^2\,cos(2\varphi)}{Z_I} \\ \frac{sin(2\varphi)v_I}{Z_I} & \frac{(2pv_I - g)cos(2\varphi)}{Z_I} & 4p\frac{(g - pv_I)sin(2\varphi)}{Z_I} \\ \frac{cos^2(\varphi)v_I}{{Z_I}^2} & \frac{(g - 2pv_I)sin(2\varphi)}{2{Z_I}^2} & -p\frac{2(pv_I - g)cos(2\varphi) + g}{{Z_I}^2} \end{bmatrix}$$

(Eq. 6)

To find all conditions in which the matrix $\mathcal{O}$ is not full rank, we solve for its determinant being zero. We find several solutions. Most are impossible physically.

But, the state is not strictly locally observable, as $p = 0$ and $\varphi = 0$ lead to a range of solutions.

=> Since p is a control input and can be set nonzero, and $\varphi = 0$ will be a transient state for nonzero p, the system is likely globally observable.

de Croon et al., *Nature*, 2022

=> We have proved the stability of the feedback loop based on this estimate

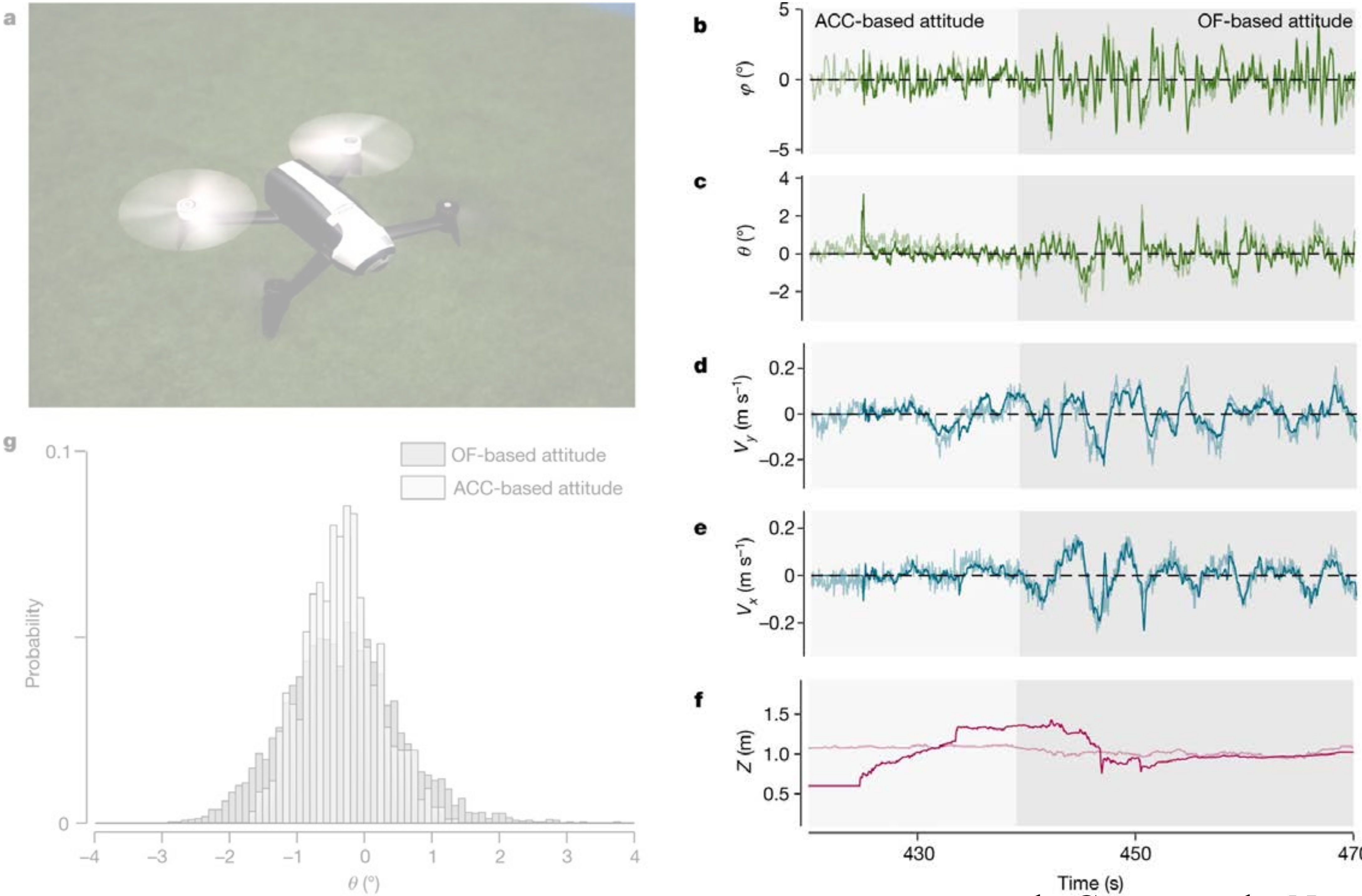

de Croon et al.. *Nature*. 2022

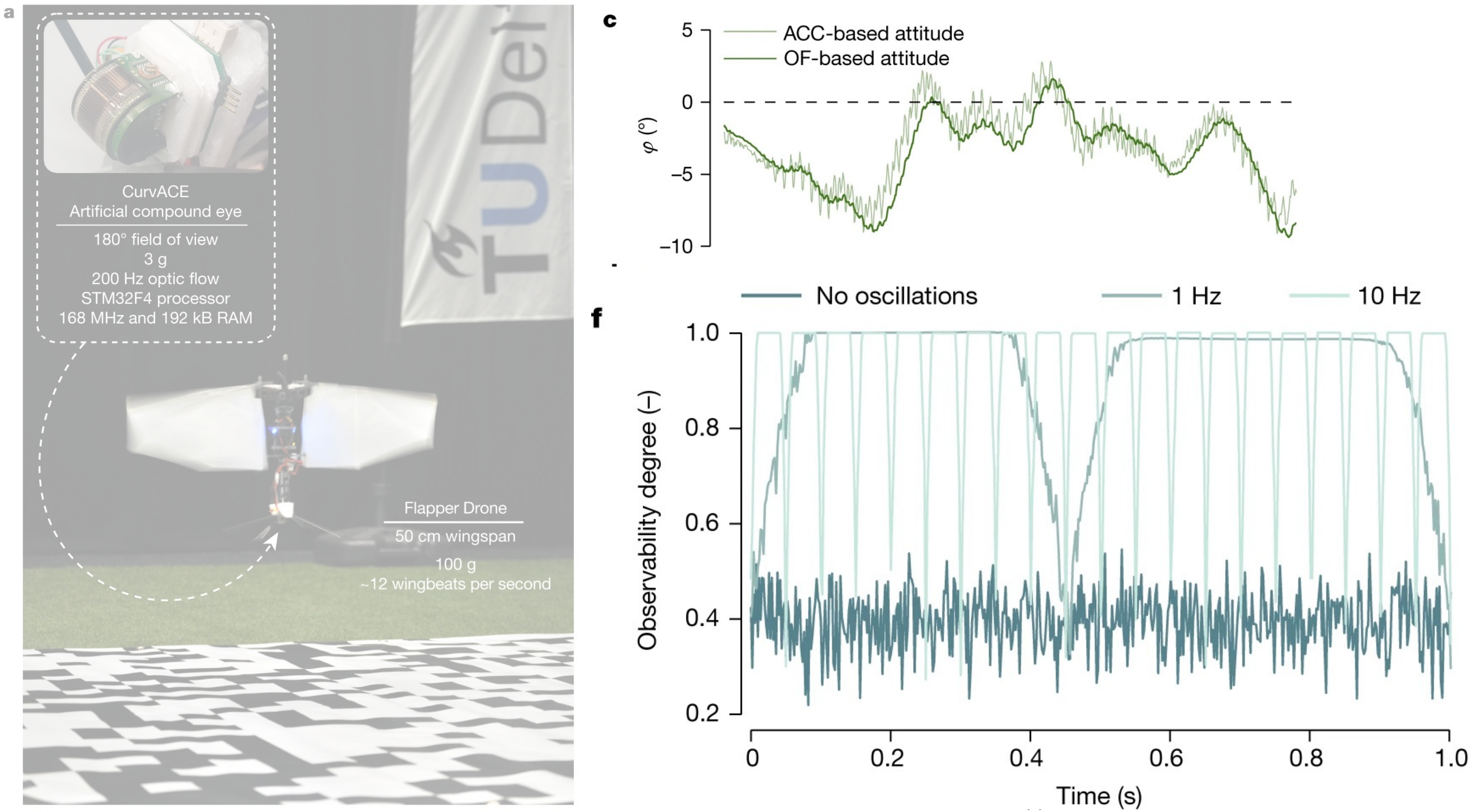

de Croon et al., *Nature*, 2022

III. Vision is enough to trigger collective movements

Diego CASTRO, Franck RUFFIER, Christophe ELOY
ISM - Biorobotics / IRPHE
Aix Marseille Université

No interdistance info, solely vision

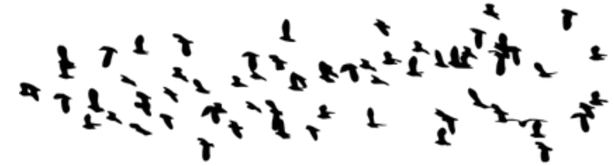

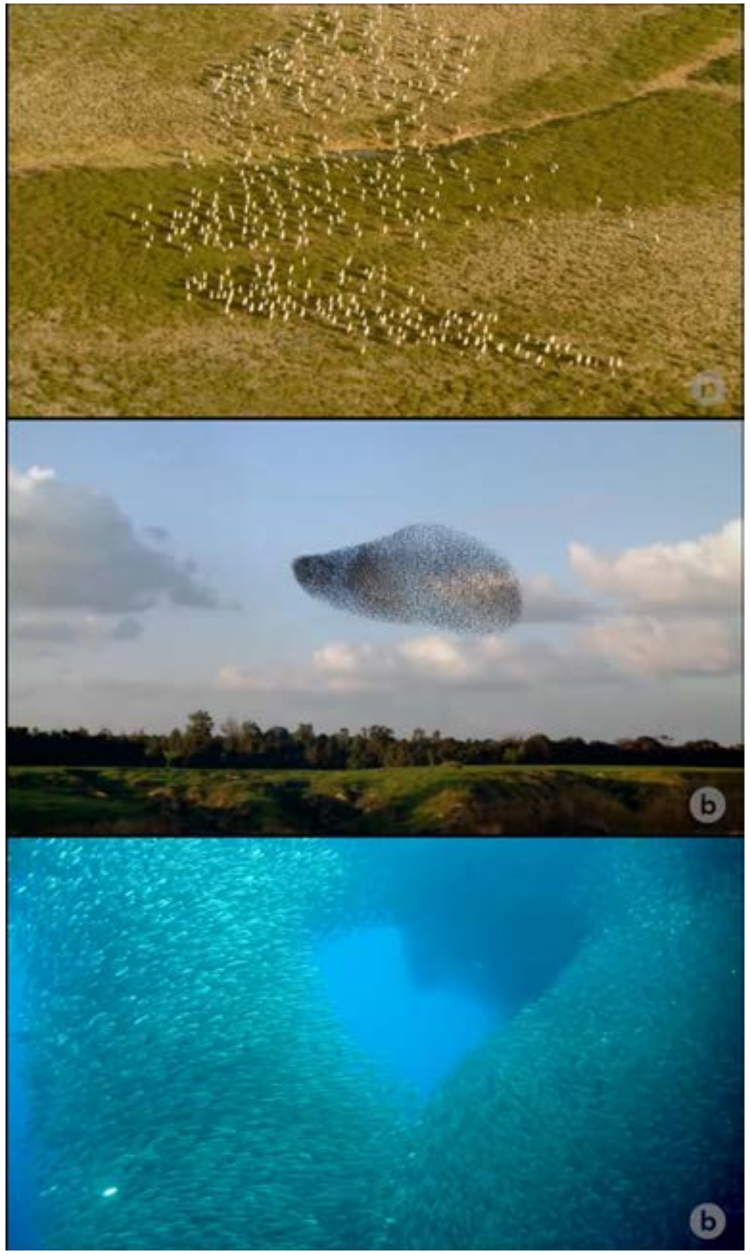

BioGraphicMagazin – Max Planck Institute
https://www.youtube.com/watch?v=Y-5ffl5_7AI

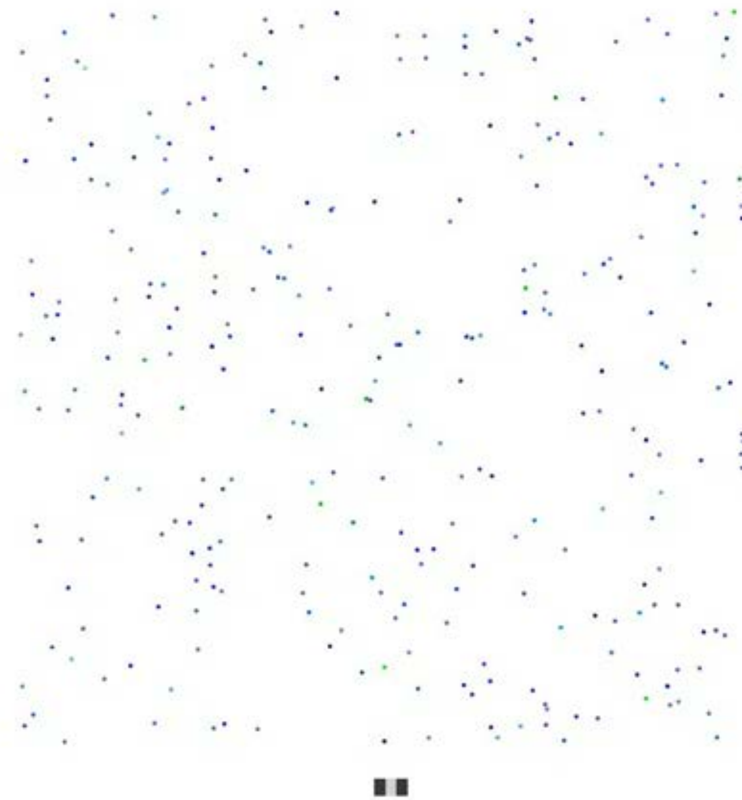

Milling N=300

Castro, Ruffier, Eloy, *PR Research*, 2024

No interdistance info, solely vision

Visual Shades produced by individuals in the FoV

Apparent Distance

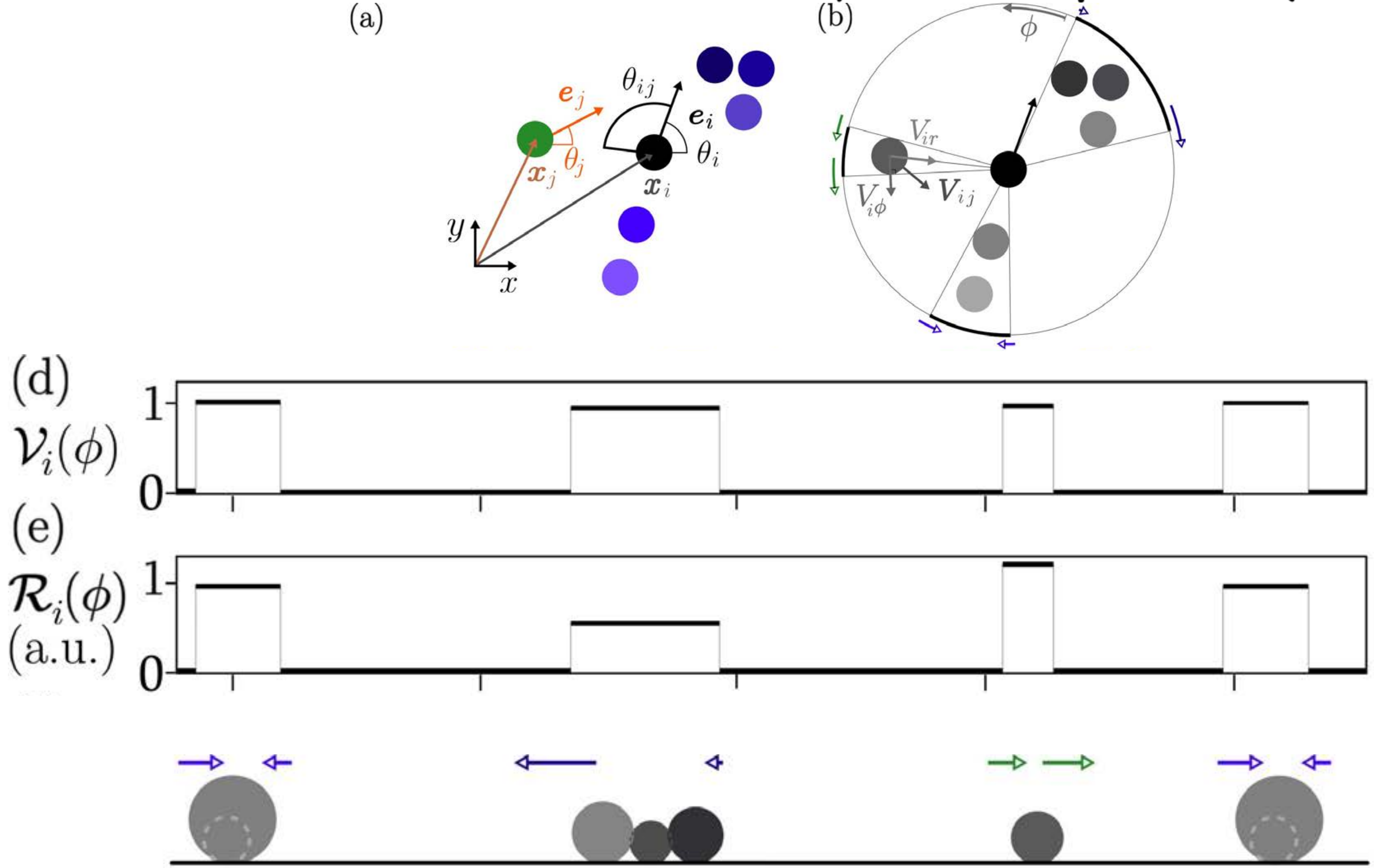

Castro, Ruffier, Eloy, *PR Research*, 2024

No interdistance info, solely vision

Visual Shade

Apparent Distance

Optic Flow

Divergence of Optic Flow

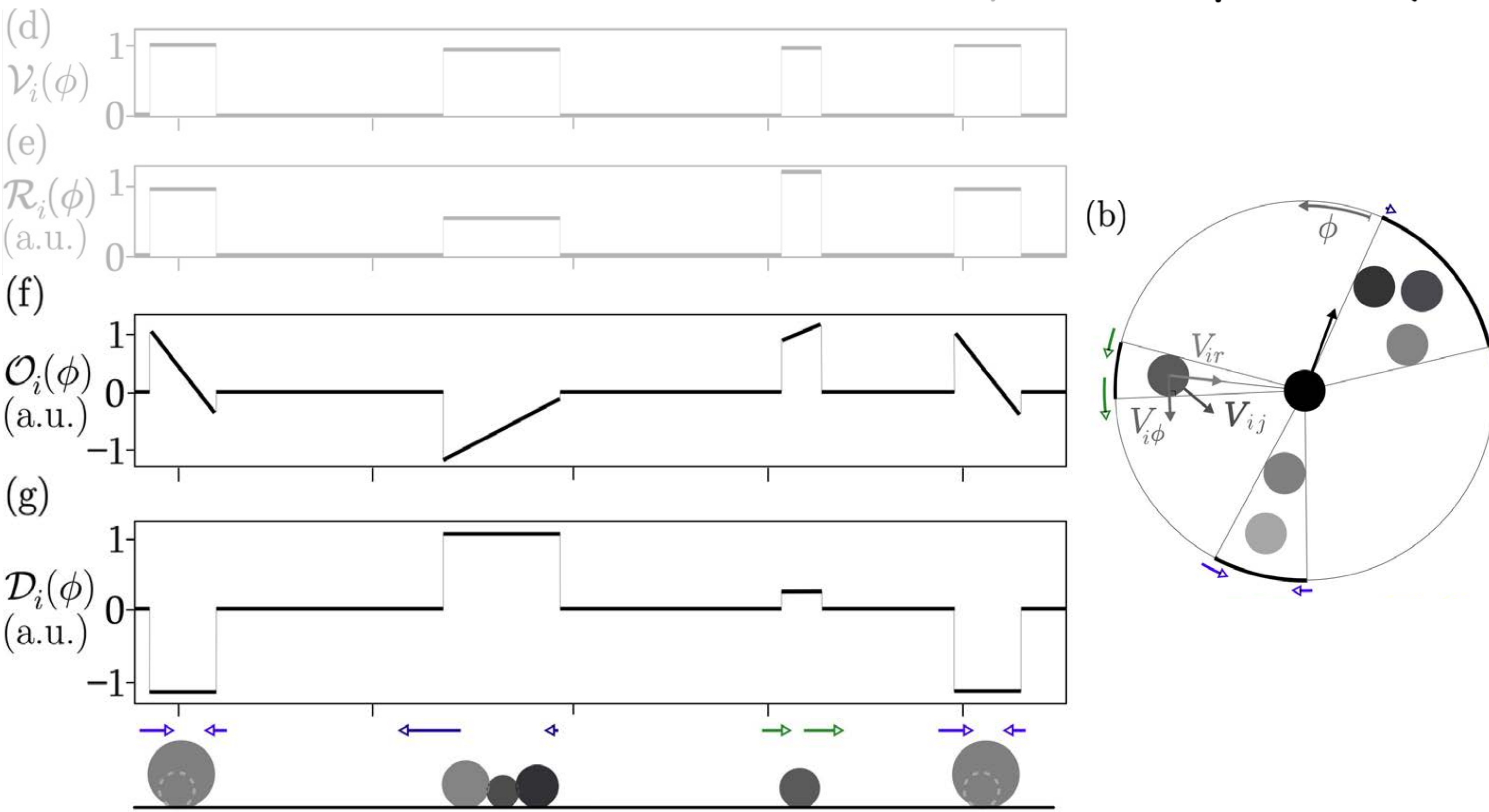

Castro, Ruffier, Eloy, *PR Research*, 2024

Self-propelled Particles Model

$$\dot{\boldsymbol{x}}_i = U\boldsymbol{e}_i,$$
$$\dot{\theta}_i = k_{\odot}\,\omega_{\odot} + k_{||}\,\omega_{||} + k_{\eta}\,\eta,$$

$$\omega_{\odot}^{\text{visu.}} = \left\langle \int_{-\pi}^{\pi} \mathcal{R}_i^2(\phi) b_{\epsilon}(\phi) \sin\phi \, d\phi \right\rangle,$$

$$\omega_{||}^{\text{visu.}} = \left\langle \int_{-\pi}^{\pi} \frac{\boldsymbol{e}_i \times \boldsymbol{V}_{ij}}{U\mathcal{R}_i(\phi)} b_{\epsilon}(\phi)\, d\phi. \right\rangle,$$

If we develop using visual cues

$$\frac{\boldsymbol{e}_i \times \boldsymbol{V}_{ij}}{U\mathcal{R}_i(\phi)} = \frac{-\mathcal{D}_i(\phi)\sin\phi + \mathcal{O}_i(\phi)\cos\phi}{U}$$

Castro, Ruffier, Eloy, *PR Research*, 2024

Phases using vision alone

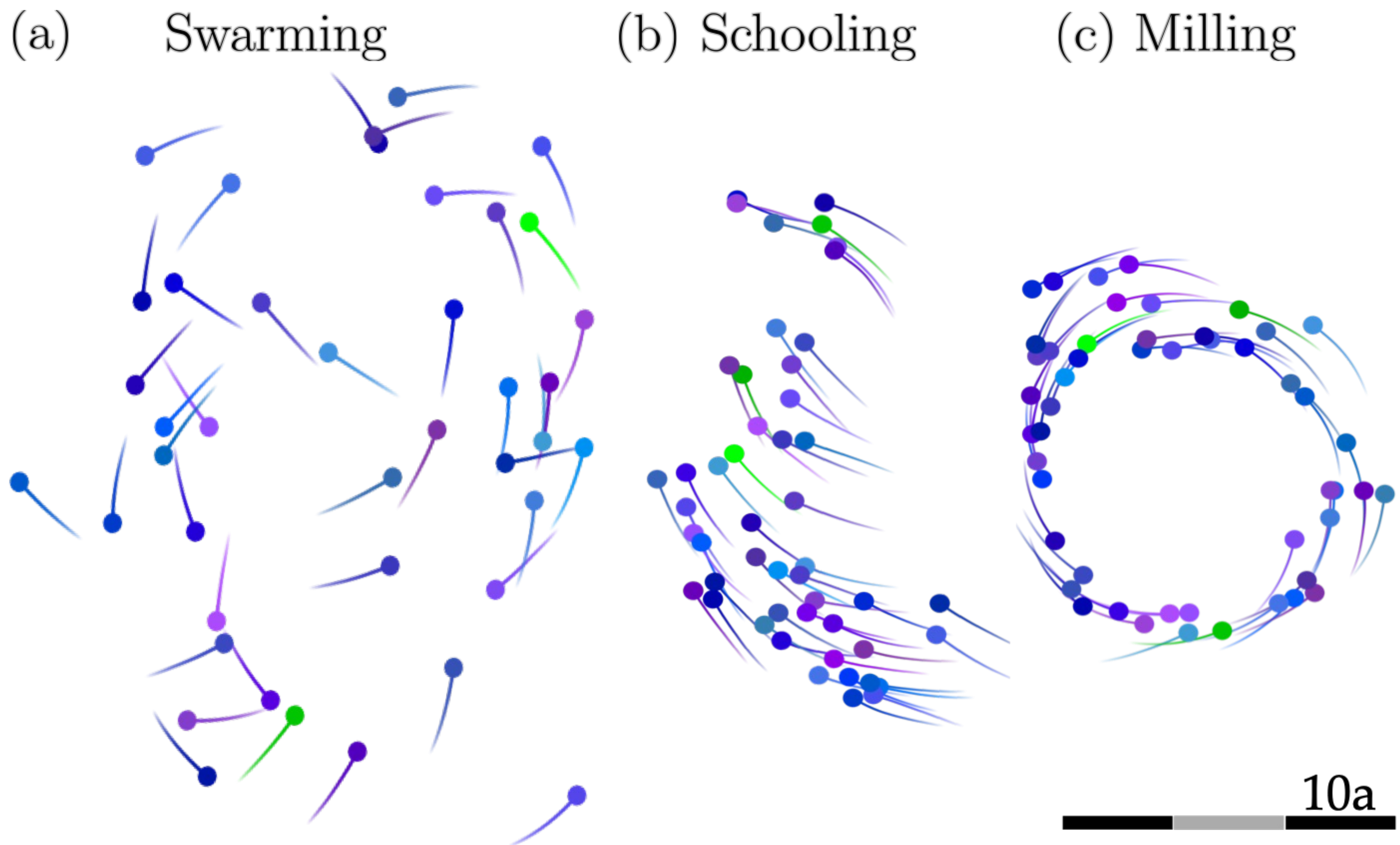

Phase Diagrams

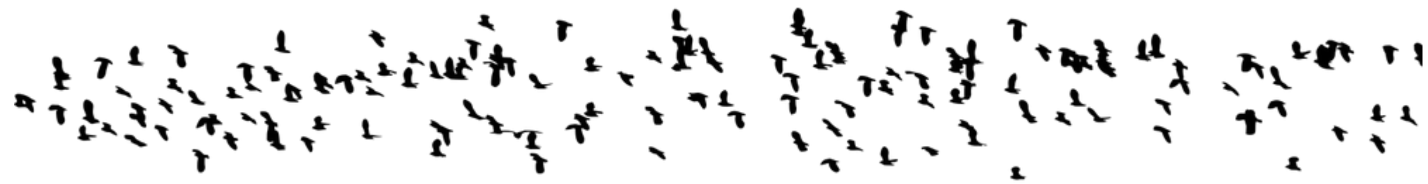

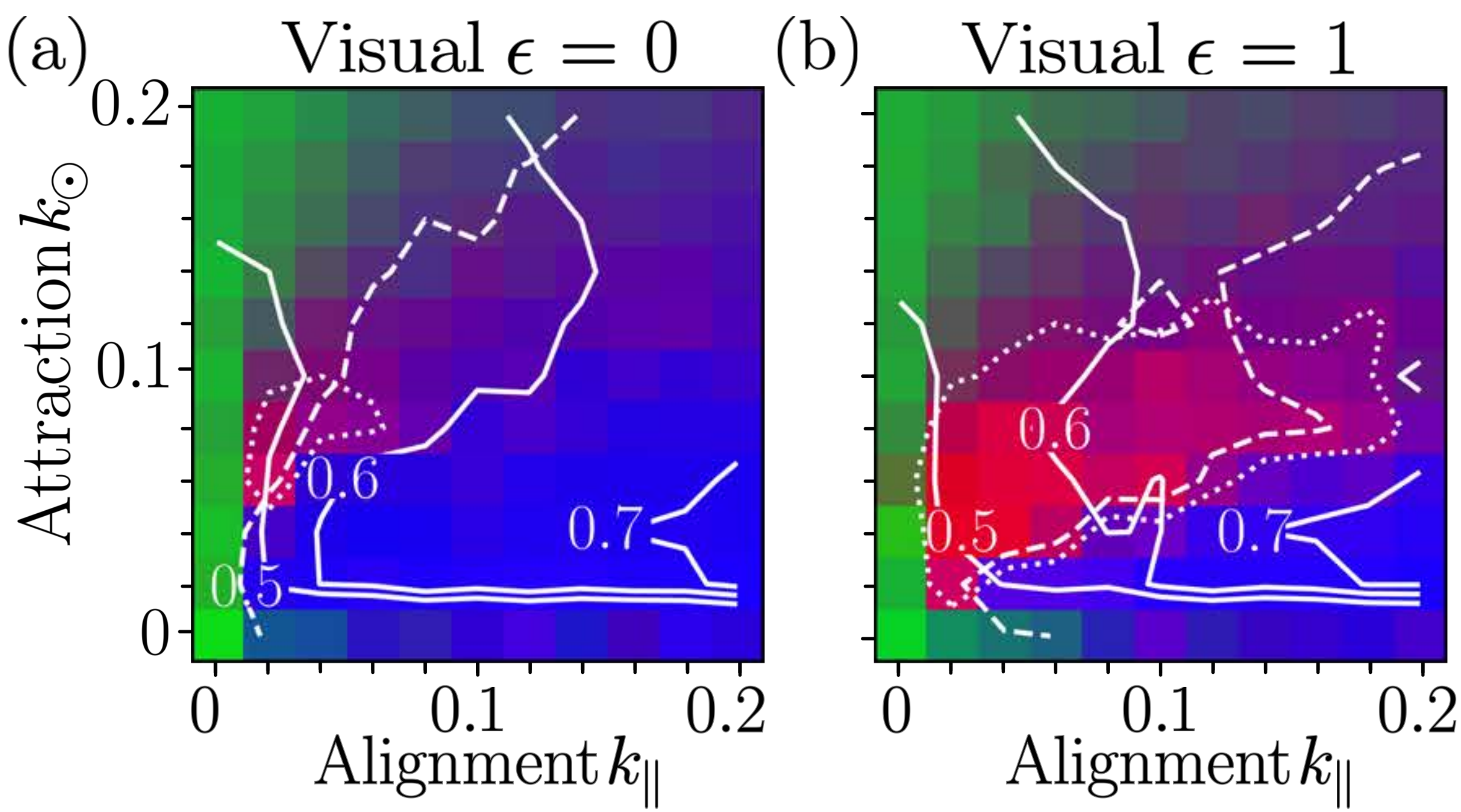

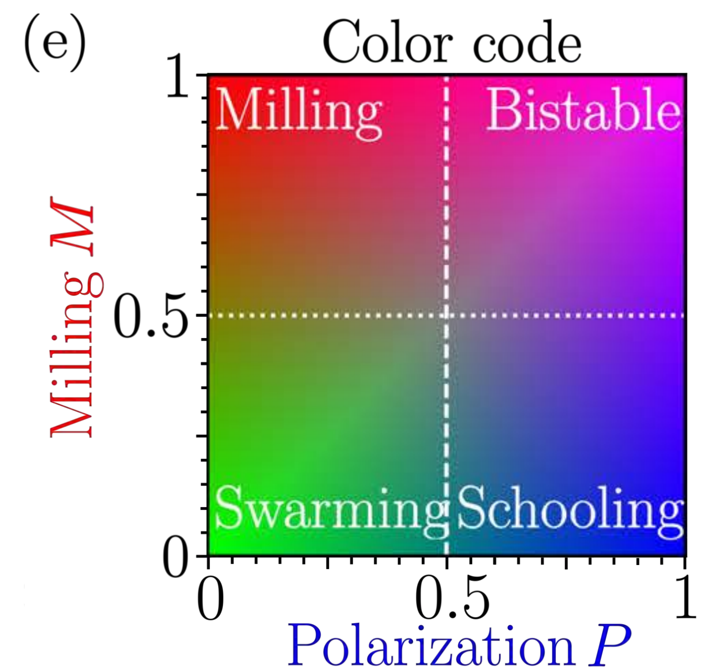

$$P = \|\overline{\boldsymbol{e}_i}\|,$$
$$M = \|\overline{\boldsymbol{y}_i \times \boldsymbol{e}_i}\|$$

Castro, Ruffier, Eloy, *PR Research*, 2024

Phases using vision alone

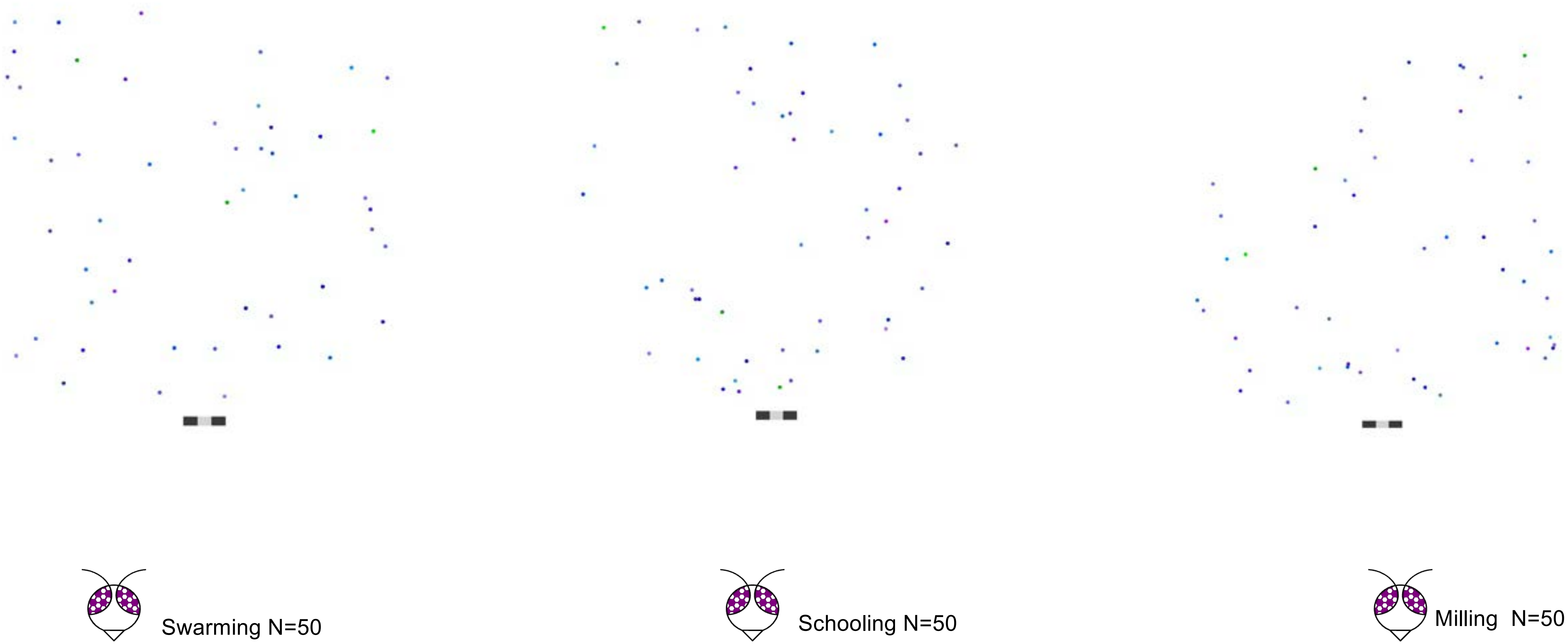

Castro, Ruffier, Eloy, *PR Research*, 2024

Next Step

(here at 0.2m/s)

- *Sphero Bolt* : a stabilized wheel equipped with a display panel

- We implemented the previous model with these *“Hardware in the loop”*

- We use the Color LED display panel to localize each *Sphero* with a camera attached to the ceiling

- **Optic flow and retinal cues created by other individuals is computed in real time for each *Spheros* FoV thanks this localization**

=> We Add a Repulsion function to limit collision

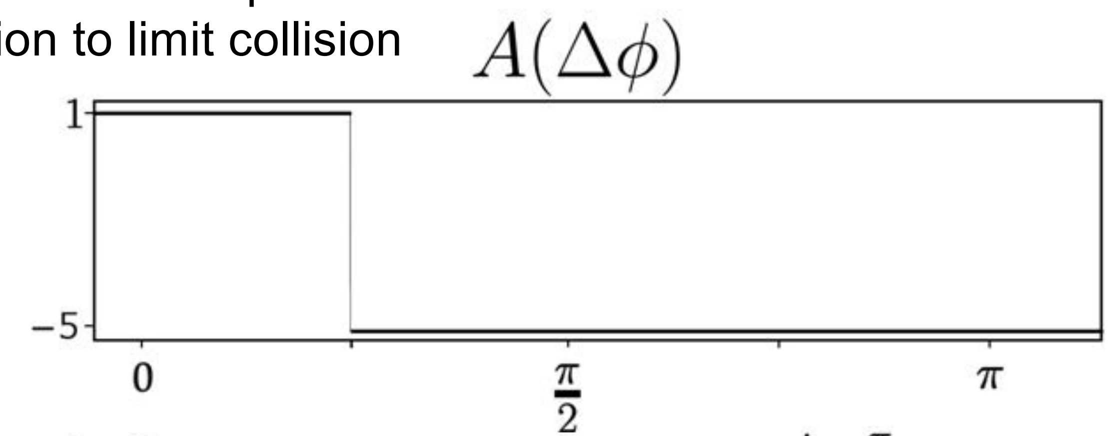

$$\omega_{\odot} = \left\langle \int_{-\pi}^{\pi} A(\Delta\phi)\mathcal{R}^2(\phi) b_\epsilon(\phi) \sin\phi \, d\phi \right\rangle \qquad \omega_{\parallel} = \left\langle \int_{-\pi}^{\pi} A(\Delta\phi) \frac{(\boldsymbol{e}_{ij} \times V_{ij})}{\mathcal{R}^2(\phi)} b_\epsilon(\phi) \, d\phi \right\rangle$$

Castro, Eloy, Ruffier *In prep*


Many Thanks !!
Biorobotics Lab.